Molecular regulation of ethylene-induced hyponasty

Molecular regulation of ethylene-induced hyponasty

Moleculaire regulatie van ethyleen geïnduceerde hyponastie

(met een samenvatting in het Nederlands)

Proefschrift

ter verkrijging van de graad van doctor aan de Universiteit Utrecht op gezag van de rector magnificus, prof. dr. G.J. van der Zwaan, ingevolge het besluit van het college voor promoties in het openbaar te verdedigen op woensdag 11 april 2012 des ochtends te 10.30 uur

door

Joanna Katarzyna Polko

geboren op 22 Februari 1983,
te Tychy, Polen

Promotor: Prof. dr. L. A.C.J. Voesenek
Co-promotoren: Dr. A. J.M. Peeters and Dr. R. Pierik

Cover design: Joanna Polko
Layout: Joanna Polko

ISBN: 978-90-393-5745-3

Table of contents

CHAPTER 1

Petiole hyponasty: an ethylene-driven, adaptive response to changes in the environment

Joanna K. Polko, Laurentius A.C.J. Voesenek, Anton J.M. Peeters and Ronald Pierik

Plant Ecophysiology, Institute of Environmental Biology, Utrecht University, Padualaan 8, 3584 CH Utrecht, the Netherlands

This chapter has been published in *AoB Plants* (2011): doi:10.1093/aobpla/plr031

SUMMARY

Many plant species can actively reorient their organs in response to dynamic environmental conditions. Organ movement can be an integral part of plant development or can occur in response to unfavourable external circumstances. These active reactions take place with or without a directional stimulus and can be driven either by changes in turgor pressure or by asymmetric growth. Petiole hyponasty is upward movement driven by a higher rate of cell expansion on the lower (abaxial) compared to the upper (adaxial) side. Hyponasty is common among rosette species facing environmental stresses such as flooding, proximity of neighbours or elevated ambient temperature. The complex regulatory mechanism of hyponasty involves activation of pathways at molecular and developmental levels with ethylene playing a crucial role. We present current knowledge on the mechanisms that promote hyponasty in the context of other organ movements, including tropic and nastic reactions together with circumnutation. We describe major environmental cues resulting in hyponasty and briefly discuss their perception and signal transduction. Since ethylene is a central agent triggering hyponasty, we focus on ethylene in controlling different stages during plant development and summarize current knowledge on the relationship between ethylene and cell growth.

INTRODUCTION

All living organisms are challenged to cope with environmental heterogeneity. For the past century, the phenomenon of phenotypic plasticity, which allows individual genotypes to adjust to multiple environments, has been a focus of much interest. Due to lack of short-term migration ability, plants have evolved a range of traits and processes which allow them to maintain their functions in dynamic environments (Bradshaw, 1965; Schlichting, 1986; Sultan, 2000). Ultimately, these processes lead to morphological and physiological modifications, some of which appear to have an adaptive role (Van Kleunen and Fischer, 2005; Ghalambor *et al.*, 2007).

Plant organ movements play a special role in coping with ambient changes

and have been given much attention since the birth of modern plant biology. According to the commonly accepted classification they are divided into three arbitrary categories: tropisms, nutations and nastic movements. Tropic reactions are triggered by an exogenous directional stimulus to which a plant can react either with asymmetric axial (differential) growth or changes in turgor status (Shropshire, 1979). Although the vast majority of studies have been carried out on photo- and gravitropsim (Shropshire, 1979; Hart, 1990), which are induced by light and gravity, respectively (Firn and Digby, 1980; Morita and Tasaka, 2004; Iino, 2006), the classification of tropisms extends far beyond that. There are other tropic reactions such as heliotropism (sun-tracking) (Jaffe, 1970; Ehleringer and Forseth, 1980), thigmotropism (reaction to touch or physical contact with an object) (Shropshire, 1979), chemotropism (response to a chemical substance) (Tsao, 1949; Kim *et al.*, 2003), hydrotropism (Jaffe *et al.*, 1985; Takahashi, 1997) or even traumatropism (response to wounding and injuries) (Hart, 1990). Some tropic movements, however, might be induced by non-directional stimuli, e.g. ethylene application or oxygen withdrawal from the roots can cause negative shoot gravitropsim in a diageotropic *Solanum lycopersicon* mutant (Jackson, 1979).

Circumnutations are autonomous, helical movements which require a circadian oscillator (Johnsson, 1979; Stolarz, 2009). They occur usually in young organs of a wide range of plants species, e.g. *Pisum sativum* tendrils (Jaffe, 1972), *Helianthus annuus* hypocotyls (Brown *et al.*, 1990) or coleoptiles of *Avena sp*. (Anker, 1972). Alongside the numerous, rather descriptive studies on circumnutations, molecular tools for studying the regulatory mechanism have now become available. Recent studies, for example, demonstrated the importance of endodermal development and gravitropsim in circumnutational movements (Kitazawa *et al.*, 2005; Johnsson *et al.*, 2009).

Nastic movements occur without a strong directional component (Brauner, 1954; Romberger *et al.*, 1993). The most extensively studied rapid nastic movements such as closing of the *Aldrovanda* or *Dionaea* trap to catch insects (Iijima and Sibaoka, 1985; Hodick and Sievers, 1989) and seismo- and thigmonastic movements of *Mimosa* leaves (Sibaoka, 1962; Sibaoka, 1991) are based on changes in the osmotic status of specific cells. Some species, belonging to *Fabaceae* family in particular, possess specialized structures, pulvini, which consist of motor cells with elastic cell walls and a large, quickly contractable vacuole (Satter *et al.*, 1990; Romberger *et al.*, 1993). Although initially classified as movements driven by reversible turgor reactions, many nastic responses depend on unequal growth rates between two anatomically different sides of the organ (differential growth) (Romberger *et al.*, 1993). Thermonastic opening of *Tulipa* and *Crocus* tepals is one of the elegant examples of differential growth triggered by differences in tissue sensitivity to ambient temperature, where the outer epidermis of the perianth has a growth optimum about 10°C lower than the inner one (Wood, 1953).

Epinasty is usually described for leaves and floral organs and takes place when, as a result of differential growth, an organ bends outward and downward

(Kang, 1979). It is usually triggered by unfavourable ambient conditions such as waterlogging (Kawase, 1974; Jackson and Campbell, 1976), salinity stress (Jones and Elabd, 1989), drought (Ruiz-Sanchez *et al.*, 2000) or pathogen attack (Evidente *et al.*, 1996; Michielse and Rep, 2009). The complex regulation of epinastic movements consists of many factors among among which gravity, ethylene and auxin play a central role (Stewart and Freebairn, 1969; Lin *et al.*, 2008; Perez-Perez *et al.*, 2010). The opposite type of asymmetric growth, when abaxial tissue exhibits higher growth rates in comparison to adaxial cells, is called hyponasty (Kang, 1979) (**Fig.1.1**). Hyponasty has been mostly reported for leaf blades of monocots and dicots (Lippincott and Lippincott, 1968; Street *et al.*, 1992) as well as leaf petioles (Voesenek and Blom, 1989; Cox *et al.*, 2003; Pierik *et al.*, 2003). Hyponastic responses are of high functional significance in coping with a wide range of abiotic types of stress such as flooding, shade or elevated temperatures (reviewed in Van Zanten *et al.*, 2010).

Fig. 1.1 (a-b) Ethylene-induced hyponasty in *Rumex palustris* and **(c-d)** *Arabidopsis thaliana*. **(a,c)** Plants after 6h in control conditions and **(b,d)** after 6h of ethylene exposure.

HYPONASTY IN RESPONSE TO ABIOTIC STRESS

Flooding

Various types of environmental stress can cause plant organs to grow hyponastically. Studies on semi-aquatic species led to the identification of a suite of submergence escape characteristics which include hyponasty (reviewed in Voesenek *et al.*, 2006). Waterlogging, partial and total submergence have a significant effect on leaf angle of *Rumex palustris* (Voesenek and Blom, 1989), *Leontodon taraxoides* (Grimoldi *et al.*, 1999), *Paspalum dilatatum* (Insausti *et al.*, 2001) or *Rorippa sylvestris* (Stift *et al.*, 2008). Although initial studies on submergence–induced differential growth fo-

cused mostly on species naturally occurring in occasionally flooded habitats, recent experiments revealed that hyponasty in *Arabidopsis thaliana* can be used to unravel mechanisms explaining flooding-induced hyponasty (Peeters *et al.*, 2002; Millenaar *et al.*, 2005; Pierik *et al.*, 2005; Vashisht *et al.*, 2011). Hyponasty in flood tolerant species is a prerequisite for non-differential petiole/leaf blade elongation (Cox *et al.*, 2003). The combined action of hyponasty followed by accelerated linear elongation helps the plant to re-establish contact with air and, in turn, restore successful gas exchange (Voesenek and Blom, 1989) and aerial photosynthesis (Mommer *et al.*, 2005). The significance of hyponasty preceding petiole elongation has been demonstrated with experiments where submerged *R. palustris* petioles were fixed at certain angles. If the angle was set below 40° relative to the horizontal plane, rates of underwater elongation were much lower than in control plants, whereas fixing the angle closer to the vertical (approximately 80°) permitted petiole elongation rates to increase. In the first instance, faster elongation rates were restored when the below 40° fixation angle was released (Cox *et al.*, 2003). The volatile phytohormone ethylene plays a central role in this complex regulatory mechanism of hyponastic response. Its diffusion from submerged tissues is severely reduced when submerged and as a result its endogenous concentrations significantly increase (Jackson, 1985; Voesenek *et al.*, 1993; Banga *et al.*, 1996). This physical entrapment is crucial for both hyponasty and non-differential linear petiole or internode elongation (Voesenek and Blom, 1989; Banga *et al.*, 1997; Kende *et al.*, 1998). Ethylene involvement is indicated by the strong inhibition of petiole angles in submerged *R. palustris* plants by application of the ethylene perception inhibitor 1-methylocyclopropene (1-MCP) (Cox *et al*., 2004). Moreover, it has been demonstrated that ethylene regulates two crucial events during the first phase of submergence response: a rapid acidification of the apoplast (Vreeburg *et al*., 2005) and up regulation of expansin transcript levels (Vriezen *et al*., 2000; Vreeburg *et al*., 2005). Different stages of submergence-induced hyponasty can be positively regulated by auxin (IAA) and gibberellins (GA) as downstream targets for ethylene, whereas the growth inhibitory hormone, abscisic acid (ABA), negatively influences the response. Since deblading experiments resulted in a dramatic delay in the hyponastic response to submergence, it has been concluded that the onset of petiole hyponasty depends on auxin transport from the leaf lamina (Cox *et al.*, 2006). Furthermore, the stage when hyponastic growth is fastest coincides with a lateral redistribution of IAA (Cox *et al.*, 2004). Importantly, the stimulating effect of auxin and ethylene on hyponasty is independent of the effect of these hormones on the subsequent non-differential linear petiole elongation. Submergence depresses endogenous levels of ABA within 2 h of submergence. This decrease is an outcome of an inhibition of ABA biosynthesis and has a stimulatory effect on all stages of submergence-induced hyponasty (initiation, speed and maintenance). In contrast, following the reduction of ABA levels, increased concentrations of GA serve a promoting function during the speeding-up phase of differential growth (Benschop *et al.*, 2006). Recently, it has been discovered that the increase in expression of *SNORKEL* genes, which belong to the ethylene response factor (ERF) family, is required for submergence-induced internode elongation in deepwater rice

(Hattori *et al.*, 2009) and that it might act through the GA signalling pathway. Since the hyponastic response in dicot species is also GA dependent, ethylene response factors (ERFs) could be crucial components of the mechanism also in this case.

Shade

Many plants, particularly angiosperms, display the so-called shade avoidance syndrome (SAS) when growing in dense communities. SAS consists of various phenotypic adjustments which affect all stages in a plants life cycle, influencing their germination, chloroplast development, extension growth, apical dominance, distribution of assimilates and flowering time (Smith and Whitelam, 1997; Smith, 2000). Depending on the overall plant morphology, extension growth applies to different organs. It can stimulate elongation of internodes, as in *Sorghum bicolor* (Finlayson *et al.*, 1998), *Urtica dioica, Senecio vulgaris* (Morgan and Smith, 1979), prairie ecotype of *Stellaria longipes* (Sasidharan *et al.*, 2008), *Datura ferox* (Ballaré *et al.*, 1990) or in case of the rosettes species, such as *Arabidopsis* or *R. palustris*, causes hyponastic growth and elongation of petioles (Pierik *et al.*, 2005). When proximity of other plants reduces photosynthetic performance, petiole hyponasty is a successful escape strategy (Hutchings and de Kroon, 1994; Ballaré *et al.*, 1995; Schmitt, 1997; Pierik *et al.*, 2003; Pierik *et al.*, 2004). Experiments on two *Potentilla* species demonstrated that, despite the lack of homology between petioles and internodes, they show a similar response to shade (Huber, 1996). This is in accordance with the hypothesis that analogous organs which share ecological function can show similar plasticity in response to environmental changes (Ballaré, 1994). Discovery of the Red:Far-red (R:FR) ratio as the primary signal triggering SAS prior to actual physical shading (Morgan and Smith, 1976; Ballaré *et al.*, 1987; Ballaré *et al.*, 1990) has generated a wide interest in this area and contributed to our current understanding of the molecular sensory mechanism for detecting the threat of shade. Photoreceptors involved in the perception of light changes include a set of phytochromes responding to altered R:FR ratio's (Quail *et al.*, 1995; Neff *et al.*, 2000; Smith, 2000) together with blue light-induced cryptochromes and phototropins (Briggs and Huala, 1999; Christie *et al.*, 1998; Cashmore *et al.*, 1999). Molecular aspects of signal transduction and transcriptional regulation upon shade has been rigorously reviewed by Franklin (2008). Studies on dense canopies of *Nicotiana tabacum* demonstrated that the perception of ethylene plays a crucial role in competition for light. In canopies, ethylene concentrations are elevated by almost four-fold compared to the ambient atmosphere and ethylene-insensitive plants display delayed shade avoidance responses in comparison to the wild type (Pierik *et al.*, 2003; Pierik *et al.*, 2004). Not surprisingly, auxin and its transport, which play an important role in most of the differential growth processes, are key players in the regulation of growth responses upon shade (Morelli and Ruberti, 2000; Keuskamp *et al.*, 2010; Kozuka *et al.*, 2010; Keuskamp *et al.*, 2011). Detailed studies by Tao *et al.* (2008) have confirmed that activation of tryptophan-dependent pathway of auxin synthesis is absolutely necessary for SAS. Additionally, the blockage of auxin receptor TIR1 as well as impairment of a trans-

porting protein, PIN3, lessens the auxin gradient thereby reducing shade avoidance symptoms, including hyponasty (Keuskamp *et al*., 2010). Auxin acts synergistically with brassinosteroids (BR) since the inhibition of both hormones almost entirely blocks elongation of the hypocotyl (Keuskamp *et al*., 2011). Although these experiments were carried out on hypocotyls, it is likely that such contributory function of BRs applies to hyponasty since the exclusive role of auxin in ethylene-induced hyponasty is still under debate (Van Zanten *et al*., 2009a). Notably, a set of BR responsive genes is essential for petiole elongation in shade (Kozuka *et al*., 2010). Gibberellins (GAs) and GA-mediated DELLA degradation have been demonstrated to contribute to SAS (Djakovic-Petrovic *et al.*, 2007), however, there is evidence that the GA pathway acts in an ethylene and auxin-independent manner (Pierik *et al.*, 2009). At a cellular level, low R:FR ratios and green shade lead to the apoplastic acidification and increase in the levels of certain cell wall modifying enzymes – expansins and xyloglucan endotransglucosylases/ hydrolases (XTHs) (Sasidharan *et al*., 2008; 2010).

Studies from the past decade have demonstrated that light perception interacts tightly with temperature signaling and that phytohormones and transcriptional regulators probably serve as nodes in this crosstalk (Franklin, 2009; Koini *et al.*, 2009). Common responses to these stresses include clear morphological changes such as hypocotyl elongation (Gray *et al.*, 1998) or early flowering (Balasubramanian *et al.*, 2006). Interestingly, elevated temperatures lead also to hyponastic responses (Koini *et al.*, 2009; Van Zanten *et al.*, 2009b) and ethylene has been shown to regulate heat-induced hyponasty negatively (Van Zanten *et al.*, 2009b). Previous experiments have revealed that leaf inclination is tightly associated with leaf temperature and that elevated angles influence cooling properties (Medina *et al.*, 1978). According to King (1997), vertical leaf orientation in *Eucalyptus sp.* is highly beneficial when dealing with low temperatures.

As mentioned above, ethylene is one of several key regulators of hyponastic responses to various environmental changes. As shown by Pierik *et al*. (2005) application of ethylene alone can mimic the response of plants to flooding or shaded conditions in both *Arabidopsis* and *R. palustris*. Therefore, ethylene-induced hyponasty is a suitable study system to help identify the regulatory network and developmental switches in differential petiole growth.

ETHYLENE AND PLANT DEVELOPMENT

A number of observations that illuminating gas leaking from pipes in orchards had a dramatic effect on plants growing in the vicinity (Girardin, 1864) led to the discovery of ethylene as a plant hormone. The analysis of active compounds in the illuminating gas performed by Neljubow (1901) identified ethylene as a component responsible for its strong morphogenetic effects at high dilution. Subsequently, a number of descriptive reports, such as ethylene's influence on the development of flowers in carnations (Crocker and Knight, 1908) or epinasty and leaf abscission

(Doubt, 1917) promoted much subsequent interest in ethylene biology.

The mosaic effect of ethylene on plant growth concerns alterations of fundamental processes at all developmental stages. Due to technical challenges, little is known about the role of ethylene during zygotic embryogenesis. The peak of ethylene concentration in *Brassica napus* embryos has been detected at the torpedo stage (Johnson-Flanagan and Spencer, 1994) and, as shown by studies on microspore-derived embryos, ethylene is necessary for the lateral expansion of cotyledons (Hays *et al.*, 2000), whereas antagonistic interaction between ethylene and ABA leads to breaking of dormancy (Koornneef *et al.*, 2002; Gniazdowska *et al.*, 2010). At the post-embryonic stage, the best recognized effect of ethylene during skotomorphogenesis is the so called triple response. It consists of inhibition of hypocotyl and root elongation, exaggeration of the apical hook and hypocotyl thickening (Knight and Crocker, 1913; Pratt and Biale, 1944) and has been used as an efficient bioassay in identifying ethylene-related mutations (Bleecker *et al.*, 1988; Guzman and Ecker, 1990). During formation of the apical hook, ethylene causes differential cell elongation (Lehman *et al.*, 1996; Raz and Ecker, 1999) and, as revealed by detailed study on the kinetics of the response, prevents it from opening (Lehman *et al.*, 1996; Gallego-Bartolome *et al.*, 2011). Smalle and Van Der Straeten (1997) showed that ethylene has a stimulatory effect on hypocotyl expansion in light. In the below-ground tissues, ethylene stimulates roots to expand radially (Dolan, 1997; Smalle and Van Der Straeten, 1997), regulates adventitious root formation (Jusaitis, 1986; Liu *et al*., 1990), affects differentiation pattern of atrichoblasts and trichoblasts (Schneider *et al.*, 1997) and, through crosstalk with auxin, inhibits lateral root formation (Ruzicka *et al.*, 2007; Ivanchenko *et al.*, 2008; Negi *et al.*, 2008; Lewis *et al.*, 2011). Its role in reproductive development includes flowering induction, e.g. in *Ananas sativus* (Burg and Burg, 1966) and promoting female sex determination in *Cucumis sativus* and *Cucumis melo* (McMurray and Miller, 1968; Boualem *et al.*, 2008; Wang *et al.*, 2010). Other thoroughly studied properties of ethylene concern the final events in plant development such as fruit ripening (Burg and Burg, 1962; Barry and Giovannoni, 2007) onset of leaf senescence (Zacarias and Reid, 1990; Thomas *et al.*, 2003) and leaf abscission (Abeles and Rubinstein, 1964). Interestingly, as shown by Summers *et al*. (1996) the complete absence of ethylene biosynthesis does not cause a disturbed overall development in *Potamogeton pectinatus* Accordingly, ethylene-insensitive mutant and transgenic genotypes under optimal growth chambers conditions do not display disturbed growth (Tholen *et al*., 2004).

ETHYLENE AND ORGAN GROWTH

Cell expansion

Early observations of cell growth in the presence of ethylene provided data about its inhibitory function on various types of tissues (Hayashi and Maclachlan, 1984). A number of experiments on *Arabidopsis* roots have shown that ethylene treatment

leads to isodiametric cell growth which is dependent both on auxin biosynthesis in the root tip (Stepanova *et al.*, 2005; Swarup *et al.*, 2007) and rootward auxin transport (Ruzicka *et al.*, 2007). Often, ethylene–treated cells do not cease their growth entirely but, instead, start to expand in a radial dimension, e.g. in epicotyl cells of *Pisum sativum* (Apelbaum and Burg, 1971). It is not clear, though, if this effect is a result of cell wall metabolism and matrix composition changes due to ethylene treatment (Eisinger *et al.*, 1983). On the other hand, studies on *Picea abies* show that ethylene can negatively affect the incorporation of wall carbohydrates (Ingemarson *et al.*, 1991). Naturally, this lateral expansion requires a different orientation of cortical cytoskeleton and, therefore, ethylene has also been associated with longitudinal organization of cortical microtubules (CMTs) (Yuan *et al.*, 1994; Steen and Chadwick, 1981; Lang *et al.*, 1982; Roberts *et al.*, 1985; Soga *et al.*, 2010).

Although obviously legitimate, this classical concept of ethylene's inhibitory effect on cell elongation has been complemented with reports of its stimulatory properties (reviewed in Pierik *et al.*, 2006). These include stem elongation in *Callitriche platycarpa* (Musgrave *et al*., 1972), previously mentioned cell expansion-driven petiole elongation in submerged *R. palustris* plants (Cox *et al.*, 2004), internode elongation in submerged deepwater rice (Kende *et al*., 1998) or *Arabidopsis* hypocotyl elongation in light (Smalle and Van Der Straeten, 1997; Le *et al.*, 2005). Moreover, it has been demonstrated that low-nutrient grown *Arabidopsis* seedlings exhibit transverse (elongation stimulating) CMT orientation upon treatment with the ethylene precursor, 1-aminocyclopropane-l-carboxylic acid (Le *et al.*, 2005). Recently, a study of cell sizes at two sides of ethylene-treated *Arabidopsis* petioles provided evidence that ethylene and ad- and abaxial identity defines whether the orientation of cytoskeleton is transverse or longitudinal (Polko *et al*., 2012, Chapter 2). The two contrasting ideas on the effect of ethylene on the direction of cell expansion can be species as well as concentration dependent. In some plants, e.g. *Triticum aestivum*, low ethylene concentrations stimulate growth whereas high levels have an inhibitory effect. Almost 4 decades ago Konings and Jackson (1979) already highlighted this dual role of ethylene which was coined the *Janus face* of ethylene by Pierik *et al*. (2006) in their review of a biphasic model for growth control by ethylene.

Cell division and endocycle

Apelbaum and Burg (1972) showed that ethylene dramatically reduces cell division frequencies in meristematic tissues of *Pisum sativum* and that it is likely due to lower rates of DNA synthesis. A similar decrease was observed in prothallia of a fern, *Onoclea sensibilis*, (Edwards and Miller, 1972) which suggests that this inhibitory effect on cell proliferation might be conserved within the plant kingdom. On the other hand, studies on the early petiole ontogeny in *Nymphoides peltata* revealed that ethylene stimulates cell proliferation in a dose dependent manner (Ridge and Amarasinghe, 1984). More recent analysis of growth responses in vascular cambium of *Populus* showed that ethylene can have a positive effect on cell divisions in this

meristem leading to stimulation of xylem growth (Love *et al.*, 2009). As shown by Kazama *et al.* (2004) in *Cucumis sativus*, ethylene does not only affect cell divisions *per se*, which results in increased stomata and trichome abundance, but also alters cell polarity and division planes. Another well-known response of cells to ethylene is enhanced ploidy which results from increased number of DNA replication rounds without mitosis. This endoreduplication is, in turn, often coupled with increased cell sizes e.g. in hypocotyls of *Cucumis* (Gendreau *et al.*, 1999; Dan *et al.*, 2003) or in *Arabidopsis* petal tissue (Roeder *et al.*, 2010). The possibility of ethylene directly affecting the cell cycle has generated a wide interest in unravelling its targets in the cell cycle machinery. A study by (Skirycz *et al.*, 2011) demonstrated that ethylene acts on cell cycle progression by reducing the activity of CDKA1, possibly by post-transcriptional regulation. The exact mechanism of this interaction, though, has yet to be elucidated.

CONCLUSIONS and FORWARD LOOK

For the last decade, hyponasty has been given considerable attention as part of a general escape mechanism from unfavourable ambient conditions. Despite the broad knowledge on the functionality and hormonal regulation of ethylene-induced hyponasty (reviewed in Van Zanten *et al.*, 2010) and growing insights into the developmental alterations leading to upward petiole movement, there are still many important questions to be answered. Since hyponasty involves asymmetric cell expansion, a process that often coincides with enhanced endoreduplication, one might expect differential regulation of cell cycle-related components. Our current knowledge on the co-ordination of cell expansion during the organogenesis allows the assumption that specific gradients of the growth-regulating factors might play a role in the regulation of hyponasty. Although auxins are major regulators of hyponasty in response to light and temperature, their role in ethylene-induced hyponasty might be marginal (Van Zanten *et al.*, 2009a; Franklin *et al.*, 2011). Another group of growth stimulating hormones, BRs could serve as potential players. Experiments have demonstrated BR perception and signal transduction are crucial for the occurrence shade avoidance-related traits (Kozuka *et al.*, 2010; Keuskamp *et al.*, 2011) and that under certain conditions, BR-ethylene crosstalk is crucial for elongation responses in hypocotyls (De Grauwe *et al.*, 2005). Moreover, as shown by Gonzalez-Garcia *et al.* (2011) the progression in cell cycle in the *Arabidopsis* root meristem is BR dependent which suggests a hypothetical role for both in regulation of hyponasty. Integration of multidisciplinary approaches such as plant physiology, developmental biology, biophysics and modelling not only could help in understanding the complex mechanism of hyponasty, but any other alterations of plant architecture resulting from diverse external stresses.

ACKNOWLEDGEMENTS

We thank Ronald Leito (Imaging and Design, Utrecht University, the Netherlands)

for help with Figure1.1.

OUTLINE OF THE CHAPTERS

The focus of this thesis is the cellular basis and molecular regulation of ethylene-induced hyponastic growth in *Arabidiopsis thaliana*. In **Chapter 2** morphological changes during hyponasty are described. A detailed analysis of the epidermal cell sizes revealed that, upon ethylene treatment, longitudinal cell expansion occurs in a localized zone of the abaxial side of the petiole. This result was confirmed by the study of cortical microtubule (CMT) reorientation events in the same tissue. The region in which cells elongate exhibits a transverse orientation of CMT which stimulates longitudinal expansion. On the other hand, the adaxial side of the petiole shows a longitudinal CMT organisation, which, in turn, inhibits cell elongation in that part of the organ. Based on the cell length data a mathematical model is provided that predicts petiole angle change which is highly similar to the observed value. The subsequent chapters focus on the results from genetic screens using two different transgenic populations. The methodological C**hapter 3** describes the use of next generation Illumina sequencing technique as a way of mapping T-DNA insertions in activation-tagging lines. Identification of T-DNA loci in such lines is occasionally problematic due to the complexity of integration events. In a screen of T-DNA activation-tagging lines carrying 35S CaMV enhancers, four candidates were selected. These lines exhibited aberrant petiole angles in control conditions, ethylene and low light treatments. The genomic DNA of those lines was pooled and subjected to Illumina sequencing which resulted in identification of three out of four insertion loci. One of the selected candidates, which exhibited decreased petiole angle in all treatments and was designated *ddd1*, was studied in detail and the results are presented in **Chapter 4**. The phenotype of *ddd1* is linked to the T-DNA insertion in the intragenic region of *ROTUNDIFOLIA3* (*ROT3*) gene which encodes an enzyme involved in the synthesis of brassinosteroids (BRs). The lack of cell expansion in *ddd1* upon ethylene exposure led to the hypothesis about an interrelation of ethylene and BRs during cell elongation. This is supported by the pharmacological experiments which indicate a potential role of ethylene in sensitisation the tissue to BRs. **Chapter 5** aims to describe the involvement of ethylene response factors (ERFs) in regulation of hyponasty. A forward genetic screen of plants over-expressing ERFs resulted in a selection of several candidate *ERF* genes. Their transcriptional regulation during ethylene treatment is shown and possible scenarios of their involvement during the induction of hyponasty are discussed. **Chapter 6** describes the role of cell cycle-related mechanisms in regulation of the magnitude of hyponastic response. Over-expression of a core cell cycle gene, *CYCA2;1*, leads to enhanced hyponasty independent of endoreduplication. It is shown that ethylene inhibits the progression of a mitotic cell cycle and mathematical modelling shows that this fine-tuning process provides a subtle balance between cell expansion and cell division which controls the degree of an upward petiole movement. **Chapter 7** is a summation of research presented in this thesis and aims to discuss future perspectives regarding the insight

into the mechanisms regulating hyponasty.

CHAPTER 2

Ethylene-induced differential petiole growth in *Arabidopsis thaliana* involves local microtubule reorientation and cell expansion.

Joanna K. Polko[1], Martijn van Zanten[1], Jop A. van Rooij[2,3], Athanasius F.M. Marée[3], Laurentius A.C.J. Voesenek[1], Anton J.M. Peeters[1], Ronald Pierik[1]

[1] Plant Ecophysiology, Institute of Environmental Biology, Utrecht University, Padualaan 8, 3584 CH Utrecht, the Netherlands
[2] Theoretical Biology and Bioinformatics, Utrecht University, Padualaan 8, 3584 CH Utrecht, the Netherlands
[3] Department of Computational and Systems Biology, John Innes Centre, Norwich Research Park, Colney, NR4 7UH Norwich, United Kingdom

This chapter has been published in *New Phytologist* (2012); **193**: 339-348

SUMMARY

Hyponastic growth is an upward petiole movement induced by plants in response to various external stimuli. It is caused by unequal growth rates between adaxial and abaxial sides of the petiole, which bring rosette leaves to a more vertical position. The volatile hormone ethylene is a key regulator inducing hyponasty in *Arabidopsis thaliana*. We studied whether ethylene–mediated hyponasty occurs through local stimulation of cell expansion and if this involves reorientation of cortical microtubules (CMTs). To study cell size differences between two sides of petioles in ethylene and control conditions, we analysed epidermal imprints. We studied involvement of CMT orientation in epidermal cells using the tubulin marker line as well as genetic and pharmacological means of CMT manipulation. Our results demonstrate that ethylene induces cell expansion at the abaxial side of the- petiole and that this can account for the observed differential growth. At the abaxial side ethylene induces CMT reorientation from longitudinal to transverse, whereas at the adaxial side has an opposite effect. Inhibition of CMTs disturbed ethylene-induced hyponastic growth. This work provides evidence that ethylene stimulates cell expansion in a tissue-specific manner and that it is associated with tissue-specific changes in arrangement of CMTs along the petiole.

INTRODUCTION

The capacity to adjust to changes in the environment is a fundamental property of living organisms. To cope with environmental changes, plants evolved plasticity in a range of metabolic, physiological and morphological processes, which allow them to survive unfavourable conditions (Lambers *et al.*, 1998). Plant organ movements are

an adaptation to, mainly abiotic, stresses and have been given much attention ever since Darwinian times. Some species, such as rain tree (*Samanea saman)* (Satter *et al.*, 1974), sensitive plant (*Mimosa pudica)* (Allen, 1969) and runner bean (*Phaseolus coccineus) (*Mayer *et al.,* 1985), possess specialized structures, pulvini, which allow rapid collapse and closing movements (Kang, 1979). Tropic movements position organs directionally to the environmental stimulus, e.g. phototropism and gravitropism in which plants bend their stems towards the light or away from the gravitational vector, respectively (Firn and Digby, 1980; Morita and Tasaka, 2004; Iino, 2006). Nastic movements occur without a directional external stimulus. Among the best described examples is upward leaf movement called hyponastic growth, which is a rapid reaction of plants in response to several external stimuli (Kang, 1979; Van Zanten *et al.*, 2010). A number of plant species, including the model species *Arabidopsis thaliana* (*Arabidopsis*), use hyponasty as part of an escape mechanism from unfavourable conditions such as complete submergence (Pierik *et al.*, 2005; Voesenek *et al.*, 2006), proximity of neighbors (Ballare and Scopel, 1997; Keuskamp *et al.*, 2010) low light intensity (Millenaar *et al.*, 2005) and supraoptimal temperatures (heat) (Koini *et al.*, 2009; Van Zanten *et al.*, 2009b).

The volatile phytohormone ethylene is one of the main factors controlling hyponastic growth in *Arabidopsis* (Cox *et al.*, 2003; Cox *et al.*, 2004; Van Zanten *et al.*, 2010) and has been used as a tool to unravel the underlying control mechanisms. When plants are exposed to ethylene, it induces a marked hyponastic growth response and accordingly ethylene accumulation is required for the induction of submergence-induced hyponastic growth (Millenaar *et al.*, 2005). However, ethylene is not involved in the control of low light-induced hyponastic growth (Millenaar *et al.*, 2009) and even acts antagonistically to heat-induced hyponasty (Van Zanten *et al.*, 2009a). Cox *et al*. (2003) showed that hyponasty in flooded semi-aquatic *Rumex palustris* is driven by differential cell expansion on the abaxial side of the petiole. *R. palustris* belongs to a group of flood-tolerant species which respond to high concentrations of ethylene by cell expansion (Voesenek *et al.*, 2006) and can only respond positively to high ethylene concentrations once a minimal hyponastic leaf angle has been achieved (Cox *et al.*, 2003; Heydarian *et al.*, 2010). Most plant species, including *Arabidopsis*, are not flood-tolerant (Peeters *et al.*, 2002; Vashisht *et al.*, 2011) and typically show growth inhibition by high concentrations of exogenous ethylene (Abeles *et al.*, 1992; Pierik *et al.*, 2006; Pierik *et al.*, 2007).

Despite the increasing insight into the physiological and hormonal regulation of ethylene-induced hyponasty, we still lack fundamental knowledge about the anatomical and morphological changes that lead to the upward petiole movement in *Arabidopsis*. A clear correlation between arrangement of cortical microtubules (CMTs) and the direction of cellular expansion has been demonstrated in a variety of plant species and it is well known that growth stimulating hormones, such as auxins or gibberellins, promote a transverse alignment of CMTs which favours cell elongation (reviewed in (Shibaoka, 1994; Inada and Shimmen, 2000; Wiesler *et al.*, 2002; Foster *et al.*, 2003; Li *et al.*, 2011). Although the functional correlation between CMT

alignment and directional cell expansion is complex and still debated, it is probably also associated with CMT-mediated delivery of cellulose synthases and other proteins to the plasma membrane (Gutierrez *et al.*, 2009; Fujita *et al.*, 2011). In pea (*Pisum sativum*) ethylene induces reorientation of CMTs from transverse to longitudinal, allowing lateral cell expansion of epidermal cells and arresting longitudinal growth (Yuan *et al.*, 1994). However, it has been shown that the ethylene precursor, 1-aminocyclopropane-l-carboxylic acid, can promote the transverse orientation in light-grown *Arabidopsis* seedlings on low-nutrient medium (Le *et al.*, 2005). If hyponasty in *Arabidopsis* involves a local stimulation of cell expansion in abaxial epidermis cells, a stimulation of transverse CMTs would be predicted.

We tested whether ethylene–mediated hyponasty in *Arabidopsis* occurs through local stimulation of cell expansion and if this involves reorientation of CMTs. Since the epidermal cell layer has an important role in both driving and limiting plant growth (Savaldi-Goldstein *et al.*, 2007), we focused our study on this tissue, both on the abaxial and the adaxial sides of petioles. Our data demonstrate that ethylene primarily induces hyponastic petiole growth by driving longitudinal cell expansion specifically in a restricted abaxial region, proximal to the shoot Analysis of CMT orientation revealed that ethylene-induced reorientation from longitudinal to transverse also occurs predominantly at this proximal, abaxial side of the petiole and disruption of CMTs prevented ethylene-induced hyponasty. Together with evidence from a geometrical model, these data show that localized cell expansion drives hyponasty in *Arabidopsis*.

MATERIALS and MEHODS

Plant material and growth conditions

Arabidopsis thaliana Col-0 (N1092) was obtained from the Nottingham *Arabidopsis* Stock Centre (NASC), *35S::TUA6:GFP* (Ueda *et al.*, 1999) was a gift of Douglas Muench (University of Calgary) and *mor1-1* seeds (Whittington *et al.*, 2001) were provided by David Collings (University of Canterbury). Seeds were dark stratified for 4 days at 4ºC on filter papers. Germinated seedlings were transferred onto pots containing fertilized mixture of soil and perlite (RHP, 's Gravenzande, the Netherlands) in a 1:2 ratio and grown in a controlled growth chamber (20ºC, 70% relative humidity and 200 µmol m^{-2} s^{-1} photosynthetic active radiation (PAR); 9 h photoperiod) as described in Millenaar *et al*., 2005. Each day at the start of the photoperiod plants were automatically watered until saturation.

Ethylene treatment and petiole angle measurements

For all experiments 30 day old plants in stage 3.9 (Boyes *et al.*, 2001) were used. To allow acclimation, plants were transferred to the experimental setup (Microclima 1750 growth cabinet; Snijders Scientific, Tilburg, the Netherlands), with similar conditions to the growth chambers (described above), one day before the start of the

experiment. Ethylene (Hoek Loos, Amsterdam, the Netherlands) application started (t=0 h) 1.5 h after the beginning of the photoperiod to prevent the effects of diurnal leaf movements. The experimental setup was flushed with 1.5 ppm ethylene which is a saturating concentration for hyponastic growth (**Fig. 2.1**) with a continuous flow of 75 L h^{-1}. For the dose response experiment pure ethylene and air were mixed at different flow rates to achieve the concentrations between 10 ppb and 10 ppm. The concentrations were checked on a gas chromatograph (GC995, Synspec, Groningen, the Netherlands). Plants were placed in glass cuvettes (18 L, 8 plants per cuvette) and subjected to different concentrations of ethylene.

For petiole angle measurements, side pictures were taken with a digital camera (Canon PowerShot A530, Amstelveen, the Netherlands) at the start of the experiment and after 6 h of ethylene/control treatment. Petiole angles were measured relative to the horizontal plane, by drawing a straight line from the petiole base to the leaf base, using ImageJ software (Abramoff *et al.*, 2004). The differential angle was calculated as the difference between the angle of ethylene treated petioles and the control at the same time point (Benschop *et al*., 2007).

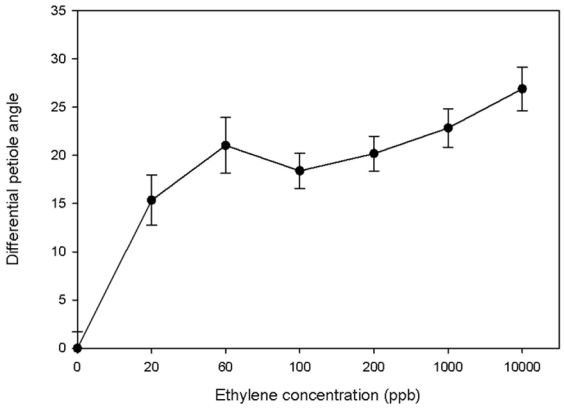

Fig. 2.1 Dose response curve for the petiole hyponasty in ethylene (means ±SE).

Epidermal cell length measurements and calculations

To obtain epidermal imprints, petioles of 1 cm or 5 mm length were covered with polyvinylsiloxane paste (type 3) (Coltene Whaledent, Langenau, Germany). After solidification, the imprint was removed and brushed with 1 layer of transparent nail polish. When dried, the film was placed on a microscopic slide and observed under an Olympus BX50WI microscope. Pictures were taken with an Olympus DP70 camera and the obtained photos were merged in Paint (Microsoft). Cell length measurements were performed with the use of a custom made macro, in KS400 software (Carl Zeiss Vision, Oberkochen, Germany). Cell width measurements were done on the first 3mm of the petiole using ImageJ software.

To allow calculations of average cell sizes relative to the distance along the petiole, each cell was assigned to a 200 µm class, depending on its position relative to the most proximal part (close to the stem) of the petiole (see **Fig. 2.2a** for details).

Disruption and visualization of CMTs

To inhibit the expansion of cells driving hyponastic growth, oryzalin (Sigma Aldrich, Zwijndrecht, the Netherlands) solution (200 µM in water and 0.2% dimethyl sulfoxide (DMSO); containing 0.1% Tween 20) was applied 24 h before the start of the experiment at the abaxial side of each petiole. To genetically disrupt the organization of CMTs, the heat-inducible *mor1-1* mutant was used (Whittington *et al.*, 2001). Plant were treated with ethylene at noninductive 20°C and inductive 30°C and after 6 h compared with controls at the corresponding temperatures.

The arrangement of CMTs was studied with *35S::TUA6:GFP* reporter lines (Ueda *et al.*, 1999). Four week-old plants were subjected to ethylene/control treatment and after 5 h CMTs of petiole epidermal cells were visualized using an inverted confocal laser scanning microscope (Leica CS SPII, 63x C-apochromat objective, excitation wavelength of 488 nm, collecting at 505-530 nm for GFP emission). Petioles were divided in 4 parts depending on their distance from the base and the abaxial and adaxial sides were observed separately. CMT areas at least twice as long as cell width were taken into account (Himmelspach and Nick, 2001). The CMTs were grouped in categories relatively to the long cell axis: transverse (0°), oblique 30°, oblique 60°, longitudinal (90°) and randomly oriented according to (Himmelspach and Nick, 2001).

Analysis of At1g20190 (*EXPA11*) expression

Col-0 petioles of 8-12 mm length were harvested, divided in quarters (**Fig. 2.3a**) and snap frozen in liquid nitrogen. RNA was isolated using the RNeasy extraction kit (Qiagen, Venlo, the Netherlands) and genomic DNA was removed with the on-column DNase digestion (Qiagen). 1 µg of total RNA was used for cDNA synthesis conducted with random hexamer primers using the SuperScript III RNase H Reverse Transcriptase kit (Invitrogen, Breda, the Netherlands). Real time RT-PCR was performed using the MyiQ Single-Color Detection System (Bio-Rad, Veenendaal, the Netherlands) with iQ SYBR Green Supermix Fluorescein (Bio-Rad) and gene specific primers (At1g20190, 5'-TGCTTTGCCTAACAACAACG-3', 5'-TCGCTCAGGGAGAAAAGAAA-3'). Relative mRNA values were calculated using the $2^{-\Delta\Delta Ct}$ method (Livak and Schmittgen, 2001) with *β-Tubulin-6* (At5g12250 5'-ATAGCTCCCCGAGGTCTCTC-3', 5'-TCCATCTCGTCCATTCCTTC-3') as an internal reference gene.

A mathematical model to predict petiole angles from cell length data

In the model, the petiole is divided into a series of consecutive sections, denoted *s*. Each section is represented by an arc with a constant radius (see **Fig. S2.1**). Since the relative size of those sections determines the spatial resolution of the model, we used sections equal in size to the classes of the cell length data (i.e. 200 µm). Each arc can be defined by its radius, which is calculated relative to the centre of the petiole cross-section, and its angle. Both can be calculated from the adaxial and abaxial section length and the petiole thickness:

$$r_s = \frac{d \cdot (i_s + j_s)}{j_s - i_s} \quad (1)$$

$$\theta_s = \frac{i_s}{r_s - \frac{d}{2}} \quad (2)$$

Where r_s = the arc radius; θ_s = the arc angle; d = the petiole diameter; i_s = the adaxial arc length; j_s = the abaxial arc length; and a positive value of r_s indicates an upward bend. The model seeks to link observed changes in cell length under ethylene treatment to the observed changes in petiole shape. To do so, we used the observed petiole shape under air treatment as a reference shape. A detailed description is given in Methods S2.1, but basically, given the known petiole shape under air treatment and a measured petiole thickness of d = 700 μm we can straightforwardly calculate the adaxial and abaxial arc length for each segment i_s and j_s. Moreover, the measured cell length data supplies us with the information needed to calculate, under air treatment, the average number of cells spanning each segment along both the adaxial and abaxial side. Using this reconstruction as the starting point, we then want to predict the petiole shape under ethylene treatment. To do so, we calculate a predicted change in length for each adaxial and abaxial section, using the measured changes in mean cell length due to the ethylene treatment (see Methods S2.1 for details and a discussion on the role of cell division). Once i_s and j_s are estimated, equations (1) and (2) allow to calculate for each segment the corresponding arc angle. The predicted petiole shape can be calculated from the arc angles in the following way. The relative x and y coordinate of the end-point of each arc are given by:

$$x_s = r_s \cdot sin(\theta_s) \quad (3)$$

$$y_s = r_s - r_s \cdot cos(\theta_s) \quad (4)$$

To correct for the curvature of the previous petiole sections, the x, y coordinates of each section are rotated using the cumulative angle of all previous sections. The initial angle (θ_0) at which petiole emerges from the shoot is also taken into account:

$$\phi_s = \sum_{t=0}^{s-1} \theta_t \quad (5)$$

$$x'_s = \cos(\phi_s) \cdot x_s - sin(\phi_s) \cdot y_s \quad (6)$$

$$y'_s = \sin(\phi_s) \cdot x_s + cos(\phi_s) \cdot y_s \quad (7)$$

Where ϕ_s is the cumulative rotation until section s and x_s' and y_s' are its rotated x,y coordinates. Finally, the absolute x and y coordinates of each section

are calculated:

$$x_s'' = \sum_{t=1}^{s} x_t' \quad (8)$$

$$y_s'' = \sum_{t=1}^{s} y_t' \quad (9)$$

Where x_s'' and y_s'' and are the absolute coordinates of the end-points of section *s*. These coordinates of each section can be used to plot the predicted petiole shape. Additional details about calibration of the model are given in the Supporting Information, Methods S1.

RESULTS

Epidermal cells at the abaxial, proximal side of the petiole elongate upon ethylene exposure

Differential petiole growth depends on unequal growth rates between the ab- and adaxial sides of an organ (Kang, 1979). In the case of hyponasty this can be achieved either by an arrest of longitudinal cell expansion at the adaxial side, by enhancement of cell elongation - at the abaxial side of a petiole, or a combination of both. To determine which of these events occur during ethylene-induced hyponasty, we first performed a comparative analysis of cell lengths using epidermal imprints of both the adaxial and abaxial part of 1 cm long petioles. To this aim, petioles of plants subjected for 10 h to a saturating concentration of 1.5 ppm ethylene (**Fig. 2.1**) and control treated plants were used since the hyponastic growth response is strongest at this time point (Millenaar *et al.*, 2005). No difference in cell length (see **Fig. 2.2a** for experimental details) was found at the adaxial surface between ethylene and control treatment (**Fig. 2.2 b**). By contrast, cell length at the abaxial side was significantly increased upon ethylene treatment in approximately first 3-4 mm from the base (**Fig. 2.2 c)** which suggests that the expansion does not occur along the entire petiole, but is restricted to the region proximal to the shoot Moreover, we observed a significant reduction of lateral expansion in this region at the abaxial side of the petiole and widening of cells of the adaxial epidermis (**Fig. S2.2a, b**). Interestingly, in the case of younger petioles (5 mm), the pattern of cell expansion differs. The increase in longitudinal cell size occurs abaxially along the entire organ (**Fig. S2.3b**). This implies that the cells involved in hyponastic growth differ between developmental stages.
Cell wall loosening proteins are well known downstream target genes involved in cell elongation in many organ types and species (Cosgrove, 2005). We examined the expression of *EXPANSIN11* (*EXPA11*) in the petiole as a marker to identify the region of elongation in ethylene exposed petioles. This gene has been shown in a genome-wide gene expression profiling study to be differentially expressed in petioles upon ethylene treatment (Millenaar *et al.*, 2006). To assess the differential expression of *EXPA11* along petiole segments, we analyzed distinct parts of the petiole (**Fig. 2.3a**). A significant increase in expression between ethylene and control treated plants

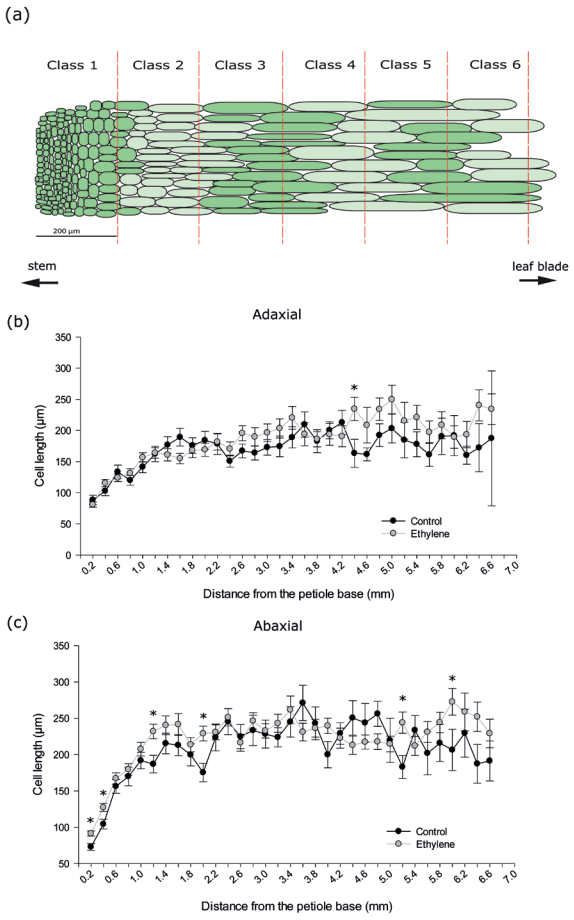

Fig. 2.2 (a) Schematic representation of the classes used for cell length calculations in the petiole epidermis. Cells are classified depending on their distance from the base of a petiole. Each class consists of 200 µm. **(b-c)** Epidermal cell length of a 1 cm petiole. Data points represent the means ±SE of cell lengths of the first 6.6 mm at the adaxial **(b)** and abaxial **(c)** side of a petiole after 10h of ethylene and control treatment. Asterisks indicate significant differences relative to the cell lengths of control treated petioles (P<0.05), n=17.

was observed in sections located on the abaxial side of the petiole (sections 2 and 4) (**Fig. 2.3b**). Strikingly, the highest up regulation was noted in the abaxial proximal region, where ethylene-induced cell elongation was observed (**Fig. 2.2c**). Taken together, these data support the hypothesis that cell expansion at the proximal abaxial petiole side, rather than inhibition of cell growth at the adaxial side, drives ethylene-induced hyponastic growth.

Ethylene induces the local reorientation of CMTs in petiole epidermis

A transverse arrangement of CMTs is associated with cell elongation, whereas the longitudinal promotes the lateral expansion (Yuan et al., 1994). To study the involvement of CMTs in ethylene-induced hyponastic growth, 24 h prior to exposing plants to ethylene, we applied oryzalin which prevents the polymerization of tubulin (Morejohn *et al.*, 1987). After 6 h of ethylene treatment, oryzalin-treated plants had a significantly lower leaf angle than mock treated plants (P<0.05). Calculation of the differential angle change (which is the difference between the mock and treat-

ed plants at the same time point) confirmed that oryzalin inhibits the hyponastic growth response to ethylene (**Fig. 2.4a**). The ±50% reduction in the response persists also after 10h of ethylene exposure when in control plants the differential response is at its maximum (data not shown).

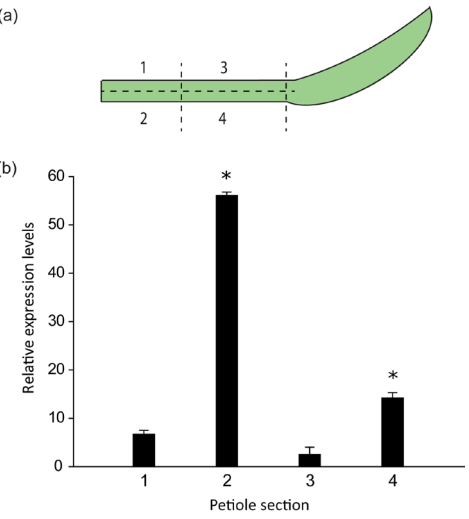

Fig. 2.3 (a) Schematic representation of petiole quarters used for studies of *EXPA11* expression. **(b)** Expression of *EXPA11* upon ethylene treatment. Petioles were divided in 4 quarters and the expression measurements done separately on each quarter. Data points represent the fold change of *EXPA11* expression (means ±SE) after 6 h of ethylene exposure relative to the control conditions and relative to *β-Tubulin-6*. Asterisks indicate significant differences between the two treatments (P<0.05).

To test the involvement of CMTs in hyponastic growth genetically, we used a temperature sensitive mutation in *MICROTUBULE ORGANIZATION1 (MOR1),* which is required for CMT organization in plants by controlling their polymerization (Whittington *et al.*, 2001). The petiole angles of *mor1-1* in mock and ethylene treated plants are similar to wild type plants at non-inductive 20°C, whereas at inductive 30°C they are significantly reduced (**Fig. 2.4b**). Together, these experiments support the hypothesis that reorientation of CMTs is required for ethylene-induced hyponasty.

To gain further insight into the involvement of CMTs in ethylene-induced hyponastic growth, we investigated CMT arrangement in the epidermal cells at both the ad- and abaxial sides of the petiole. Transgenic plants carrying a *35S::TUA6:GFP* reporter construct, which exhibits normal hyponasty in response to ethylene (**Fig. S2.4**), were subjected to ethylene and control treatments and images of the epidermal cells were taken using confocal microscopy. Ad- and abaxial sides were divided into four segments (**Fig. 2.5a**) and, subsequently, the CMT orientation was classified for each section. Figure 2.5b-c shows a typical CMT orientation in air and control conditions, whereas Figure 2.5d-e the detailed frequency of CMTs in a transverse orientation (promoting cell expansion) and longitudinal (inhibiting cell expansion) (Wilms and Derksen, 1988; Wasteneys and Williamson, 1993). The complete coverage including the intermediate (oblique 30°, 60°) and random orientations is presented in the supporting information (**Fig. S2.5**).

The orientation of CMTs in control conditions is largely transverse at the adaxial side of the petiole and longitudinal at the abaxial side. Upon ethylene treatment, these proportions change significantly in the first 3 classes with the adaxial side displaying the highest frequency of longitudinal CMTs, whereas the elongation-stimulating transverse orientation at the abaxial side increases from 5% to ±30%. Moreover, in case of the abaxial side, there is a reduction in the frequency of trans-

verse CMTs towards the leaf lamina. The sections which have the highest abundance of this type of CMTs (1ab-2ab) co-localize with the region in which we detected cell expansion and elevated levels of *EXPANSIN11* mRNA (**Fig. 2.2c** and **2.3b**).

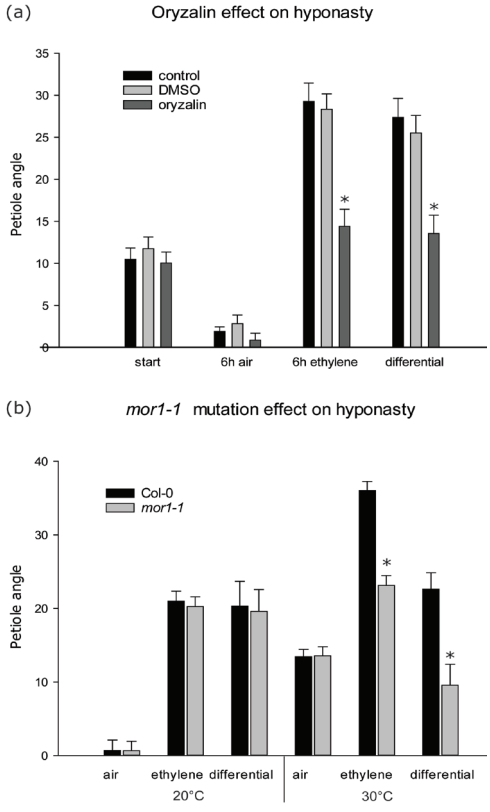

Fig. 2.4 (a) Effect of 200 µM oryzalin on petiole angle in control and 6 h ethylene treatment. **(b)** Effect of the heat-inducible *mor1-1* mutation on hyponasty. Asterisks indicate significant differences (P<0.05) relative to the angles of mock and untreated petioles (**a**) or differences between Col-0 and *mor1-1* plants **(b)** (P<0.05). Data points represent means ±SE of petiole angles, n=40-63.

To calculate whether ethylene-induced changes in longitudinal cell expansion can explain the observed hyponastic growth, we have constructed a geometrical model that predicts petiole shape from the measured ad- and abaxial cell lengths. Our model is related to the one used by Cox *et al*., 2004, which calculates the ratio between petiole angles from the difference in adaxial and abaxial petiole length. To allow prediction of local changes in petiole shape, we divided the petiole into sections and calculated the curvature for each of these sections separately. The results show that, if we normalize for the observed petiole elongation due to ethylene treatment (derived from (Millenaar *et al.*, 2005)), the hyponastic growth and resulting petiole shape are correctly predicted from the measured cell lengths (**Fig. 2.6**). The prediction is accurate to within a single degree. As an overall conclusion, the model supports the hypothesis that hyponastic growth observed during ethylene treatment is caused by increased abaxial cell elongation.

DISCUSSION

Ethylene-induced hyponastic leaf movement depends on unequal growth rates between the ad- and abaxial sides of the petiole. In this work, we investigated what event drives this process. In accordance to the observation by Cox *et al*. (2003) that hyponasty is driven by differential cell expansion in submerged *Rumex palustris*, we found that epidermal cells at the abaxial side of *Arabidopsis* petioles elongate rapidly upon ethylene treatment, while cells on the adaxial side do not. We did not assess elongation of underlying mesophyll tissues because elongation

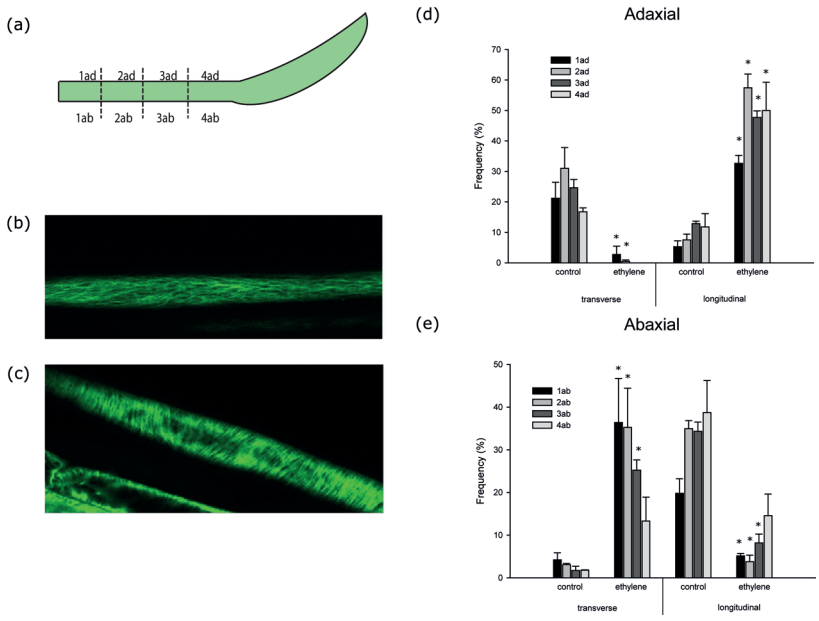

Fig. 2.5 (a) Schematic illustration of the experimental setup of CMT visualization. Petioles were divided in 4 sections, and the adaxial parts (1ad, 2ad, 3ad, 4ad) were observed separately from the abaxial (1ab, 2ab, 3ab, 4ab). The orientation of CMTs in petiole epidermal cells changes upon 6-10 h of ethylene treatment. Confocal images of a longitudinal arrangement of CMTs at the abaxial side of a petiole upon control conditions **(b)** and a transverse orientation in ethylene **(c)**. **(d-e)**Data points refer to the average number of areas representing either a transverse or a longitudinal class of CMT orientation ±SE, *n*=3. **(d)** The frequency of CMT categories at the adaxial side and **(e)** the abaxial side. Asterisks indicate significant differences ($P<0.05$) between the frequency in control and ethylene treated plants.

growth of the epidermis is considered both required for and sufficient to drive and restrict growth of underlying basal tissues (Savaldi-Goldstein *et al.*, 2007; Savaldi-Goldstein and Chory, 2008). In accordance, prediction of the resulting leaf angle matched the observed hyponastic leaf movement measured after ethylene treatment, suggesting that the observed cell elongation is sufficient to drive hyponasty. Our non-invasive method of epidermal imprints allowed studying changes in cell size without affecting the biomechanical integrity that would be distorted upon tissue excision.

The measurements performed on 1 cm petioles revealed that the expansiontakes place in the most proximal zone of the abaxial side of the petiole, approximately within the first 3-4 mm. By contrast, in younger (5 mm) petioles hyponasty is triggered by elongation of all cells along the petiole, rather than in a restricted part of the organ (**Fig. S2.3**). The latter was previously observed for ethylene-induced epinasty in castor oil plant (*Ricinus sp.*), *Datura sp.*, coleus (*Coleus sp.*) and *Hibiscus* sp. (Doubt, 1917). This observation would be consistent with the idea that petiole epidermis cells loose the capacity to elongate upon ethylene treatment when they become older.

Several lines of independent evidence strongly suggest that CMT reorganization is involved in ethylene-induced hyponastic growth. First, application of

the drug oryzalin inhibited ethylene-induced hyponasty. Oryzalin has been successfully used to assess the role of CMTs in plant development in several other studies before (Morejohn *et al.*, 1987; Baskin *et al.*, 1994). Microtubule depolimerization by oryzalin causes swelling of cells and prevents CMTs from orienting in a transverse direction, thereby arresting the anisotropic growth (Grandjean *et al.*, 2004; Hamant *et al.*, 2008). Application of oryzalin at the abaxial side of the petiole resulted in a significant reduction in the petiole angle already before induction of hyponastic growth by ethylene treatment and also significantly reduced the response to this hormone. Since the petiole inclination in response to ethylene was not completely absent, it can be concluded that besides the anisotropic growth, there may be other factors playing a role in the induction of hyponasty. A similar effect was observed in studies on apical meristem growth, where oryzalin only partially prevented the organ outgrowth (Hamant *et al.*, 2008). The additional, more specific, genetic approach involving plants carrying the temperature sensitive *mor1-1* mutation (Whittington *et al.*, 2001; Sugimoto *et al.*, 2003; Collings *et al.*, 2006) confirmed the role of CMT reorganization in the induction of hyponastic growth.

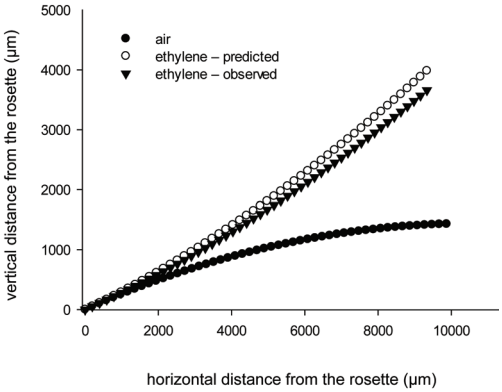

Fig. 2.6 Geometrical model predicting petiole curvature after ethylene treatment (ethylene predicted) that is consistent with observed differential growth values (ethylene observed) upon 6 h of ethylene exposure.

Subsequent visualization of CMT orientation demonstrated that two types of CMT reorientation events take place. At the adaxial side ethylene changes the alignment of CMTs from transverse (stimulating elongation) to longitudinal. However, at the abaxial side of the petiole, CMTs reorient from longitudinal to transverse, thus indicating local cell expansion. The frequency of the CMTs in the transverse category is the highest in the region located at the petiole base (proximal) and decreases towards the leaf lamina (distal). This matches our observation that ethylene-induced cell elongation is strongest at the proximal, abaxial side of the petiole and is likely sufficient for the occurrence of hyponasty.

Since cell expansion requires primary cell wall modifying agents which, according to the acid growth hypothesis, bring about the wall loosening (Rayle and Cleland, 1970; Cosgrove, 1989), we used the expression of an expansin gene as another marker for cell expansion. A previous microarray study on whole petioles showed *EXPA11* to be the only cell wall modifying enzyme differentially regulated in petioles upon ethylene treatment (Millenaar *et al.*, 2005). The spatial analysis of *EXPA11* expression, which is most strongly induced in the proximal abaxial region, is consistent with our observations on cell expansion and CMT rearrangement which also occur in the same region. It has previously been demonstrated that ethylene specifically regulates transcription of one *EXPA* gene in petioles of submerged *R.*

palustris (Vreeburg *et al.*, 2005), which was associated with enhanced physiological cell wall loosening activity. It is possible that only few specific members of this family are recruited by ethylene to adjust the plant phenotype but control at levels other than transcription is certainly also possible. To obtain a more comprehensive understanding of the involvement of cell modifying proteins in the regulation of ethylene-induced hyponasty in *Arabidopsis* it would be crucial to test expression profiles as well as knockout mutant phenotypes of more expansins and other cell wall modifying agents in future studies.

High ethylene concentrations are frequently associated with inhibitory growth effects on terrestrial plants (reviewed in Pierik *et al.,* 2006). In *Arabidopsis* this includes the triple response, characterized by an inhibition of hypocotyl and root elongation, and an exaggerated apical hook formation (Guzman and Ecker, 1990; Abeles F.B. *et al.*, 1992). In accordance, ethylene has been so far mostly implicated in promoting the longitudinal orientation of CMTs, thereby causing lateral expansion (Steen and Chadwick, 1981; Lang *et al.*, 1982; Roberts *et al.*, 1985; Soga *et al.*, 2010). Our results provide evidence of an opposite effect of high ethylene levels at the cellular level and provide support for the dual role of ethylene in growth control (Pierik *et al.*, 2006; Pierik *et al.*, 2007 and references therein). Interestingly, the ad- and abaxial sides of a petiole respond differently to ethylene treatment, making it an elegant example of asymmetric growth. This is in line with a growing number of studies, which indicate its stimulatory function, e.g. *Arabidopsis* hypocotyl elongation in light (Smalle *et al.*, 1997; Le *et al.*, 2005; Pierik *et al.*, 2006), submergence escape by petiole elongation and hyponastic growth in *Rumex palustris* (Cox *et al.*, 2003; Cox *et al.*, 2004; Vreeburg *et al.*, 2005), elongation growth in rice (Kende *et al.*, 1998) and shade-avoidance by hyponasty and internode elongation in tobacco (Pierik *et al.*, 2004). It has been reported that ethylene can stimulate endoreduplication levels in *Arabidopsis* (Gendreau *et al.*, 1999; Dan *et al.*, 2003) and cucumber hypocotyls (Dan *et al.*, 2003). Increased ploidy levels are also tightly associated with cell size in *Arabidopsis* petal tissue (Roeder *et al.*, 2010) and in peri- and mesocarp in tomato fruit (Cheniclet *et al.*, 2005; Nafati *et al.*, 2011). It is, therefore, possible that local, tissue-specific ethylene induced stimulation of cell expansion might involve control through the endocycle.

ACKNOWLEDGEMENTS

We thank J. M. H. Ammerlaan, R. A. M. Welschen and J. C. M. Granneman for technical assistance. JvR was financed by the Netherlands Consortium for Systems Biology (NCSB) which is part of the Netherlands Genomics Initiative / Netherlands Organisation for Scientific Research (NGI/NWO).

CHAPTER 3

Illumina sequencing technology as a method of identifying T-DNA insertion loci in activation-tagging *Arabidopsis thaliana* plants

Joanna K. Polko[1], Martijn van Zanten[1,2], Mohamed-Ramzi Temanni[3], Wilbert van Workum[3], Sven Iburg[1], Ronald Pierik[1], Laurentius A.C.J. Voesenek[1], Anton J.M. Peeters[1]*

[1] Plant Ecophysiology, Institute of Environmental Biology, Utrecht University, Padualaan 8, 3584 CH Utrecht, the Netherlands
[3] ServiceXS B.V., Plesmanlaan 1d, 2333 BZ Leiden, the Netherlands

Modified version of this chapter has been accepted for publication in *Molecular Plant*

SUMMARY

T-DNA activation-tagging method has been used to identify novel gene functions in *Arabidopsis thaliana*. Its popularity and usefulness are expressed by the possibility of isolating dominant phenotypes and characterizing genes belonging to large families where redundancy is a common phenomenon. Standard ways of mapping T-DNA insertions in activation-tagging lines include, *e.g*. plasmid rescue or Thermal Asymmetric Interlaced–PCR (TAIL–PCR). In some cases, however, these methods fail to provide satisfactory results, usually due to post-insertional rearrangements within T-DNA and/or plant DNA. Here, we describe the use of the next generation sequencing technique to identify T-DNA insertion loci. Genomic DNA of four T-DNA activation-tagging lines, selected for their aberrant hyponasty phenotypes, was pooled and subjected to Illumina sequencing. The bioinformatics analysis and further PCR confirmation enabled us to identify three out of four insertion loci. Our results show that next generation sequencing methods can be successfully used to identify problematic activation-tagging candidates.

INTRODUCTION

Forward and reverse genetics provide successful means to identify novel components of genetic pathways and to characterize functions of genes. Reverse genetics aims to isolate mutations in known sequences and, in plants, include methods such as homologous recombination, gene silencing, random mutagenesis, TILLING or ectopic expression (reviewed in Alonso and Ecker, 2006). Forward genetic screens are a common unbiased tool in which initially selected phenotypes are linked back to a gene linked to the expressed phenotype. In *Arabidopsis thaliana* forward genetic screens using T-DNA activation tagging methods are a common way of identifying genes (crucial) in various biological processes. Vectors with cassettes containing multimerised copies of 35S promoters derived from cauliflower mosaic virus (35S

CaMV) have been widely used as means of achieving dominant, over-expression, gain of function phenotypes (Hayashi *et al.*, 1992; Kardailsky *et al.*, 1999; Weigel *et al.*, 2000; Nakazawa *et al.*, 2003). They allow studying members of large gene families which are often functionally redundant and, therefore, hard to identify in loss of function screens. Another advantage is that these gain-of-function mutations are dominant and able to be recognized already in T_1 generations (Ostergaard and Yanofsky, 2004). Plasmid rescue and thermal asymmetric interlaced PCR (TAIL-PCR) (Liu *et al*., 1995) have been effectively employed in order to recover *Arabidopsis* sequences flanking T-DNA insertions (Behringer and Medford, 1992; Mandal *et al*., 1993; Weigel *et al*., 2000; Nakazawa *et al*., 2003). In some instances, however, these two techniques do not yield expected results, possibly due to potential sequential complexities following integration events (Palin *et al*., 1998; McElver *et al*., 2001).

Illumina sequencing belongs to the next generation sequencing techniques and its popularity has been growing throughout the last years. It incorporates an attachment of single-stranded DNA fragments of 300-500 bases to a solid flow-cell using adapters. The DNA-adapter hybrid subsequently bends over, forming a "bridge" which serves as a template for PCR amplification. After a series of complementary strand formation events, a cluster of approximately 1000 copies is formed. Consequently, these clusters are sequenced in a parallel manner which is possible due to attachment of fluorescent reversible chain terminator nucleotides (Bentley, 2006; Morozova *et al*., 2008; Quail *et al*., 2008). Each sequencing reaction bears reads of 50-75 bases. Illumina sequencing has been widely used in identifying, *e.g*. transposon insertions in *Zea mays* (Williams-Carrier *et al.*, 2010), obtaining large transcript sequences in *Sesamum indicum* (Wei *et al.*, 2011) and in sequencing of chloroplast genomes (Cronn *et al.*, 2008) .

In this chapter, we present how the Illumina technique can be used to identify T-DNA loci in activation-tagging *Arabidopsis* plants. We conducted a genetic screen for plants with aberrant petiole angle in ethylene and low light, two factors that induce upward leaf movement, called hyponasty, which resulted in selection of four candidate lines. The standard techniques of plasmid rescue and TAIL-PCR failed to provide insertion loci in these lines. The Illumina sequencing method performed on a pool of genomic DNA from selected candidates provided a set of potential breakpoints. Subsequently, we confirmed three out of four T-DNA insertion sites responsible for the hyponasty-related phenotypes.

MATERIALS and METHODS

Plant material and growth conditions

Arabidopsis thaliana Col-7 (N1092) and activation tagged lines (N21991, N23153 (Weigel *et al*., 2000) were obtained from the Nottingham Arabidopsis Stock Centre (NASC). Before potting, seeds were dark stratified for 4 days at 4°C on moisturized filter papers. Germinated seedlings were transferred onto pots containing fertilized

mixture of soil and perlite (RHP, the Netherlands) in a 1:2 ratio and grown in a controlled growth chamber (20°C, 70% relative humidity and 200 µmol m^{-2} s^{-1} photosynthetic active radiation (PAR); 9 h photoperiod) as described in Millenaar *et al*., 2005. At the start of each photoperiod plants were automatically watered until saturation.

Screening, ethylene treatment and petiole angle measurements

17.500 plants carrying the Cauliflower Mosaic Virus (CaMv) 35S enhancer (Weigel e*t al*,. 2000) were screened. Plants were examined for initial petiole angle at the start of the screen, after 6h ethylene treatment and overnight recovery, and after 6h of low light exposure. Candidates selected in the screen were designated according to the principle: '*S*' was used for similar, '*E*' for enhanced and '*D*' for decreased in i) initial petiole angle, ii) angle after ethylene treatment and iii) petiole angle after low light treatment respectively. For classification as '*E*' or '*D*', an arbitrary threshold of minimal 5 degrees was set. Plants with petiole angles within 5 degrees of difference were assigned to the '*S*' category.

For all experiments 30 day old plants in stage 3.9 (Boyes *et al*., 2001) were used. To allow acclimation, one day before the start of the experiment plants were transferred to the experimental setup with similar conditions to the growth chambers (Microclima 1750 growth cabinet; Snijders Scientific, Tilburg, the Netherlands). Ethylene (Hoek Loos, Amsterdam, the Netherlands) application started (t=0 h) 1.5 h after the beginning of the photoperiod. The experimental setup was flushed with 1.5 ppm ethylene with a continuous flow of 75 L h^{-1}. For low light experiments the photosynthetic active radiation (PAR) levels were reduced to 20 µmol m^{-2} s^{-1} without changing light quality.

At the start of the experiment and after 6 h of ethylene/control treatment side pictures of plants were taken with a digital camera (Canon PowerShot A530). Petiole angles were measured relative to the horizontal plane using ImageJ software (http://rsbweb.nih.gov/ij/; Abramoff *et al*., 2004). The differential angle was calculated as the difference between the angle of ethylene treated petioles and the control at the same time point (Benschop *et al*., 2007).

Segregation analysis

Candidate lines containing a phosphinothricin resistance gene (BAR) (Weigel *et al*., 2000) were crossed with wt Col-7 plants as a female receiver and self-pollinated. The F_2 progeny was sown on agar plate containing 8 gL^{-1} plant agar (Duchefa, Brussels, Belgium), 0.22 g L^{-1} Murashige-Skoog (Duchefa) and 50 µg mL^{-1} phosphinothricin/ glufosinate ammonium (also known as BASTA®) (Duchefa). Following sowing seeds were dark stratified for 4 days at 4 °C and then transferred to a growth chamber with conditions described above. The survival rates were scored after 3 weeks.

Illumina sequencing

Equimolar concentrations of genomic DNA of four individual activation-tagged lines (*SDS2*, *SDS4*, *DDD1* and *EDD1*) were pooled. One sample preparation according to the Illumina protocol "Preparing Samples for Paired-End Sequencing" was performed (http://tucf.org/htseq_Paired-End_Seq_SamplePrep_1005063_RevA.pdf). The sample was clustered on one lane of a flow cell for sequencing on the Genome Analyzer IIx (GAII; Illumina, San Diego, USA) according the Paired-End Sequencing protocol. The quality and integrity of the DNA sample(s) was analysed by gel electrophoresis on a 0.6% agarose gel. Sample quality met the requirements for sample preparation. The Illumina 'Paired-End DNA sequencing Sample Prep Kit (cat# 1001809)' was used to process the sample. Fragmentation of the DNA by nebulisation, ligation of sequencing adapters, and PCR amplification of the resulting product was performed according the Illumina protocol 'Preparing Samples for Paired-end Sequencing (1005063 Rev. A)'. The quality and yield after sample preparation was measured with Lab-on-a-Chip analysis. The size of the resulting product was consistent with the expected size of approximately 300 bp after excision from a 2% agarose gel. The sample was sequenced on the GAII. Clustering and DNA sequencing using the GAII was performed according manufacturer's protocols. A total of 8 pmol DNA was used. Two sequencing reads of 51 cycles each using the Read 1 sequencing and Read 2 sequencing primers were performed with the flow cell.

PCR and RT-PCR

For PCR analysis leaves were harvested and snap frozen in liquid nitrogen. Genomic DNA isolation was carried out using the Nucleon Phytopure DNA extraction kit (GE Healthcare/Amersham, Den Bosch, the Netherlands). PCR was conducted on 100 ng of DNA with TDNA and *Arabidopsis* specific primers (Table 3.1). For RT-PCR RNA from 8-12mm petioles which had been harvested and snap frozen in liquid nitrogen was isolated using the RNeasy extraction kit (Qiagen, Venlo, the Netherlands) and genomic DNA was removed with the on-column DNase digestion (Qiagen). 1 µg of total RNA was used for cDNA synthesis conducted with random hexamer primers using the SuperScript III RNaseH- Reverse Transcriptase kit (Invitrogen, Breda, the Netherlands). Real time RT-PCR was performed using the MyiQ Single-Color Detection System (Bio-Rad, Veenendaal, the Netherlands) with iQ SYBR Green Supermix Fluorescein (Bio-Rad) and gene specific primers (Table S3.1). Relative mRNA values were calculated using the $2^{-\Delta\Delta Ct}$ method (Livak and Schmittgen, 2001) with *β-Tubulin-6* (At5g12250 5'-ATAGCTCCCCGAGGTCTCTC-3', 5'-TCCATCTCGTCCATTCCTTC-3') as an internal reference gene.

RESULTS and DISCUSSION

Screening and selection of candidate lines

To identify molecular components during hyponastic growth in *Arabidopsis thaliana*

(for reviews on this topic see Van Zanten *et al.*, 2010 and Polko *et al.*, 2011), we conducted a forward genetic screen on a population of plants carrying a tetramer of 35S CaMV enhancer (pSKI015) (Weigel *et al.*, 2000). Prior to the actual mutant screen, we verified that low light-induced hyponasty would not be affected by a previous ethylene treatment the day before. Indeed, ethylene treatment did not interfere with the response to low light the following day (data not shown). Plants were screened for altered petiole angles at the start of the experiment (initial), after 6h of ethylene exposure (6h ethylene) and after 6h in low light conditions (6h low light). A set of candidate lines with aberrant petiole angle phenotypes was isolated and classified. Lines addressed in this study were designated *SDS2*, *SDS4, DDD1*, and *EDD1* (**Fig. 3.1a-e**).

Fig. 3.1. Visual phenotypes of activation-tagged lines selected in a screen.

SDS2 and *SDS4* have a wt-like initial petiole angles and decreased angles in ethylene, line *DDD1* exhibits decreased hyponasty at the start of the experiment and in both treatments, and line *EDD1* has a constitutively high petiole angles but decreased responses to ethylene and low light (**Fig 3.2a**). To verify the number of T-DNA insertions in each line, we back-crossed them with wt Col-7 and scored the phosphoinotricin resistance in self-pollinated F_2 progeny. Since herbicide resistance is a dominant trait, the Mendelian segregation (75% resistant, 25% non-resistant) would correspond with one T-DNA insertion in each line. As shown in Fig. **3.2b**, 75% of plants in *SDS2, SDS4* and *DDD1* are resistant. The lack of phosphoinotricin resistance in *EDD1* is not likely due to loss of insertion since the amplification of T-DNA sequences in *EDD1* gave positive results (data not shown). It is possible that the selection marker site has been silenced in subsequent generations. Silencing of exogenous DNA through methylation is a known in case of retrotranspozons (Suzuki *et al*., 2007) or siRNA-mediated silencing of T-DNA (Schubert *et al*., 2004; Daxinger *et al*., 2008).

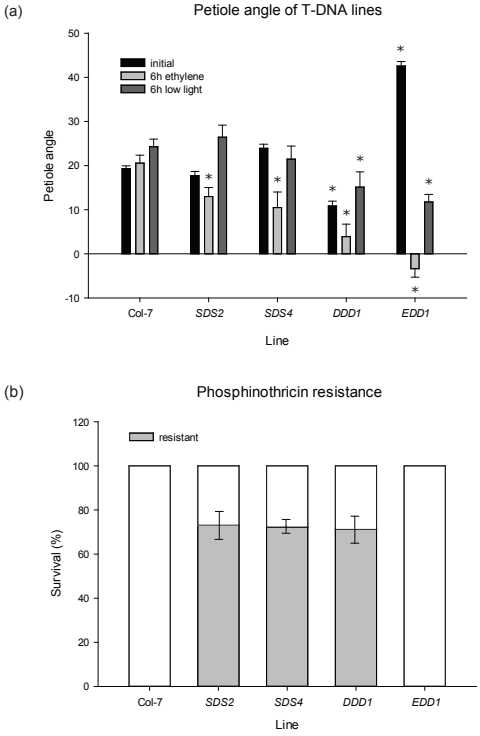

Fig. 3.2. (a) Peiole angles of activation-tagged candidate lines. The initial petiole angle is an absolute angle; 6h ethylene and 6h low light indicate the differential petiole angle (difference between petiole angle in ethylene/low light exposure and control treatment) n>15 ± SE. Asterisks indicate significant differences in petiole angle between an activation-tagged line and wt Col-7 in the same treatment (P<0.05). **(b)** phosphoinothricin resistance scores in F2 progeny of backcrosses between each activation-tagged line and wt Col-7.

Illumina sequencing and data analysis

To identify TDNA insertion loci in *SDS2*, *SDS4, DDD1* and *EDD1,* we followed a novel approach using Illumina next generation sequencing. Genomic DNA of four lines was pooled and subjected to sequencing as described in "Materials and Methods". 50 bp paired reads with 204 +/- 63 bases insert size were used. The total number of reads

in the lane was 20,419,624 reads. The data generated by the GAII was a set of 2 files; one file contained the forward reads and the second file contained the reverse reads. The files were in a proprietary format called SCARF (Solexa compact ASCII read format). First, the files were converted to the standard/Sanger FASTQ format. Subsequently, the forward and reverse reads were aligned separately to the reference genome of T-DNA (pSKI015) and *Arabidopsis* using the Bowtie aligner (Langmead *et al*. 2009). Aligned reads were stored and for each sequence the chromosome, the position and the orientation was added. Unaligned reads were stored in a different fastq file. The aligned reads were then paired based on their ID using R programming language (R Development Core Team. 2009). As shown in Fig. **3.3a**, three types of pairing are possible: *Arabidopsis*/*Arabidopsis*, T-DNA/T-DNA, and *Arabidopsis*/T-DNA. The detection of T-DNA insertion locus is possible based on the latter pairing (*Arabidopsis*/T-DNA). The unaligned reads may be of interest, as some reads can map over the breakpoint and thus be composed of a bases coming from T-DNA and the other bases coming from *Arabidopsis*. Such reads, if identified, would give the exact location of the breakpoint. In order to detect such sequences, unaligned reads were blasted against reference genomes and sub-sequences of the same read that map both to *Arabidopsis* and T-DNA were selected and analysed. The pipeline used

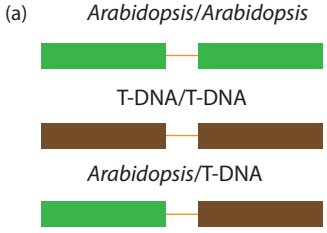

Fig. 3.3. (**a**) Illustration of the possible reads obtained with Illumina sequencing. Reads can cover either only Arabidopsis sequences, only T-DNA sequences or both Arabidopsis and T-DNA sequences harbouring a potential breakpoint. (**b**) Breakpoint 1- a read mapping over the breakpoint.

(b)

T-DNA *Arabidopsis*

ACTCATTGCTGATCCATGTAGAT CTCTACATGTACGTCCACCACGTCAT

for searching the *Arabidopsis*/T-DNA paired reads detected three majors breakpoints having two or more supporting paired-reads and 7 breakpoints with only one supporting paired-read (**Table S3.2**). For the breakpoint 1 we also found a read which maps over the breakpoint (**Fig. 3.3b**; T-DNA in brown, *Arabidopsis* in green). The position of this breakpoint is: 7742 (T-DNA)/ 17189850 (*Arabidopsis*).

Sequencing confirmation

The next step involved a validation of the sequencing results and identification of particular breakpoints in lines selected in our screen. Based on the sequences from pair-reads (**Table S3.2**), we designed primers and conducted a PCR on each candidate line separately. To amplify a substantial part of DNA primers were designed at

~200bp up- and downstream from each breakpoint. The PCR amplification yielded satisfactory results for three out of four lines: *SDS2*, *SDS4*, *DDD1*. The results are presented in **Table 3.1**.

Breakpoint 1, detected on chromosome 4, in the intragenic region of At4g36380, corresponds with line *DDD1*. Breakpoint 2 is situated on chromosome 2, in the intragenic region of At2g20050 and corresponds with line *SDS2*. Breakpoint 3 was detected line *SDS4* on chromosome 1, in the intergenic region between At1g60050 and At1g60060. We were not able to identify the insertion locus for *EDD1*. One possibility is that that the T-DNA insertion in *EDD1* is situated in a repeat area and thus difficult to detect. Following the confirmation, we studied expression of genes in the vicinity of the T-DNAs (**Fig. 3.4**).

RT-Q-PCR analysis revealed that in *DDD1* transcript levels of *ROTUNDIFOLIA3* (*ROT3*; At4g36380) were substantially lower in comparison to wt Col-7 plants. Two more genes in the vicinity - *PURPLE ACID PHOSPHATASE 25* (*PAP25*; At4g36350) and D-*2-HYDROXYGLUTARATE DEHYDROGENASE* (*D2HGDH*; At4g36400) had slightly but significantly disturbed levels of mRNA (**Fig. 3.4a**). In the case of *SDS2*, the insertion resulted in lower transcript levels of *T2G17.15* (At2g20050) compared to Col-7. Also, mRNA levels of two other genes - *T2G17.13* (At2g20070) and *T2G17.10*, basic helix-loop-helix (bHLH) DNA-binding superfamily protein (At2g20100) were down regulated (**Fig. 3.4b**). The third breakpoint in *SDS4* resulted in a tremendous (~550 times) up regulation of mRNA levels of At1g60060 which encodes the serine/threonine-protein kinase WNK (With No Lysine)-related protein. The expression of other genes flanking the insertion site was not substantially affected (**Fig. 3.4c**). These data illustrate various possible scenarios of T-DNA integration in the Arabidopsis genome. In principle, the presence on 35S enhancers lead to an over-expression of gene(s) flanking the insertion but might also, when inserted in the intragenic region, result in a knock-down of a gene. In this case of just 4 phenotypically selected lines the number of intragenic insertions is high.

Our results show that Illumina sequencing can serve as a method to successfully map T-DNA insertions and potentially other insertion constructs in *Arabidopsis*. We were able to map T-DNA in three out of a pool of four candidates. We do not know what the limit of number in the pool might be, but it may be that with longer reads more resolution can be obtained and therefore more lines could be screened in one sequencing event. With the constant improvement of the next generation sequencing techniques which provide longer reads, identification of more difficult inserts will soon be possible.

Table 3.1. Localisation of detected breakpoints in activation-tagged lines; position (+) corresponds with forward reads and (-) with reverse reads; primers (forward; Fwd, and reverse; Rev) used for confirmation of the sequencing and a corresponding activation-tagged line.

Breakpoint	Position (+)	Position (-)	Primer T-DNA	Primer *Arabidopsis*	Line
Breakpoint 1	17189850	7742	TAACGCTGCGGACATCTACA (Rev)	CTCCCAATTCCAATTTACGC (Fwd)	*DDD1*
Breakpoint 2	4272	851419	CGTCTTCAAAGCAAGTGGA (Fwd)	TGGAATCACTAACGAGTATGACAA (Rev)	*SDS2*
Breakpoint 3	22137398	7736	TAACGCTGCGGACATCTACA (Rev)	TGCAAGTTGCTAACCTTTTTGA (Fwd)	*SDS4*

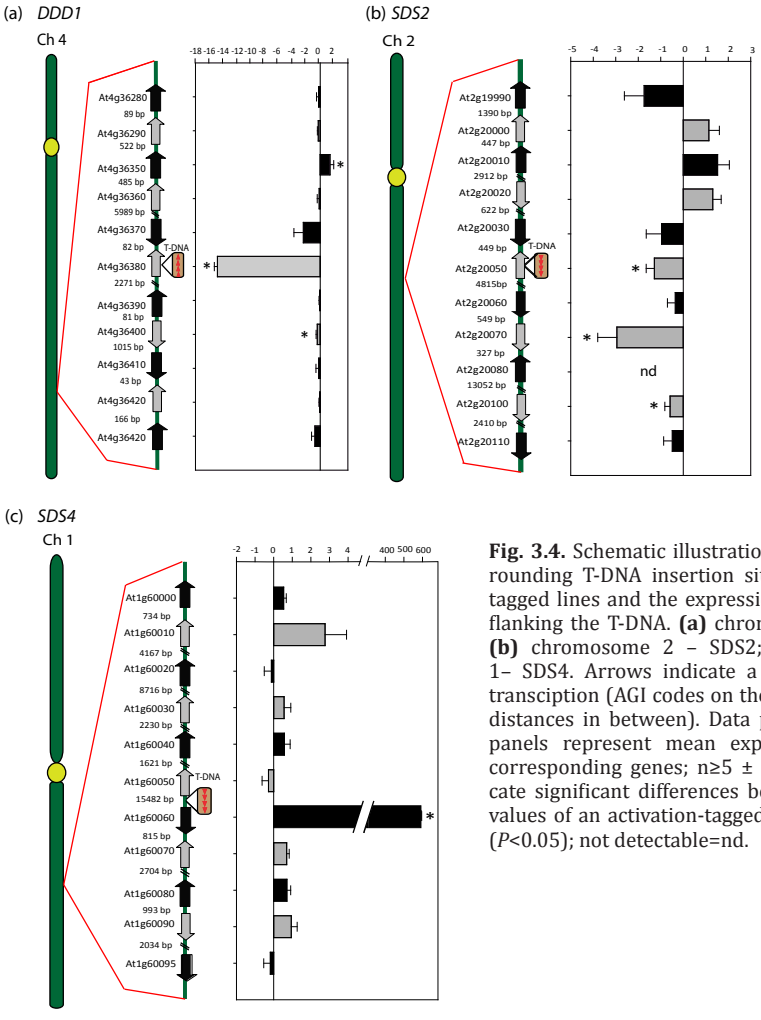

Fig. 3.4. Schematic illustration of the locus surrounding T-DNA insertion site in 3 activation-tagged lines and the expression values of genes flanking the T-DNA. **(a)** chromosome 4 - DDD1, **(b)** chromosome 2 – SDS2; **(c)** chromosome 1– SDS4. Arrows indicate a direction of gene transciption (AGI codes on the left hand side, bp distances in between). Data points in the right panels represent mean expression values of corresponding genes; n≥5 ± SE. Asterisks indicate significant differences between expression values of an activation-tagged line and wt Col-7 (P<0.05); not detectable=nd.

CHAPTER 4

Ethylene promotes upward leaf movement through interaction with brassinosteroids

Joanna K. Polko[1], Ronald Pierik[1], Martijn van Zanten[2], Laurentius A.C.J. Voesenek[1] and Anton J.M. Peeters[1]

[1]Plant Ecophysiology, Institute of Environmental Biology, Utrecht University, Padualaan 8, 3584 CH Utrecht, the Netherlands
[2]Molecular Plant Physiology, Institute of Environmental Biology, Utrecht University, Padualaan 8, 3584 CH Utrecht, the Netherland

SUMMARY

Hyponastic leaf growth is an example of the ability of plants to cope with adverse environmental conditions. It is an active repositioning of organs, mainly petioles and leaves, which occurs as a consequence of differential growth. The exact hormonal regulation depends on the signal that initiates hyponasty. Ethylene is a central player in the regulation of the hyponastic response during flooding, heat or shade and its application alone can successfully mimic hyponastic responses. In *Arabidopsis thaliana* ethylene promotes epidermal cell expansion in a proximal zone of the abaxial side of a petiole which leads to leaf movement. Brassinosteroids (BRs) are a class of phytohormones involved in many developmental processes including organ growth, cell expansion, cell division and responses to abiotic and biotic stresses.
Here, we tested the interaction between BRs and ethylene in the control of hyponastic growth and provide evidence that response to BRs is a crucial step in the regulation of ethylene-induced hyponasty. We show that BR biosynthesis mutants have reduced differential growth and that pharmacological inhibition of BR synthesis leads to similar reduction in petiole angle. Analysis of epidermal imprints together with gene expression studies indicate a role for BRs in regulating longitudinal cell expansion at the abaxial side of the petiole during hyponasty.

INTRODUCTION

Upward petiole movement, referred to as hyponastic growth, is an active response of several plant species to adverse environmental conditions such as flooding, elevated temperatures or dense canopies (Ballaré and Scopel, 1997; Cox *et al*., 2003, Koini *et al*., 2009; Keuskamp *et al*., 2010). Hyponasty is an increase in petiole angle which is an outcome of unequal growth rates between two (ad- and abaxial) sides of the organ. Ethylene-induced hyponasty has been given much attention due to the discovery that ethylene is a key player in the regulation of hyponasty in *Arabidopsis* and that exogenous ethylene application on its own rapidly induces plants to show hy-

ponastic growth (Cox *et al.*, 2003; Millenaar *et al*., 2005). The cellular mechanism of this nastic movement consists of enhanced longitudinal cell expansion at the abaxial side of the petiole which requires the reorientation of cortical microtubules and recruitment of cell wall modifying proteins in a region proximal to the rosette (Cox *et al*., 2003, Polko *et al*., 2011, Chapter 2). A number of studies have contributed to today's understanding of the regulation and significance of ethylene-induced hyponasty and have indicated an interaction between ethylene and other plant hormones (*i.e.* auxin, ABA and GA; reviewed in van Zanten *et al.*, 2010).

Brassinosteroids (BRs) are a family of plant steroid hormones involved in many, generally growth promoting, processes. Initially purified from *Brassica napus* pollen (Mitchell *et al.*, 1970; Grove *et al.*, 1979), they are widespread among the entire plant kingdom and present in various organs (Rao *et al.*, 2002). The highest concentrations of BRs, however, are found in young tissues, reproductive organs, seeds and fruits (reviewed in Symons *et al.*, 2008). The impressive range of developmental processes they control include cell elongation and division, cell cycle progression, vascular differentiation and fruit ripening (Szekeres *et al*., 1996; Altmann, 1998; Hu *et al*, 2000; Nakaya *et al*., 2002; Cano-Delgado *et al*., 2004; Symons *et al*., 2006; Gonzalez-Garcia *et al.*, 2011). Therefore, BRs are an integral part of several signaling cascades during biotic and abiotic stress responses (reviewed in Krishna, 2003). Since their discovery and purification from plant tissue, a great number of studies expanded our knowledge and understanding of both regulatory processes they are involved in and their signal transduction (Kim *et al*., 2010). In contrast to animal steroids, which bind to nuclear receptors (Mangelsdorf *et al.*, 1995), the perception of BRs starts at the plasma membrane by their binding to the receptor-like kinase BRASSINOSTEROID INSENSITIVE (BRI1). This initiates a signal transduction cascade leading to activation of several transcription factors controlling gene expression (reviewed in Clouse, 2011) involved in e.g. ion exchange, water uptake and cell wall modifications which lead to cell expansion (Zhang *et al.*, 2005; Xie *et al.*, 2011). During the plant life cycle BRs interact with other phytohormones. Due to their general growth-stimulating function in plant development they interact with auxin having even the same molecular targets (Halliday *et al*., 2004). Despite the differences in the complexity of downstream signaling, brassinosteroids and auxin share a considerable number of responsive genes, e.g. from the *Auxin/Indole-3-Acetic Acid* (*Aux/IAA*) *or Small Auxin Up RNAs (SAUR)* gene families (Nakimamura *et al.*, 2003; Goda *et al.*, 2004; Nemhauser *et al.*, 2004; Nakamura *et al.*, 2006; Vert *et al.*, 2008). In contrast to increasing knowledge regarding potential nodes in the auxin-BR crosstalk, relatively few studies have focused on a functional interdependence of these two hormones. These particularly include a crosstalk between auxin and BRs in responses to light cues (Kozuka *et al.,* 2010; Keuskamp *et al.,* 2011). De Grauwe *et al*. (2005) have shown an brassinosteroid-auxin interplay in development of the apical hook in dark-grown seedlings which changes in light. Furthermore, mutant and pharmacological analyses demonstrated that exogenous application of the ethylene precursor, 1-aminocyclopropane-1-carboxylic acid (ACC), also induces expression of

BR-related genes, suggesting an elaborate network between these three hormones. Ethylene and brassinosteroids have been shown to affect one another in various ways (Schlagnhaufer and Arteca, 1985; Arteca *et al.*, 1983). More recent, studies attempting to elucidate this interaction have shown that brassinopride, a novel inhibitor of BR action, additionally promotes ethylene synthesis (Gendron *et al.*, 2008). In a study by Deslauriers *et al*. (2010) *FERONIA* (*FER*), a gene typically responsible for male-female gametophyte interplay during pollen tube reception (Huck *et al*., 2003), was shown to function as a node in the inhibitory interaction between BRs and ethylene during hypocotyl elongation in darkness. Interestingly, BR also acts in crosstalk with ethylene during thermotolerance and salt stress (Divi *et al.*, 2010).

We recently performed a screen to isolate activation-tagged lines affected in petiole hyponasty in *Arabidopsis*. One of the lines, showing reduced hyponasty in ethylene treatment, is here reported to be allelic to a mutant in *ROTUNDIFOLIA3* (*ROT3*), a BR biosynthesis-related gene. We report that *rot3* mutants have a reduced petiole hyponasty in ethylene and that this reduction is reflected at the cellular level. We further provide evidence for BR importance in the occurrence of hyponastic growth. We conclude that brassinosteroids control differential cell expansion during ethylene-induced hyponasty.

MATERIALS and METHODS

Plant material and growth conditions

Arabidopsis thaliana Col-0 (N1092), Col-7 (N3731), activation tagged lines (N21991, N23153 (Weigel *et al.*, 2000), *rot3-1* mutant (N3727), SALK 043566C (N670634) and SALK 003225C (N671057) were obtained from the Nottingham Arabidopsis Stock Centre (NASC; Stock numbers between brackets). SALK lines belong to a homozygous collection and were confirmed by a PCR amplification with T-DNA-specific (LBb1.3) primer and At-specific (RP) primer, as described on http://signal.salk.edu/. Seeds were dark stratified for 4 days at 4ºC on moist filter papers and thereafter kept in light for three days. Seedlings were subsequently transferred to pots containing a fertilized mixture of soil and perlite (RHP,'s-Gravenzande, the Netherlands) in a 1:2 ratio and grown in a growth chamber under controlled conditions (20ºC, 70% relative humidity and 200 µmol m^{-2} s^{-1} photosynthetic active radiation (PAR); 9 h photoperiod) as described by Millenaar *et al*., 2005. For hypocotyl experiments seeds were surface sterilized in an ethanol : bleach solution (8:2), sown on agar plates containing 8 g L^{-1} agar and 0.22 g L^{-1} Murashige and Skoog medium (both Duchefa, Haarlem, the Netherlands), dark-stratified for 4 days at 4ºC and transferred to the indicated growth cabinets.

Ethylene and green shade treatment

30 day-old plants in stage 3.9 (Boyes *et al.*, 2001) were used for all experiments. One day before the start of the treatment plants were transferred to the experimen-

tal setup with similar conditions to the growth chambers (Microclima 1750 growth cabinet; Snijders Scientific, Tilburg, the Netherlands). To exclude a rapid downward petiole movement due to diurnal leaf oscillation, ethylene (Hoek Loos, Amsterdam, the Netherlands) application always started (t=0 h) 1.5 h after the beginning of the photoperiod. The setup was flushed with 1.5 μL L^{-1} ethylene with a continuous flow of 75 L h^{-1}. The control treatment was done in the same experimental cabinet. For green shade experiments, Lee 122 Fern Green (Lee Hampshire, United Kingdom) filters were applied, reduced the photosynthetic active radiation (PAR) to 65 μmol m^{-2} s^{-1}, R/FR to 0.19 and blue light to < 2 μmol m^{-2} s^{-1}. The control experiment was carried out under white light at a PAR of 140 μmol m^{-2} s^{-1} and R/FR of 2.1. For ethylene treatment of seedlings, after 4 days in 4°C plates were uncovered and placed in the experimental setup flushed with 5 μL L^{-1} ethylene at a continuous flow of 75 L h^{-1}. High humidity (95%) prevented agar plates from drying out. Hypocotyl length was measured using ImageJ software (Abramoff *et al.*, 2004).

Petiole angle measurements and camera setup

Side pictures were taken (Canon PowerShot A530) at the start of the experiment, after 6 h of ethylene/control treatment, or in case of green shade experiment - after 24h of treatment. Petiole angles were measured relative to the horizontal plane and the rosette base, using ImageJ software (Abramoff *et al.*, 2004). The differential angle was calculated as a difference between the angle of ethylene treated petioles and the control at the same time point (Benschop *et al.*, 2007). For petiole kinetics measurements, we used a custom-built digital camera system as described in Millenaar *et al*. (2005). Plants were placed in glass cuvettes and side pictures were taken every 10 min for 24h in constant light. Petiole angles were measured with the use of a custom made macro (KS400, Carl Zeiss Vision, Hallbergmoos, Germany).

Epidermal cell length measurements and calculations

Cell length measurements were performed on epidermal imprints as described in Chapter 2 with the use of a custom made macro in KS400 software (Carl Zeiss Vision, Oberkochen, Germany). To allow calculations of average cell sizes relative to the distance along the petiole, each cell was assigned to a 200 μm class, depending on its position relative to the most proximal part (close to the stem) of the petiole (Polko *et al.*, 2011).

Pharmacological treatments

For the hypocotyl experiments, seeds were sterilized as described above and the agar medium was supplemented with 1-aminocyclopropane-1-carboxylic-acid (ACC) (Sigma Aldrich, Zwijndrecht, the Netherlands), brassinazole (Brz) (TCI Europe, Hannover, Germany) or epi-brassinolide (BL) (Sigma Aldrich, Zwijndrecht, the

Netherlands).

For petiole experiments 100µM Brz solution (TCI Europe, Hannover, Germany) containing 0.1% DMSO and 0.1% Tween 20 was applied on the abaxial side of each petiole. The control treatment contained 0.1% DMSO and 0.1% Tween 20. To ensure the penetration of the tissue by Brz, the application was conducted 24, 20 and 16 hours before the start of the experiment. The abaxial sides of petioles were brushed with the solution and side pictures were taken at the beginning of the experiment and after 6h of control/ethylene exposure.

Gene expression studies

Petioles of 8-12 mm length were harvested, snap frozen in liquid nitrogen and RNA was isolated using the RNeasy extraction kit (Qiagen, Venlo, the Netherlands). Genomic DNA was removed using on-column DNase digestion (Qiagen). For the analysis of gene expression in different petiole quarters, petioles were divided in four sections and 1 µg of total RNA was used for cDNA synthesis conducted with random hexamer primers using the SuperScript III RNase H Reverse Transcriptase kit (Invitrogen, Breda, the Netherlands). Real time RT-PCR was performed using the MyiQ Single-Color Detection System (Bio-Rad, Veenendaal, the Netherlands) with iQ SYBR Green Supermix Fluorescein (Bio-Rad), *ROTUNDIFOLIA-3* (At4g36380) and *BRASSINOSTEROID-6 OXIDASE* (At5g38970) specific primers**.** Relative mRNA values were calculated using the $2^{-\Delta\Delta Ct}$ method (Livak and Schmittgen, 2001) with β-Tubulin-6 (At5g12250) as an internal reference gene. Primer sequences are listed in the table (Table S4.1).

Statistics

For the comparison of means a non-paired Student T-test was used.

Results

***decreased initial decreased ethylene decreased low light* (*ddd1*) exhibits reduced hyponasty and no cell expansion at the abaxial side of the petiole**

ddd1 was isolated in a forward genetic screen of 35S CaMV promoter-tagged plants based on its decreased petiole angles (Chapter 3). The angle measurements were carried out at the start of the screen, after 6 h in ethylene and after 6 h in low light. The isolated line was therefore named *decreased initial decreased ethylene decreased low light* (*ddd1*). A full description of the screen is presented in Chapter 3. In the vegetative stage the distinctive phenotype of *ddd1* included compact rosettes, broader leaf blades and shorter petioles compared to wild type Col-0 plants (**Fig. 4.1a, b**). Detailed analysis of *ddd1* petiole kinetics using a time-lapse camera setup shows that hyponastic response in ethylene is reduced throughout the duration of the ex-

periment (24 hours) (**Fig. 4.1c-e**) and that induction of the response is moderately delayed.

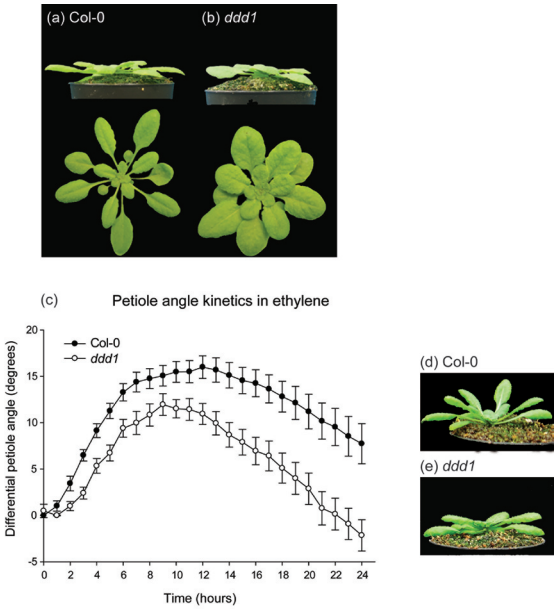

Fig. 4.1 (**a**) Phenotype of Col-0 and (**b**) *ddd1* in control conditions. (**c**) Kinetics of Col-0 and *ddd1* petiole angle in ethylene (means ±SE; *n*>10) (**d**) Col-0 and (**d**) *ddd1* after 10h of ethylene treatment.

Ethylene–induced hyponasty depends on unequal growth rates between two sides of the petiole which is driven by a local stimulation of cell expansion at the abaxial side of the petiole (Chapter 2). Since hyponasty is highly reduced in *ddd1*, we analysed epidermal imprints of 1cm petioles after 10 hours of ethylene and control treatment. In Col-0 plants, in approximately the first 3-4 mm cells at the abaxial side of the petiole increase their length (Chapter 2, **Fig. 2.2c**). Despite the small hyponastic response of *ddd1*, no difference in longitudinal cell expansion between the two treatments was observed in *ddd1* (**Fig. 4.2a, b**).

As mentioned above, the phenotype of *ddd1* consists of short petioles and relatively compact rosettes. To test whether the reduction of ethylene-induced hyponasty in *ddd1* is a result of mechanical constraints, we tested its response to green shade, which mimics dense canopy conditions leading to hyponasty and petiole elongation (Pierik *et al.*, 2005). Despite the initial difference between petiole angles of Col-0 and *ddd1* before the start of the experiment, the 24-hour green shade exposure resulted in comparable increase in petiole angles of both genotypes (**Fig. 4.3a-e**). This implies that reduced hyponastic growth in *ddd1* is not due to physical limitations but due to a molecular effect downstream of ethylene signalling.

ddd1 has reduced levels of *ROT3* expression which does not affect ethylene sensitivity

To identify the genetic nature of the *ddd1* phenotype we used Illumina® sequencing (Chapter 3) which revealed that the T-DNA insertion is located on chromosome 2 in the fourth exon of the *ROTUNDIFOLIA3* gene (*ROT3*, At4g36380). Subsequent analysis of the *ROT3* transcript levels confirmed substantial decrease in the expression of *ROT3* in the *ddd1* line (see Chapter 3 for details). To confirm that a mutation in *rot3* is causal to the *ddd1* phenotype, we tested responses of a previous described *rot3-1* (Kim *et al.*, 1998) mutant and of two additional T-DNA insertion lines in *ROT3* SALK

043566C and SALK 003225C. *Rot3-1* has a deletion of at least 1 kb in the promoter region and in the first intron (Kim *et al*., 1998) while both the SALK lines carry a T-DNA insertion in the promoter area of *ROT3* (**Fig. 4.4a**). The analysis of petiole angle in ethylene shows that the *rot3-1* mutant had a significantly reduced hyponastic response, comparable to *ddd1* (**Fig. 4.4b**), whereas the two SALK lines did not. Moreover, the phenotype of *rot3-1* consists of compact rosettes, broad leaves and shorter petioles clearly resembling *ddd1* (**Fig. 4.4c, d**). To confirm the genetic interrelation between *ddd1* and *rot3-1* we performed a genetic complementation test by crossing *ddd1* and *rot3-1* and examining the resulting phenotype of the F1 offspring (**Fig. 4.4c-e**). The characteristic appearance remained in the F1, confirming that *ddd1* and *rot3-1* are allelic. Therefore the subsequent experiments were carried out using the *rot3-1* line.

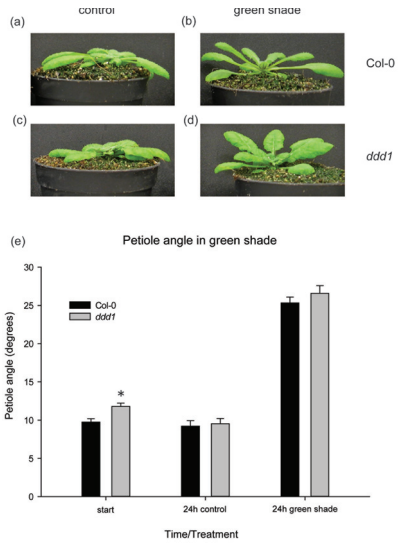

Fig. 4.3 Hyponasty under spectral (green) shade. (**a, b**) Col-0 and (**c, d**) *ddd1* plants in (**a, c**) control conditions and (**b, d**) after 24h of green shade exposure. (**e**) Petiole angles in control conditions and green shade. Data points represent means ± SE of petiole angles (n=40). Asterisks indicate significant differences relative to petiole angle in control-treated plants ($P < 0.05$).

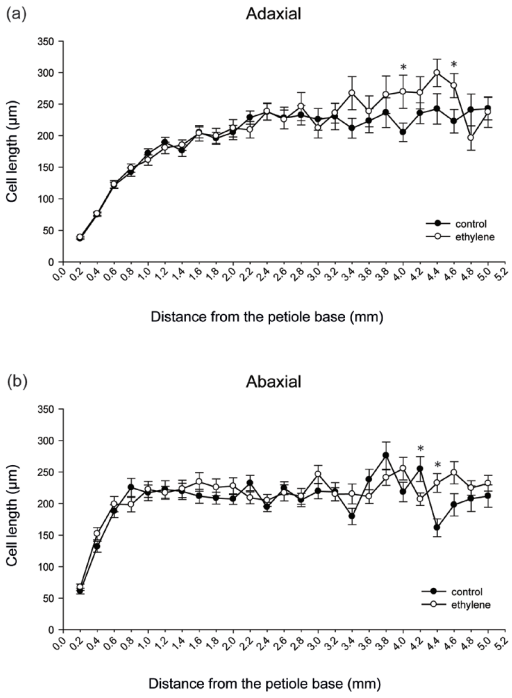

Fig. 4.2 Epidermal cell lengths of 1-cm petioles of the *ddd1* line. Data points represent the means ± SE of cell lengths at the **(a)** adaxial and **(b)** abaxial sides of petioles after 10 h of ethylene and control treatment. Asterisks indicate significant differences relative to the cell lengths of control-treated petioles ($P < 0.05$), n = 12-16.

Ethylene sensitivity can be studied using the so called triple response assay which in *Arabidopsis* consists of inhibition of hypocotyl elongation, exaggerated apical hook and swelling of the hypocotyl in darkness (Bleecker *et al.*, 1988; Guzman and Ecker, 1990). To exclude that impaired hyponasty of *rot3-1* is due to a generally reduced responsiveness to ethylene, we tested the mutant's hypocotyl elongation in presence of

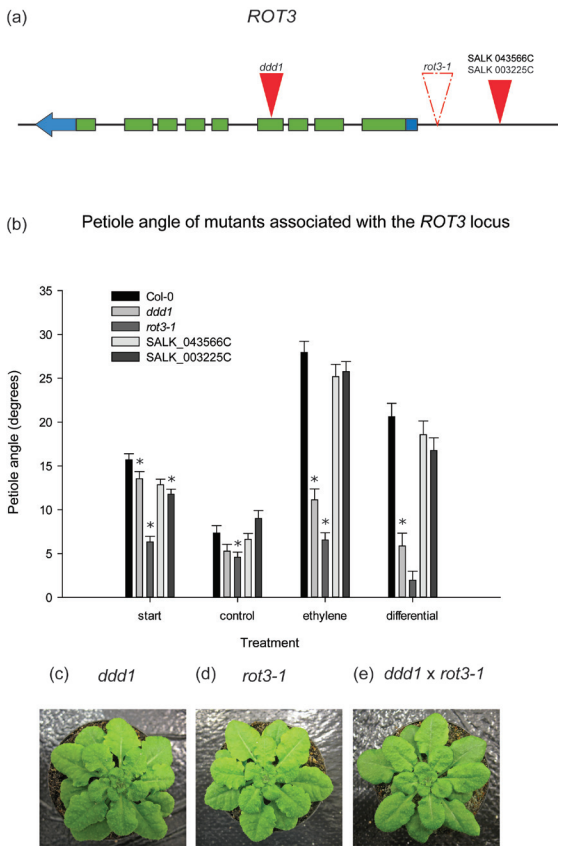

Fig. 4.4 Mutations associated with the *ROT3* locus. **(a)** Schematic illustration of the insertion sites within the *ROT3* locus. **(b)** Hyponasty in lines with disrupted *ROT3* expression. Data points represent means ± SE of petiole angles (n=15); asterisks represent significant differences between mutants and wild type Col-0. **(c)** The phenotype of ddd1 **(d)** *rot3-1* and **(e)** F1 of a cross between the two lines (*ddd1* and *rot3-1).*

exogenous ACC. *Rot3-1* has typically less elongated hypocotyls in darkness, however the growth inhibition by ACC resembles the wild-type response (**Fig. 4.6**). This result suggests that general sensitivity to ethylene is unaffected in *rot3-1*.

Brassinosteroid action is required for ethylene-induced hyponasty

ROT3 encodes a member of the cytochrome P450 family, CYP90C1, an enzyme involved in the conversion of typhasterol (TY) to castasterone (CS), which is the last step in the synthesis of bioactive BRs (Kim *et al*. 2004, 2005). Based on the previous experiments, we hypothesized that *ROT3* acts as an important component in ethylene-induced hyponasty and that its expression might change upon ethylene exposure. We examined the transcription of *ROT3* together with another BR biosynthesis-related gene, *BRASSINOSTEROID-6 OXIDASE* (*BR6OX*), in four separate petiole segments (**Fig. 4.6a**). Surprisingly, 3 and 6 hours after start of ethylene exposure the expression of *ROT3* significantly declines in quarter 2, which corresponds with the abaxial side proximal to the rosette where hyponastic growth is known to be induced (Chapter 2). The analysis of *BR6OX* appears to be less straightforward, with only a slight reduction of gene expression in the mentioned segment.

Along with the notion that brassinosteroids play an important role in regulating ethylene-induced hyponasty, we tested whether perturbation of their synthesis reflects on the petiole angle. We applied brassinazole (Brz), an inhibitor of cytochrome CYP450 function specifically during steroid synthesis (Asami *et al.*, 2000). Clearly, Brz application reduced petiole angles in both air and ethylene. In addition, the ethylene-induced angle increase was also reduced by Brz (**Fig. 4.7**).

BR involvement in ethylene-induced leaf movement responses implies that

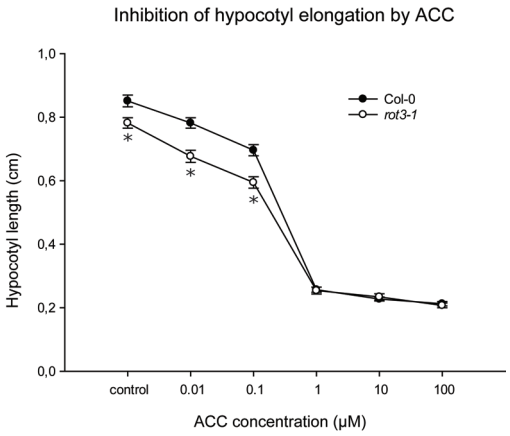

Fig. 4.5 Inhibition of hypocotyl elongation in darkness by ACC. Data points represent average hypocotyl length of Col-0 and *rot3-1* seedlings. Asterisks indicate significant differences between hypocotyl the two treatments ($P < 0.05$), $n = 70$-120.

ethylene either stimulates BR synthesis or BR responsiveness. Since BR application to petioles on itself does not affect petiole angles, we tested BR responsiveness on an alternative system that involves cell expansion. Ethylene can induce hypocotyl elongation in light-grown seedlings (Smalle *et al.*, 1997) and we used this to study whether brassinosteroid responsiveness is modulated by ethylene application. We applied a range of epibrassinolide (BL) concentrations and examined effects on hypocotyl elongation under control air and high ethylene conditions. Furthermore, we included a Brz treatment to inhibit endogenous BR biosynthesis to separate effects of ethylene on biosynthesis from effects on BR responsiveness. Brz application alone substantially inhibited hypocotyl elongation in ethylene-exposed seedlings, which suggests a role of brassinosteroids in this process (**Fig. 4.8**; De Grauwe *et al.*, 2005), consistent with observations described earlier for hyponasty. BL stimulated hypocotyl elongation in a dose-dependent manner, but was much more effective in the low concentration range in the presence of ethylene as compared to control air, indicating an ethylene-induced increase of BL responsiveness.

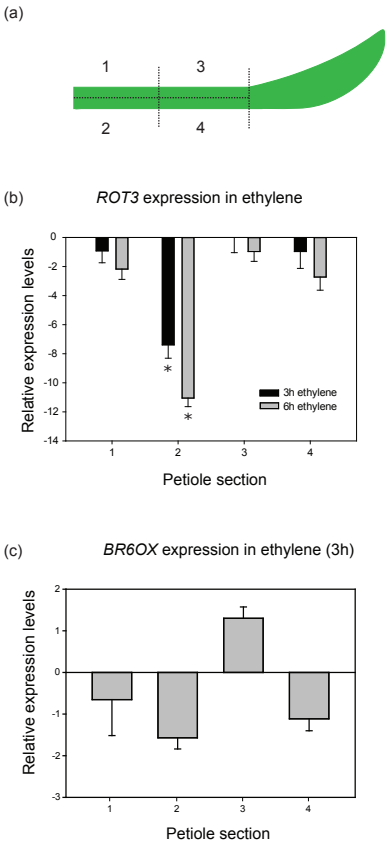

Fig. 4.6 (a) Schematic representation of petiole quarters used for studies of gene expression. Petioles were divided into four quarters and expression measurements were performed separately for each quarter. **(b-c)** Expression of *ROT3* and *BR6OX* after 3 and 6 hours of ethylene exposure. Data points represent the fold change of gene expression (means ± SE) after 3 and/or 6 h of ethylene exposure relative to the control conditions and relative to *β-Tubulin-6*. Asterisks indicate significant differences between results from ethylene and control treatments ($P < 0.05$).

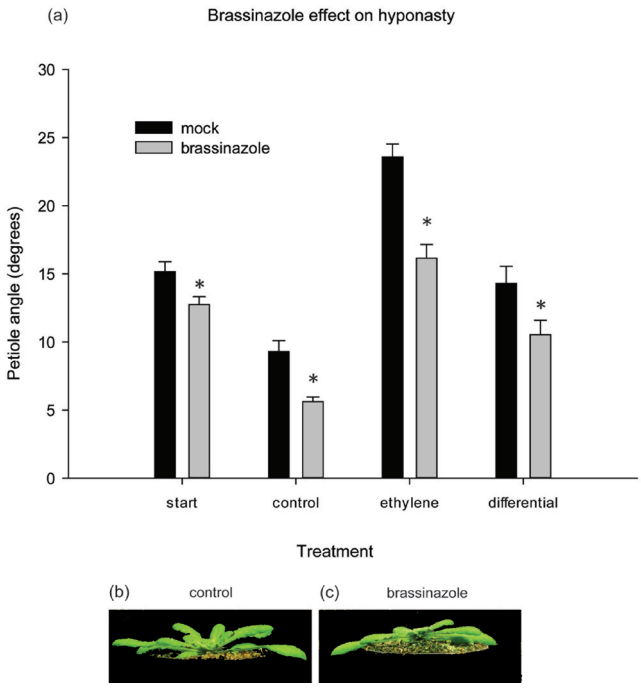

Fig. 4.7 (a) Effect of brassinazole on petiole hyponasty in ethylene. Data points show means ± SE of petiole angles and asterisks indicate significant differences ($P < 0.05$) between brassinazole and mock treatment (n=15). **(b, c)** Appearance of plants after mock and brassinazole treatment.

DISCUSSION

Hyponastic growth is driven by differential growth rates between the ad- and abaxial side of the petiole. In a previous study on cell length dynamics in ethylene we have shown that a local longitudinal expansion of cells at the abaxial side of the petiole is a driving force in hyponastic response (Chapter 2). In the current report, we present data that indicate that BRs function as an integral part of the signalling cascade towards differential tissue growth in response to ethylene. The mutant line, *ddd1*, that we isolated in our screen (Chapter 3) shows a clear reduction in the hyponastic response and consistently lacks the response at the cellular level. Given the fact that hyponasty in *ddd1* is not completely absent, it is feasible that minor changes in cell expansion dynamics still occurred beyond the resolution of the measurement and were responsible for the small angle increase. One of the explanations for the decreased hyponasty in *ddd1* would be that its distinctive phenotype - broad leaf blades, short petioles and compact rosettes - could potentially mechanically interfere with the upward petiole movement. However, in experiments using spectral (green) shade to induce hyponasty, *ddd1* has a response almost identical to wild type plants. Petioles of both genotypes reached a similar angle of ± 25 degrees indicating that reduced hyponasty in ethylene is not due to biophysical constraints and is therefore the consequence of interference with the signal transduction pathway from ethylene towards differential petiole growth. Since *ddd1* petioles in selected for this experiment were much shorter (<5mm) than petioles used for standard ethylene experiments (10 mm), they displayed a slightly yet significantly enhanced initial petiole angle in comparison to Col-0. These development-related differences in petiole angle might be due mechanical properties of compact rosettes in *ddd1*.

Sequencing of *ddd1* revealed that the T-DNA insertion is located within the *ROT3* gene (At4g36380). Previously characterized *rot3* mutants showed an identical phenotype consisting of shorter petioles and larger leaf laminas. As described by Kim *et al.*, (1998, 1999), *ROT3,* encoding an enzyme important for BR synthesis, is responsible for polar elongation of cells, specifically in leaves and flower organs. The sequencing result was confirmed by the analysis of an independent mutant associated with the *ROT3* locus, *rot3-1*. This mutant displayed a significant and similar reduction in the hyponastic response as did *ddd1*. Two other lines, harbouring T-DNA insertions in the close proximity of the *ROT3* locus, revealed a hyponastic response similar to the wild-type. This is probably caused by the position of the T-DNA insertions that were found to be in the promoter region and not in the coding sequence of the gene. Importantly, *rot3-1* does not display a general difference in sensitivity to ethylene, since the triple response induced by the ethylene precursor ACC, was nearly identical between *rot3-1* and wild type Col-0. The fact that the hypocotyl shortening at ACC concentrations ≥ 1μM is the same in both *rot3-1* and Col-0 suggests that the inhibition effect reaches its saturation.

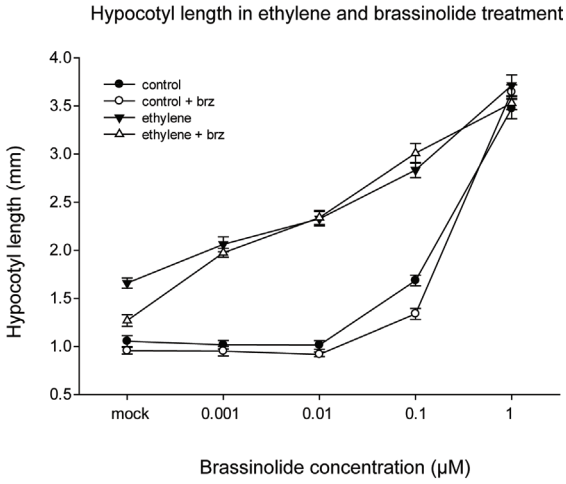

Fig. 4.8 Hypocotyl elongation in ethylene. The effect of different concentrations of BL in ethylene and control treatment. Data points show hypocotyl length of wild-type Col-0 seedlings *n*=40-50 in various treatments.

To assess whether the expression of *ROT3* and another BR biosynthesis-related gene, *BR6OX*, changes during ethylene exposure, we looked at the transcript levels of these genes in different sections of the petiole. The region in which cell expansion occurs exhibited significantly lower expression of *ROT3* and slightly lower levels of *BR6OX* transcripts already after 3 hours in ethylene. It is likely that this reduction is an outcome of a negative feedback loop between increased levels of BRs which would result in a decline in transcript abundance of genes involved in their biosynthesis. This would be in agreement with a study by Tanaka *et al*. (2005), which illustrated a tight negative feedback regulation of BR homeostasis by expression dynamics of BR metabolism-related genes. Exogenous application of BL resulted in a substantial decrease in transcript levels of *ROT3* and *BR6OX* together with other BR biosynthesis genes such as *DWARF5* (*DWF5*) or *CONSTITUTIVE PHOTOMORPHOGENIC DWARF* (*CPD*) in *Arabidopsis* seedlings already after 2 hours of hormone treatment. Even though the molecular mechanism of this negative feedback loop has not been fully recognized, a downstream component of BR signaling, *BRAS-*

SINAZOLE-RESISTANT1 (*BZR1*) has been shown to bind to cis regulatory elements of *CPD* and *DWF4* (He *et al.*, 2005), thereby negatively regulating their expression (Kim *et al*., 2006).

ROT3 encodes a cytochrome P450, CYP90C1, catalysing a late step in castasterone (CS) synthesis (Kim *et al*., 2005; Ohnishi *et al*., 2006). CS is a direct precursor of brassinolide (BL), and, together with BL, serves as an active form of BR (Grove *et al.*, 1979; Suzuki *et al.*, 1993). We used brassinazole (Brz), a chemical inhibitor of CS biosynthesis (Asami *et al*., 2000) to test in an independent way if brassinosteroid synthesis is required for hyponasty. Indeed, brassinazole modestly inhibited hyponasty, indicating that BR synthesis contributes to the occurrence of hyponasty. The fact that the reduction was not complete suggests that either BR biosynthesis was only partially inhibited by brassinazole or that other regulators are also involved. Since many studies have demonstrated synergistic relation between BRs and auxin (reviewed in Halliday *et al*., 2004), it is possible that there is a cross-talk between these two hormones in the hyponastic response in *Arabidopsis*.

It is known that ethylene application in light results in *Arabidopsis* hypocotyl elongation (Smalle *et al.*, 1997). Because the combined treatment of BL and ethylene does not lead to enhanced hyponasty (data not shown/supplementary information), we used hypocotyl elongation in seedlings as a system to assess whether or not ethylene increases responsiveness to brassinosteroids. As expected, Brz inhibits hypocotyl elongation in ethylene when no additional BL was supplied which suggests that its synthesis is crucial for hypocotyl cell elongation in ethylene. This is consistent with earlier studies on dark grown seedlings which demonstrated that apical hook formation in presence of ethylene strongly depends on a functional BR pathway (De Grauwe *et al.*, 2005). Moreover, we found that ethylene clearly sensitizes cell expansion to BL application, since very low BL levels (0.001-0.01 μM) stimulated elongation in ethylene, whilst being ineffective in control plants.

Taken together, our data provide evidence for a positive role of BRs, downstream of ethylene, in regulation of ethylene-induced increase of petiole angle. Consistent with this conclusion, BR signalling has been shown to be crucial to organ growth by controlling cell expansion in the epidermis (Savaldi-Goldstein *et al*., 2007), where also hyponasty is likely controlled. We also provide evidence that ethylene can sensitize tissue to BRs, at least in hypocotyls. Future studies should elucidate whether ethylene also promotes the synthesis of BRs, if such regulation would be tissue specific and which are the molecular mechanisms behind this interaction.

CHAPTER 5

Ethylene response factors (ERFs) in ethylene-induced hyponasty

Joanna K. Polko, Martijn van Zanten, Anita Wagemaker, Cheryl Philipsen, Laurentius A.C.J. Voesenek, Anton J.M. Peeters and Ronald Pierik

Plant Ecophysiology, Institute of Environmental Biology, Utrecht University, Padualaan 8, 3584 CH Utrecht, the Netherlands

SUMMARY

Hyponastic growth is a response of several rosette plant species, including *Rumex palustris* and *Arabidopsis thaliana,* to unfavourable environmental conditions. This response is characterized by upward repositioning of leaves driven by differential growth within a petiole. Previous studies have demonstrated that ethylene, a gaseous phytohormone, plays a crucial role during shade and submergence-induced hyponasty. Despite the substantial knowledge on hormonal regulation during ethylene-driven hyponasty, the direct molecular downstream components during this response remain to be elucidated. Ethylene response factors (ERFs) belong to a large superfamily of transcription factors involved in many biological processes such as organogenesis or response to environmental cues. They have been reported to regulate responses to biotic (such as pathogen attack) as well as abiotic stresses (e.g. drought, high salinity and flooding). Transcriptional regulation of ERFs is often induced within several hours or even minutes after perception of the external signal. Since not all ERFs are ethylene-inducible, we performed a forward genetic screen of an ORF collection of *Arabidopsis* plants over-expressing various ERFs. The aim of this study was to identify ERFs involved in ethylene-induced hyponasty which would provide a solid basis for studying their transcriptional control and downstream targets during hyponastic growth.

INTRODUCTION

Ethylene is a gaseous phytohormone controlling a wide range of events in plant development such as breaking of seed dormancy (Koornneef *et al.*, 2002), adventitious root formation (Jusaitis, 1986), sex determination (McMurray and Miller, 1968) leaf abscission (Abeles and Rubinstein *et al*., 1964), fruit ripening (Burg and Burg, 1962), enhanced shoot elongation (Bailey-Serres and Voesenek, 2008) or programmed cell death (Young *et al*., 1997). Furthermore, its production is highly regulated by diverse abiotic and biotic stresses, such as chilling and freezing, drought, hypoxia, mechanical wounding, pathogen and insect attack (reviewed in Abeles *et al*., 1992). Ethylene has been also recognized as a primary signal in triggering submergence escape responses including non-differential shoot elongation in *Oryza sativa* and differential

petiole elongation in *Rumex palustris* (Jackson, 1985; Voesenek *et al.*, 1993; Banga *et al.*, 1996; Bailey-Serres and Voesenek, 2010). The accumulation of ethylene in submerged plant tissues induces a set of downstream events including crosstalk between ABA, GA and auxin, changes in apoplastic pH, activation of cell wall modifying enzymes and, eventually, tissue growth (reviewed in Jackson, 2008; Bailey-Serres and Voesenek, 2008; Voesenek *et al*., 2006). Experiments from the last decade have demonstrated that ethylene application on its own can mimic submergence-induced hyponasty in *R. palustris* as well as in *Arabidopsis thaliana* making it a useful system for studying downstream targets of ethylene regarding differential organ growth.
In brief, ethylene biosynthesis in vascular plants (the MSAE pathway) starts with S-adenosylmethionine (SAM or AdoMet) generated in the Yang cycle. ACC synthase (ACS) converts SAM into 1-aminocyclopropane (ACC) which is then degraded into ethylene by ACC-oxidase synthase (ACO) (reviewed in Lin *et al*., 2009). This process can be induced under stressful environmental conditions and depends on a mitogen-activated protein kinase (MAPK) cascade (Liu and Zhang, 2004). Although some aspects remain unknown, many events in the ethylene perception mechanism have been unravelled (reviewed in Lin *et al.,* 2009). The earliest-described component of the pathway, ETHYLENE RESPONSE1 (ETR1), was discovered using the so called triple response (Bleecker *et al*., 1988) which, in *Arabidopsis*, consists of swelling and shortening of the hypocotyl and an exaggerated apical hook formation (Knight, 1912). Shortly, ethylene perception starts with a group of endoplasmic reticulum (ER) membrane-associated proteins: ETR1, ETHYLENE RESPONSE SENSOR1 (ERS1), ETR2 and ETHYLENE INSENSITIVE4 (EIN4). In the absence of ethylene this group of receptors physically activates a negative regulator of ethylene action, (CONSTITUTIVE TRIPLE RESPONSE) (CTR1), which in turn represses downstream ethylene responses. In the presence of ethylene, however, CTR1 dissociates from the membrane complex and the repression is inactivated. Thereafter, a positive component of ethylene signalling, EIN2 promotes downstream transcription factors, EIN3 and EIN3-LIKE proteins (EILs) which activate ethylene-regulated gene expression through, e.g. ETHYLENE RESPONSE FACTOR1 (ERF1) (reviewed in Lin *et al*., 2009). Ethylene response factors (ERFs) belong to an ERF subfamily of AP2/ERF superfamily of transcription factors (TFs) which were initially identified in *Nicotiana tabacum* as ethylene-responsive element-binding proteins (EREBP's) and subsequently renamed as ERFs (Suzuki *et al*., 1998). ERF proteins bind to GCC-boxes in ethylene responsive genes (Ohme-Takagi and Shinshi, 1995). According to Sakuma *et al*. (2002) there are 121 genes in the ERF subfamily in the *Arabidopsis* genome, whereas Nakano *et al.* (2006) distinguishes 122 genes. The latter study resulted in the construction of the ERF phylogenetic tree which consists of 10 subgroups.

ERFs have been implicated in various biological processes including regulation of developmental events such as petiole development (Van der Graaff *et al*., 2000) and shoot regeneration (Banno *et al*., 2001). Moreover, they play a central role in regulation of plant defence mechanisms (Yamamoto *et al*., 1999; Gu *et al*., 2000; Cao *et al*., 2005, Pré *et al*., 2008) and responses to abiotic stresses such as drought and salt stress (Karaba *et al*., 2007; Trujillo *et al*., 2008; Abogadallah *et al*., 2011),

submergence (Fukao and Bailey-Serres, 2008; Fukao *et al*., 2011) or hypoxia (Yang *et al*., 2011). Recently, it has been demonstrated that in low oxygen conditions one of the *Arabidopsis* plasma membrane-associated ERFs, RAP2.12, is released from the plasma membrane-bound acyl-CoA binding proteins (ACBP's) and transported to the nucleus where it activates hypoxia-related genes. Upon re-oxygenation RAP2.12 functions as a substrate for the N-end rule-regulated protein degradation (Licausi *et al*., 2011; Gibbs *et al*., 2011).
Regardless of their name, not all ERFs are ethylene-inducible (reviewed in Ohme-Takagi et al., 2000). The goal of this report was to identify ERFs which both positively and negatively regulate ethylene-induced hyponasty. Here, we present results from a forward genetic screen of *Arabidopsis* ERF-over-expression lines which exhibit altered petiole hyponasty upon ethylene exposure. The established set of candidate *ERF* lines with aberrant petiole angle has been then tested for ethylene biosynthesis. To understand their role in petiole hyponasty, we consequently examined transcriptional regulation of ERFs of interest during ethylene treatment. These results provide a platform for future studies regarding ERF functioning in various developmental and physiological aspects of ethylene signalling pathway.

MATERIALS and METHODS

Plant growth

Arabidopsis thaliana Col-0 (N1092) and SALK 063727 (N563727) were obtained from the Nottingham Arabidopsis Stock Centre (NASC; stock numbers between brackets). SALK 063727 line belongs to a homozygous collection and was confirmed by a PCR amplification with T-DNA-specific (LBb1.3) primer and At-specific (RP) primer, as described on http://signal.salk.edu/. The collection of ERF over-expression lines (Weiste *et al*., 2007) was a gift from Prof. Wolfgang Dröge-Laser (University of Göttingen, Germany). Seeds were sown on moisturised filter papers and dark stratified at 4ºC for 4 days. Afterwards, seeds were transferred to a growth chamber (20ºC, 70% relative humidity and 200 µmol m^{-2} s^{-1} photosynthetic active radiation (PAR); 9 h photoperiod) where they were left for germination and after 4 days potted on a fertilized mixture of soil and perlite (RHP,'s-Gravenzande, the Netherlands) in a 1:2 ratio. The growth conditions were as described by Millenaar *et al*., 2005.

Ethylene treatment and petiole angle measurements

30 day-old plants in stage 3.9 (Boyes *et al.*, 2001) were used for all experiments. One day before the start of the treatment, plants were transferred to the experimental setup with similar conditions to the growth chambers (Microclima 1750 growth cabinet; Snijders Scientific, Tilburg, the Netherlands). Ethylene (Hoek Loos, Amsterdam, the Netherlands) application always started (t=0 h) 1.5 h after the beginning of the photoperiod. The setup was flushed with 1.5 µL L^{-1} ethylene with a continuous flow of 75 L h^{-1} and the control treatment was conducted in the same experimental

cabinet. Side pictures were taken with a digital camera (Canon PowerShot A530) at the start of the experiment, after 6h in control or ethylene treatment. Petiole angles were measured relative to the horizontal plane using ImageJ software: http://rsb.info.nih.gov/ (Abramoff *et al.*, 2004). The differential angle was calculated as a difference between petiole angles of 6 h ethylene- and control-treated plants as described by (Benschop *et al.*, 2007).

Validation of ERF over-expression lines and gene expression studies

For DNA extraction leaf material was harvested and snap-frozen in liquid nitrogen. Genomic DNA was extracted using the Nucleon Phytopure DNA extraction kit (GE Healthcare/Amersham, Den Bosch; the Netherlands). To identify *ERF* genes over-expressed in an individual line, PCR amplification was conducted on 100 ng of DNA with Gateway® att specific primers as described by Weiste *et al*. (2007). Obtained product was purified and sequenced (BaseClear®, Leiden; the Netherlands).
For the Real Time qPCR (RT-Q-PCR) RNA from 8-12mm petioles, that were snap-frozen in liquid nitrogen, was isolated using the RNeasy extraction kit (Qiagen, Venlo; the Netherlands) and genomic DNA was removed with on-column DNase di gestion (Qiagen). 1 µg of total RNA was used for cDNA synthesis conducted with random hexamer primers using the SuperScript III RNase H Reverse Transcriptase kit (Invitrogen, Breda; the Netherlands). RT-Q-PCR was performed using the MyiQ Single-Color Detection System (Bio-Rad, Veenendaal, the Netherlands) with iQ SYBR Green Supermix Fluorescein (Bio-Rad) and gene specific primers. Relative mRNA values were calculated using the $2^{-\Delta\Delta Ct}$ method (Livak and Schmittgen, 2001) with *β-Tubulin-6* (At5g12250) as an internal reference gene. Primer sequences are presented in Table S5.1.

Ethylene production measurements

Fresh leaf material (0.3 g) from 28-day-old plants was collected and placed in a 2.5 mL syringe. After 15 minutes, the formed overhead gas was transferred to another syringe of 1 mL volume and injected into a gas chromatograph (GC) (GC955; Synspec, Groningen; the Netherlands). Obtained values (ppb) were recalculated into nmol $gFW^{-1}\,h^{-1}$.

Statistics

For the comparison of means a non-paired Student T-test was used.

RESULTS and DISCUSSION

Over-expression of several ethylene response factors (ERFs) in *Arabidopsis* affects petiole angle in response to ethylene

We conducted a forward genetic screen of an open reading frame (ORF) collection of T_2 seeds over-expressing ethylene response factors (ERFs) generated by Weiste *et al*. (2007). In an initial screen on this ERF over-expression population we selected 32 individual plants (data not shown) with either enhanced or decreased petiole angle at the start of the experiment or/and in ethylene. For the subsequent studies, we then narrowed down the selection to the 10 lines that displayed the most extreme phenotypes (**Fig. 5.1a-d**).

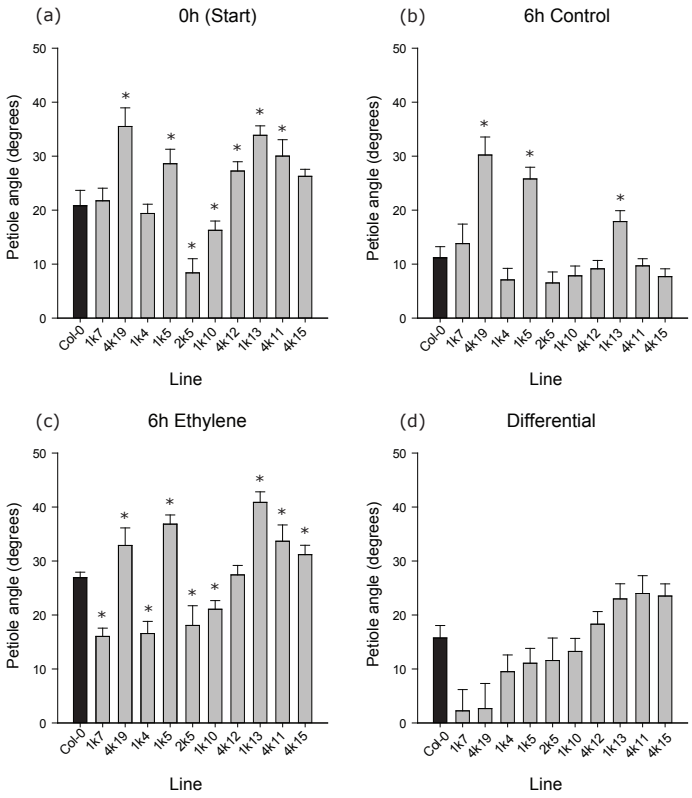

Fig. 5.1 Screen results of ERF over-expression lines showing petiole angles of selected candidate lines. **(a)** Petiole angles at the start of the experiment, **(b)** after 6 h in control conditions, **(c)** after 6 h in ethylene and **(d)** differential petiole angles as a result of subtraction between ethylene and control values. Data points represent mean values (n=10) ± SE. Asterisks indicate significant difference in comparison to wild type Col-0 plants (P < 0.05).

Most of the plants had an aberrant (increased or reduced) petiole angle upon ethylene treatment, with only one line (designated *ERF4k12*) exhibiting increased petiole angles only at the start of the experiment (0h). To identify which particular *ERF* gene is over-expressed by each line, we amplified a region with T-DNA specific primers and sequenced the product. The results are presented in **Table 5.1**. The *1k13* line harboured two independent T-DNA insertions of *ERF96* (At5g43410) and *ERF7* (At4g06746), whereas the rest of the candidates had a single insertion. Interestingly, lines *4k11* and *4k15*, which exhibit highly similar phenotypes in all treatments, both were found to harbour insertion of *ERF112* (At2g33710) and were therefore designated *ERF112a* and *ERF 112b*. **Figure 5.2a-k** shows general phenotypes of selected candidates. Most were similar to the wt Col-0 and showed no striking morphological defects. However, leaf development is strongly affected in line *ERF87*

(At1g28160) (**Fig. 5.2b**), which has no distinctive petioles and curled leaf blades. *ERF 95* (At3g23220) has a dwarfed phenotype with constitutively high petiole angles (± 36 degrees), elongated petioles and small leaf blades (**Fig. 5.2c**).

Table 5.1 Sequencing results of candidate *ERF* lines selected in a screen.

Name	At code	ERF number	Group
ERF1k7	At1g28160	*ERF87*	VIIIb
ERF4k19	At3g23220	*ERF95*	IXc
ERF1k4	At4g06746	*ERF7*	IIa
ERF1k5	At5g18560	*ERF86*	VIIIb
ERF2k5	At1g74930	*ERF18*	Ib
ERF1k10	At5g21960	*ERF16*	IIb
ERF4k12	At2g46310	*ERF68*	VI
ERF1k13	At5g43410 + At4g06746	*ERF96+7*	IXc + IIa
ERF4k11	At2g33710	*ERF112a*	Xc
ERF4k15	At2g33710	*ERF112b*	Xc

To examine whether a knock-out mutation results in a contrasting response, we then compared the response of the available SALK line (SALK063727) for the *ERF112*. *ERF112* and SALK063727 display contrasting petiole angles already at the start of the experiment, and, as expected respectively, showed an enhanced and reduced response upon ethylene exposure (**Fig. 5.3**).

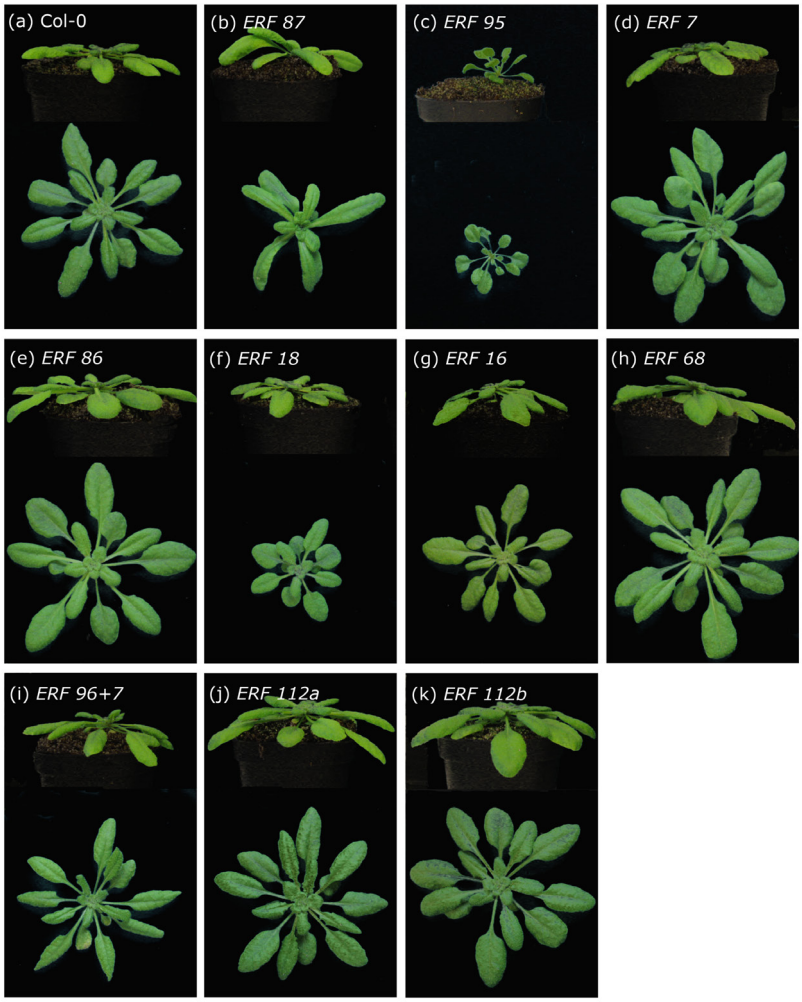

Fig. 5.2 (a-k) Phenotypes of *ERF* lines selected in a screen.

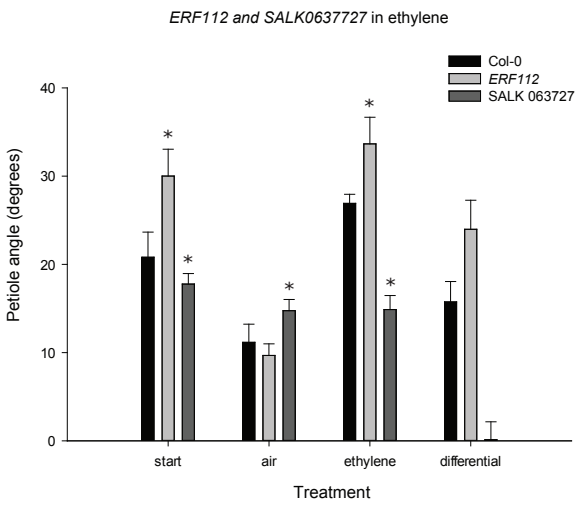

Fig. 5.3 Hyponasty of *ERF112* and SALK 063727 in ethylene. Data points indicate mean values (n=15) ± SE. Asterisks indicate significant differences in comparison to wild type Col-0 plants ($P < 0.05$).

Some of the lines selected in our screen harbour an over-expression construct of an *ERF* that has previously been described regarding responses to various stresses. *ERF18* (At74930) is involved in response to wounding, methyl jasmonate (MeJA) signalling and JA biosynthesis (Walley *et al*., 2007, Pauwels *et al*., 2008). *ERF95* (*Ethylene and salt-induced ERF - ESE1*) is implicated in response to salt stress. Recently, a study by Zhang *et al*. (2011) showed that *ESE1* is transcriptionally modulated by EIN3 which binds directly to its promoter region. Other *ERF* lines are involved in development-related processes such as *in vitro* shoot regeneration (*ERF87* or *ENHANCER OF SHOOT REGENERATION-LIKE2 - ESL2*) (Mase *et al*., 2007) or early lateral root primordium initiation (*ERF86*, *PUCHI,* At5g18560) (Hirota *et al*., 2007). The remarkable phenotype of *ERF87* with no clear petiole-leaf lamina transition resembles a previously described activation tagging line of *LEAFY PETIOLE* (*LEP*) (Van der Graaff *et al*., 2000). *LEP* (*ERF85*; At1g13910) as well as *ERF87* belong to the subgroup VIII in the ERF family and show a high degree of homology (Nakano *et al*., 2006). This implies that both genes could potentially share molecular targets during petiole development. Interestingly, *ERF112* has been described as a general stress response factor (Feng *et al*., 2005) but is also implicated in female gametophyte development (Wang *et al*., 2010), suggesting a pleiotropic role.

Next, we examined whether the selected over-expression lines have altered ethylene biosynthesis since ethylene signalling has been reported to show such feedback control. Most of the candidates show unaltered ethylene production comparable to Col-0 (**Fig. 5.4**). Significantly higher levels of ethylene were present in lines *ERF95, ERF87*, *ERF7* and *ERF96+7* which suggests a potential positive feedback between transcriptional regulation of *ERF* genes and ethylene biosynthesis. Such an effect has been previously described for *Solanum lycopersicum* and *N. tabacum* plants which exhibit an increased ethylene production upon over-expression of *LeERF2/TERF2*. This effect is most likely due to the interaction of *LeERF2/TERF2* with the *cis*-regulatory elements in *ACO* and *ACS* genes (Zhang *et al*., 2009). Ethylene is also shown to stimulate its own production during flower senescence and fruit ripening (Nakatsuka *et al*., 1997, 1998). On the other hand, it has been demonstrated that following pollination, tomato pistils exhibit highly reduced ethylene production levels

triggered by a negative feedback in which ethylene auto-inhibits its own production (Llop-Tous *et al*., 2000).

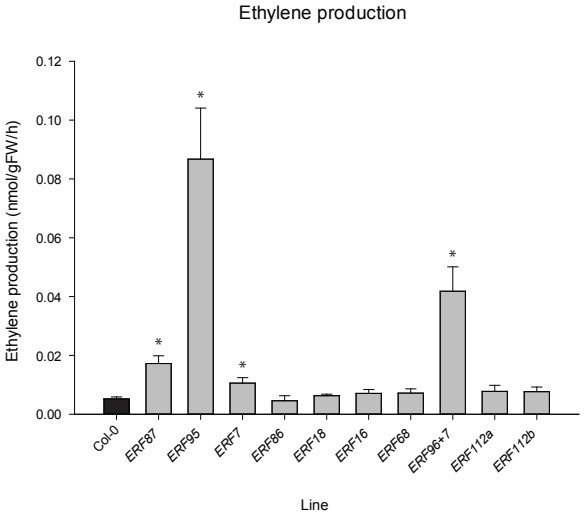

Fig. 5.4 Ethylene production in *ERF* lines. Data points indicate mean values (n=8) ± SE. Asterisks indicate significant difference in comparison to wild type Col-0 plants ($P < 0.05$).

Expression of ERF genes changes in ethylene

To test whether ethylene mediates transcriptional regulation of ERF genes in leaf angle control, we examined the kinetics of *ERF95, ERF7, ERF18, ERF68* (At2g46310) *and ERF112* expression upon ethylene application. Due to low transcript abundance, other candidate genes (*ERF87*, *ERF86* and *ERF16*) are not included in the results. In the first hour of ethylene exposure transcript levels of *ERF95, ERF68* and *ERF112* increased significantly in comparison to control conditions (**Fig. 5.5a, d, e**), whereas expression of *ERF7* and *ERF18* remained unaltered (**Fig. 5.5b, c**). Such rapid induction might imply a function in early signalling events. Accordingly, up-regulation of genes encoding TFs is usually very rapid upon perception of the inducing stimulus. Brenner *et al.* (2005) observed a substantial up-regulation of TFs in response to cytokinin treatment already after 15 min of hormone treatment. Mechanical injury in tobacco plants results in a rapid (5-30 min) induction of expression of several *ERFs* which after 1h returned to the initial or even below initial levels (Nishiuchi *et al*., 2002). Likewise, Suzuki *et al*. (1998) demonstrated a very rapid up-regulation of *ERF* transcription upon ethylene treatment which reached its peak after 30 min and disappeared soon thereafter. It is, therefore, possible that the lack of differences in expression of several of the target *ERF* genes in the current study is masked by the specific time-points we used here, which might not overlap with the transient changes in transcriptional regulation of certain ERF genes.

In Chapter 4 we presented data indicating that *ROTUNDIFOLIA3* (*ROT3*) is a positive regulator during ethylene-induced hyponasty. According to the data presented above, two ERF genes (*ERF95* and *ERF112*) are likely to have a promoting effect on petiole angle. Therefore, we tested a possible relationship between these

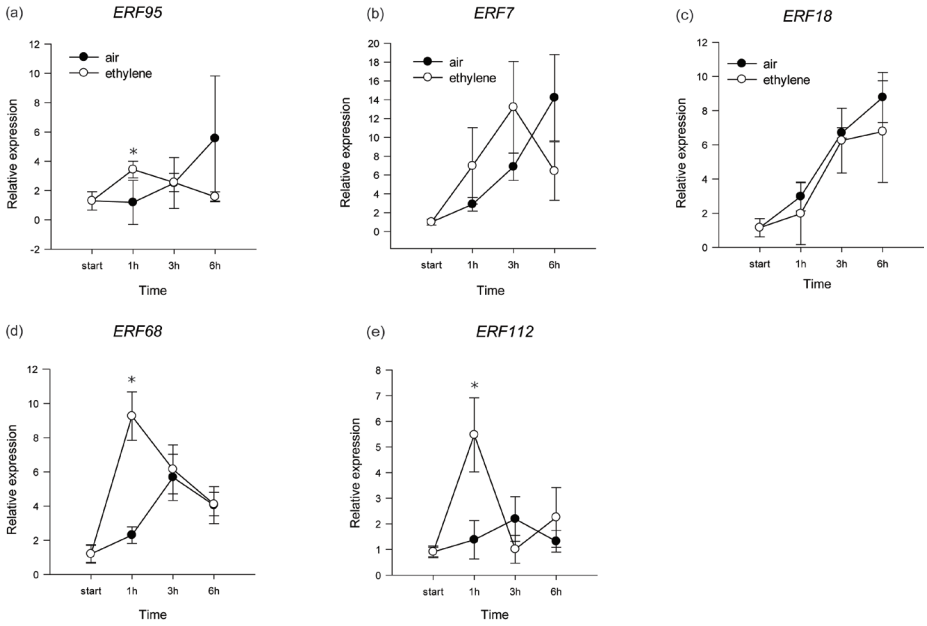

Fig. 5.5 Kinetics of ERF lines isolated in the screen. Gene expression after 1, 3 and 6 h of control and ethylene treatment. Data points represent mean values (n=5-7) ± SE. Asterisks indicate significant difference in comparison to wild type Col-0 plants ($P < 0.05$).

ERFs and *ROT3*. To do so, we measured *ROT3* transcript levels in the in over-expression lines of *ERF95* and *ERF112*. The constitutively hyponastic *ERF95* line has higher expression levels of *ROT3* which suggests a potential interaction between the ERF activity and brassinosteroid action in the control of ethylene-induced hyponasty. Since *ERF95* is also transiently induced by ethylene this could be part of the mechanism that underpins the predicted ethylene-mediated induction of brassinosteroids that is required to induce hyponastic petiole movement in *Arabidopsis*.

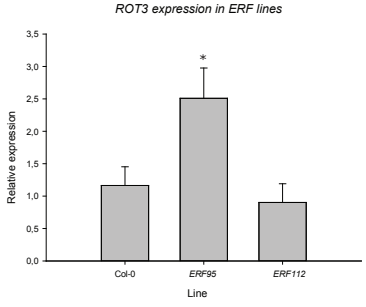

Fig. 5.6 *ROTUNDIFOLIA3* (*ROT3*) expression levels in *ERF 95* and *ERF 112*. Data points indicate mean values (n=15) ± SE. Asterisks indicate significant difference in comparison to wild type Col-0 plants ($P < 0.05$).

The exact mechanism of ERF action in hyponasty in ethylene remains unknown. Future studies focusing on detailed kinetics of gene expression, tissue localisation of ERF proteins and their molecular targets should elucidate their role in the signalling network downstream of ethylene signalling.

CHAPTER 6

Ethylene induces cell cycle inhibition during ethylene-induced hyponastic growth in *Arabidopsis thaliana*

Joanna K. Polko[1], Steffen Vanneste[2], Jop A. van Rooij[3,4], R. Pierik[1], Athanasius F.M. Marée[4], Ankie M.H. Ammerlaan[1], Fionn McLoughlin[1], Kerstin Gühl[1], Laurentius A.C.J. Voesenek[1], Frank F. Millenaar[1,5], Tom Beeckman[2], Martijn van Zanten[1], Anton J.M. Peeters[1]

[1] Plant Ecophysiology, Institute of Environmental Biology, Utrecht University, Padualaan 8, 3584 CH Utrecht, the Netherlands
[2] Department of Plant Systems Biology, Flanders Interuniversity Institute for Biotechnology, Ghent University, Technologiepark 927, B-9052, Ghent, Belgium
[3] Theoretical Biology and Bioinformatics, Utrecht University, Padualaan 8, 3584 CH Utrecht, the Netherlands
[4] Department of Computational and Systems Biology, John Innes Centre, Norwich Research Park, Colney, NR4 7UH Norwich, United Kingdom
[5] Monsanto, Leeuwenhoekweg 52, 2660 BB Bergschenhoek, the Netherlands

SUMMARY

Plant growth and survival largely depends on the ability to adjust their phenotypes to changes in the environment. Upward leaf movement (hyponastic growth or hyponasty), driven by differential petiole growth, is an example of a response operated to outgrow unfavorable conditions. Hyponastic growth is induced to a similar extent by different abiotic stimuli, including enhanced ethylene levels, shade, low light intensity and increased temperatures. Despite its functional importance, relatively little is known about the molecular mechanisms that control hyponasty. In our study we applied a forward genetic approach in which we isolated and characterized an activation-tagged *Arabidopsis thaliana* line with enhanced hyponastic response to ethylene and shade. We found that ectopic expression of the core cell cycle gene *CYCLINA2;1* causes its phenotype. Further analyses of cell cycle-related events during hyponasty indicated that ethylene triggers a reduction in cell division by affecting transcription of the core cell cycle machinery at the abaxial side of the petiole. Together with results presented in Chapter 2, these findings indicate that ethylene-induced hyponasty is a response in which one signalling component has a dual role within the same tissue; stimulation of cell expansion and inhibition of cell division.

INTRODUCTION

Plant growth and reproduction are influenced by various environmental factors. Many plant species have acquired acclimation mechanisms to increase their survival chances under unfavourable conditions. Among the strategies employed by plants to escape adverse conditions is a particular type of leaf movement called hyponastic

growth (reviewed in Chapter 1 and in Van Zanten *et al.,* 2010). Hyponasty is an upward leaf movement driven by unequal growth rates between ad- and abaxial sides of the petiole. Repositioning of leaves to a more vertical position allows plants to avoid complete submergence or shade, thereby restoring contact with the atmosphere and light, respectively (Voesenek and Blom, 1989, Cox *et al.,* 2004; Pierik *et al.,* 2005). *Arabidopsis thaliana* exhibits a marked hyponastic response upon several environmental signals, *e.g.* submergence, direct proximity of neighbours, shade or supra-optimal temperatures (Ballaré and Scopel, 1997; Hangarter *et al.,* 1997; Millenaar *et al.,* 2005, 2009; Pierik *et al.*, 2005; Mullen *et al.,* 2006; Benschop *et al.,* 2007; Koini *et al.,* 2009; Van Zanten *et al.,* 2009b). The volatile phytohormone ethylene plays a primary role in the regulatory network of responses to submergence and shade (Banga *et al*., 1997; Pierik *et al*., 2003, 2004). The complex interactions between ethylene and other plant hormones, *e.g*. abscisic acid, gibberellin or auxin in the control of hyponasty in *Arabidopsis* is relatively well understood (reviewed in Van Zanten *et al*., 2010) and the cellular basis for hyponasty in *Rumex palustris* and *Arabidopsis* has been characterized. It has been shown that longitudinal cell expansion in the proximal part of the abaxial side of the petiole is a driving force in upwards petiole movement in both species (Cox *et al*., 2004; Polko *et al*., 2011, Chapter 2). Downstream molecular targets of ethylene in this response remain largely unknown.

The tight control and coordination of the cell cycle allows growth and differentiation of all living organisms. Two major events, cell division (mitosis – M) and DNA replication (synthesis – S) are preceded by the so called gap phases G2 and G1, respectively. During the post-mitotic G1, and pre-mitotic G2, cells undergo a series of complex processes allowing completion of the preceding phase and entry into the following (reviewed in Inzé and De Veylder, 2006). Cyclin-Dependent Kinases (CDKs) are integral general components of the progression control between subsequent phases of the cell cycle. Their inactive state is removed once they bind to their cyclin (CYC) partners. The conformational changes triggered by CYC binding to CDKs are a central step in the process of kinase activation (Jeffrey *et al*., 1995). So far, 7 classes of cyclins have been characterized in plants (A – D, H, P and T) (Francis *et al*., 2007) and although some of the cyclins have been shown to interact with CDKs, their precise role in the regulation of cell cycle remains elusive. According to a generally accepted notion A-type cyclins regulate S to M phases, D-type cyclins control the G1/S progression and B-type cyclins are active during the transition between G2 to M and within the M phase itself (reviewed in Inzé and De Veylder, 2006). Four members of the A2-type cyclin family – CYCA2;1, CYCA2;2, CYCA2;3, CYCA2;4 are transcriptionally regulated starting in the S phase, with their expression peak during the G2–M progression. Additionally, they regulate the mitosis-related CDK activity (Shaul *et al*., 1996; Vanneste *et al*., 2011). Expression of CYCA2's has been associated with cells either undergoing mitosis or endoreduplication events (Imai *et al*., 2006). Yoshizumi *et al*. (2006) demonstrated that transcriptional down-regulation of *CYCA2;1* leads to increased ploidy levels and described a role for INCREASED LEVEL OF PLOIDY (ILP) as a central regulator of endocycle regulation. The relation-

ship between the plant cell cycle and stress responses has been reported in a variety of cases. For example, in *Arabidopsis* salt stress results in a transcriptional down-regulation of *CYCA2;1* and *CDC2a* (*CDKA*) genes which in turn regulates the development of lateral roots (Burssens *et al*., 2000b). A similar study by West *et al*. (2004) showed that high salinity strongly reduces the cell cycle activity, thereby affecting root meristem size. Moreover, elicitor-treated *Nicotiana tabacum* cells exhibit down-regulation of cell cycle-related gene expression which might in turn regulate growth inhibition (Suzuki *et al*., 2006; Ohno *et al*., 2011).

To identify novel components controlling upward petiole movement, we followed a forward genetic approach. From a population of 35S Cauliflower Mosaic Virus (CaMV)-promotor tagged plants (Weigel *et al.,* 2000), we selected a line (*SIMILAR INITIAL ENHANCED ETHYLENE ENHANCED LOW LIGHT ANGLE-D* (*SEE-D*)) which shows enhanced hyponasty in response to exogenous ethylene and in low light conditions. The enhanced leaf movement phenotype of *SEE-D* is caused by an ectopic expression of the core cell cycle gene *CYCLINA2;1*. We show that cell cycle-regulatory mechanisms play a crucial role in the control of the petiole hyponasty and that its magnitude is a result of a subtle balance between longitudinal cell expansion and reduction in the mitotic cell cycle.

MATERIALS and METHODS

Plant material and growth conditions

Arabidopsis thaliana lines: Col-0 (N1092), activation-tagged lines (Weigel *et al*., 2000; N21991, N23153), *cyca2;1-1* (Alonso *et al.,*2003; SALK_121077), *cyca2;2-1* (Rosso *et al.,* 2003, GABI_120D03), *ilp1-2, ILP1-1D* (Yoshizumi *et al.,* 2006), *At*TOTF-Ex ERF ectopic expression library (Weiste *et al.,* 2007) were obtained from the Nottingham Arabidopsis Stock Centre or were a gift of the authors who described them (NASC Stock IDs and authors between brackets). *35S::TUA6:GFP* (Ueda *et al.*, 1999) was a gift of Douglas Muench (University of Calgary). For detection of T-DNA inserts in SALK and GABI lines left border specific primers of the T-DNA insert (LBC1, LB_GABI) were used in combination with gene-specific primers. To generate the *35S::CYCA* lines, the full-length cDNAs were cloned through GATEWAY technology (Invitrogen, Gaithersburg, MD, USA) in pDONR221 and sub-cloned into pK2GW7,0 and pKGWFS7,0 respectively (Karimi *et al.,* 2002).

Seeds were sown on moist filter papers and dark-stratified at 4°C for 4 d. Germinated seedlings were potted on a fertilized mixture of soil and perlite (1:2; v/v) and grown at 20°C, 70% (v/v) relative humidity, 200 µmol m^{-2} s^{-1} photosynthetic active radiation (PAR), 9 h short-day photoperiod as described in Millenaar *et al.* (2005). Each day at the start of the photoperiod plants were automatically watered until saturation.

Forward genetic screen

To facilitate easy and fast screening, we first checked if *Arabidopsis* Columbia (Col-0) was able to exhibit a normal low light-induced hyponastic response after 6 h ethylene treatment and an overnight recovery. Ethylene-induced hyponastic growth was, as expected, quickly reversed by removing the ethylene source (Millenaar *et al.,* 2005) and this treatment did not interfere with low light-induced hyponasty in the subsequent photoperiod (data not shown). In total, 17.500 individual Cauliflower Mosaic Virus (CaMV) 35S enhancer (activation) tagged (Weigel *et al.,* 2000) vegetative plants in developmental stage 3.7 (Boyes *et al.,* 2001), pooled in batches of approximately 500 plants each, were screened. The plants were visually monitored for i) initial petiole angles, ii) petiole angle after 6 h ethylene treatment and after overnight recovery iii) the petiole angle after 6 h low light treatment.

Cloning of the *SEE-D* T-DNA locus

To identify the T-DNA locus in *SEE-D*, TAIL-PCR was conducted as described by Liu *et al.* (1995a, b). Genomic-DNA was isolated using Nucleon Phytopure DNA extraction kit, (GE Healthcare/Amersham, Den Bosch, the Netherlands). Subsequent TAIL-PCR was conducted using the degenerate primer: AD2; 5'- NGTCGASWGANAWGAA-3', TTCWTNTCWSTCGACN; (Liu *et al.,* 1995a, b) in combination with nested primers from the Left-border: 5'-ATCTAAGCCCCCATTTGGAC-3' (primary PCR); 5'-TAACGCTGCGGACATCTACA-3' (secondary PCR); 5'-CGGACATGAAGCCATTTACA-3' (tertiary PCR). PCR products were separated on agarose gel. Excised bands containing DNA were purified using a GFX-spin column (GE Healthcare/Amersham) and subjected to direct sequencing (Macrogen, Seoul, South-Korea) using the tertiary PCR primer.

Ethylene, low light and pharmacological treatments

30 d-old plants in stage 3.9 (Boyes *et al.*, 2001) were used for all experiments. One day before the start of the experiments plants were transferred to the experimental setup with similar conditions to the growth chambers (Microclima 1750 growth cabinet; Snijders Scientific, Tilburg, the Netherlands). Ethylene (Hoek Loos, Amsterdam, the Netherlands) application started (t=0 h) 1.5 h after the beginning of the photoperiod. The setup was flushed with 1.5 μL L^{-1} ethylene with a continuous flow of 75 L h^{-1}. The control treatment was done in the same experimental cabinet. For low light treatment PAR-level of 200 μmol m^{-2} s^{-1} was decreased to 20 μmol m^{-2} s^{-1} using spectrally neutral shade cloth. Light quality remained unaffected (checked with a LI-COR 1800 spectro-radiometer (LI-COR, Lincoln, NE, USA)).

Petiole angle measurements

Side pictures were taken (Canon PowerShot A530) at the start of the experiment, after 6 h of ethylene/low light/control treatment. Petiole angles were measured relative to the horizontal plane and the rosette base, using ImageJ software (Abramoff *et al.*, 2004). The differential angle was calculated as a difference between the angle

of ethylene treated petioles and the control at the same time point (Benschop *et al.*, 2007). For petiole kinetics measurements, we used a custom-built automated digital camera system as described in Millenaar *et al*. (2005). Plants were placed in glass cuvettes and side pictures were taken every 10 min for 24h in constant light. Petiole angles were measured with the use of a custom made macro (KS400, Carl Zeiss Vision, Hallbergmoos, Germany).

Epidermal cell length measurements and calculations

Cell length measurements were performed on epidermal imprints of 1 cm long petioles as described in Chapter 2 with the use of a custom made macro in KS400 software (Carl Zeiss Vision, Hallbergmoos, Germany). To allow calculations of average cell sizes relative to the distance along the petiole, each cell was assigned to a 200 µm class, according to its position relative to the proximal part (closer to the stem) of the petiole.

Ploidy measurements

Two petioles or petiole segments of two petioles of Col-0 plants were harvested and snap frozen in liquid nitrogen. The material was ground in 200 µl nuclei extraction buffer (CyStain UV precise buffer P; Partec, Münster, Germany) and then diluted in a Staining buffer (CyStain UV precise buffer P; Partec) containing DAPI (4',6-diamidino-2-phenylindole). Samples were analyzed on a Cytoflow ML flow-cytometer (Partec).

Real-Time Reverse Transcriptase-Q-PCR

Tissues were harvested and snap-frozen in liquid nitrogen. RNA was isolated using the RNeasy Plant Mini Kit (Qiagen, Leusden, the Netherlands). Genomic DNA was removed using the DNA-Free kit (Ambion, Cambridgeshire, United Kingdom). Superscript III RNaseH$^-$ Reverse Transcriptase (Invitrogen, Breda, the Netherlands) with Random-Hexamer Primers, was used for cDNA synthesisis. Real-Time RT- PCR reactions were performed on a MyiQ Single-Color Real-Time PCR Detection System and Software using iQ SYBR Green Supermix Fluorescein (Bio-Rad laboratories, Veenendaal, the Netherlands). Primers for *SEE-D* T-DNA flanking genes are described in Table S6.1. Primers for A2-Cyclin genes and cycle-specific genes are derived from Richard *et al.* (2001), Mariconti *et al.* (2002) and Yoshizumi *et al,* (2006). Relative mRNA values were calculated using the comparative cycle threshold (C_t) method described by Livak and Schmittgen (2001), expressing mRNA values relative to *ß-Tubulin-6* (At5g12250, 5'-ATAGCTCCCCGAGGTCTCTC-3', 5'-TCCATCTCGTCCATTCCTTC-3'; Czechowski *et al.*, 2004).

Visualization of cortical microtubules

Arrangement of cortical micro tubules (CMTs) was performed as described as in Polko *et al.,* 2011 and Chapter 2. For this aim, visualizing microtubules in a *35S::CYCA2;1* background, we crossed *35S::CYCA2;1* with *35S::TUA6:GFP* reporter lines (Ueda *et al.*, 1999). 30 d-old plants in stage 3.9 (Boyes *et al.*, 2001) were subjected to ethylene/control treatment and at 5-10 h of the treatment CMTs of petiole epidermal cells were visualized using an inverted confocal laser scanning microscope (Leica CS SPII, 63x C-apochromat objective, excitation wavelength of 488 nm, collecting at 505-530 nm for GFP emission). Petioles were divided in 4 parts depending on their distance from the base and the abaxial and adaxial sides were observed separately. CMT areas at least twice as long as cell width were taken into account (Himmelspach and Nick, 2001). The CMTs were grouped in categories relatively to the long cell axis: transverse (0°), oblique 30°, oblique 60°, longitudinal (90°) and randomly oriented according to (Himmelspach and Nick, 2001).

Theoretical analysis of cell division rates

The model that we used to predict cell division rates from measured cell lengths is similar to the one used in Chapter 2. As a first step we fitted a function to describe the petiole shape, using the measured petiole angle data describing the initial angle at which the petiole emerges from the shoot, and the final angle at the intersection between the petiole and the leaf blade (see **Fig. S6.1** and **Table S6.2** for used parameters).

In the next step, we fitted a function to the measured cell lengths along the petiole. Moreover, we tested for significant differences in cell length before and after ethylene and control treatments for each 200 µm interval along the petiole. Given that along the adaxial side we hardly found significant differences, we decided to fit all adaxial cell length data collectively to a single overarching function. In contrast, the abaxial cell length data, which are significantly different in the proximal part of the petiole, were fitted for each individual dataset (cell length data per genotype per time point and per treatment) independently, although we did introduce an extra constraint to the fitting, requiring that the maximum cell length (in the distal part of the petiole) would be the same for the different datasets, given that no significant differences could be found along this part of the petiole (see **Fig. S6.2** and **Table S6.2**).

In the next step, the curve fitted to the petiole angle for the 'start' (T0) data was divided into 200 µm sections. To each section a circular arc was fitted, and by combining the curve of the arc with the function fitted to the measured cell lengths, the number of adaxial and abaxial cells per section could be calculated. (See **box S6.1** and **Table S6.2**). We started from the null hypothesis that no cell divisions at all took place during the treatments. The number of cells per section before treatment combined with the function describing the adaxial and abaxial cell lengths for the 10 h control and 10 h ethylene treatments allows us to calculate a predicted petiole shape after treatment. The deviation from the predicted petiole shape to the observed

shape allowed us to predict adaxial or abaxial cell division. (See **box S6.2**). The thus obtained cell division rates represent relative rather than absolute values.

RESULTS

Isolation and cloning of *SEE-D*

To identify novel genetic components involved in hyponastic growth in *Arabidopsis*, we conducted a forward genetic screen using a population of 35S CaMV promoter-tagged Columbia (Col-0) plants (derived from Weigel *et al.,* 2000). Among the selected lines one candidate had an initial petiole angle similar to wild type Col-0 and an exaggerated response to both ethylene and low light treatment (**Fig. 6.1a**).

Therefore, this line was designated *SIMILAR INITIAL ENHANCED ETHYLENE ENHANCED LOW LIGHT ANGLE-D (SEE-D*). Its enhanced hyponastic growth was confirmed by a quantitative analysis of the response kinetics using a time-lapse digital camera setup (**Fig. 6.1b, c**). To check the number of T-DNA insertions in *SEE-D,* BASTA resistance in self-pollinated heterozygous *SEE-D* plants was scored. The segregation resulted in a 3:1 ratio (77.3±2.0 resistant), indicating that a single T-DNA integration locus in *SEE-D* is responsible for its phenotype (data not shown). The T-DNA flanking borders were amplified by Thermal Asymmetric Interlaced-PCR (TAIL-PCR; Liu *et al.,* 1995a, b) and sequencing revealed that the insertion locus is on chromosome 5 in the intergenic region between *ETHYLENE RESPONSE FACTOR/ APETALA2* (ERF/AP2 transcription factor subfamily B-6; *SHINE3/WAX INDUCER1*) (*SHN/WIN1*; At5g25390, *ERF5*; Nakano *et al.,* 2006) and the core cell cycle gene *CYCLINA2;1* (*CYCA2;1*; At5g25380) (**Fig. 6.2a**).

To identify the most likely candidate explaining the *SEE-D* phenotype, we measured transcript levels of the genes within 15 kb up- and downstream of the T-DNA integration site. A cluster of five genes surrounding the insertion site (four downstream and one upstream) were markedly up regulated in comparison to the wt including the T-DNA flanking genes; *SHN3/WIN1* and *CYCA2;1* (**Fig. 6.2b**). Since ETHYLENE RESPONSE FACTORs (ERFs) control many developmental and physiological processes in *Arabidopsis,* together with several ethylene-mediated responses (Nakano *et al.,* 2006; Chapter 5), we first tested if *SHN3/WIN1* (also known as *ERF5*) could be responsible for the enhanced differential petiole growth of *SEE-D.* Ectopic over expression of *SHN3/WIN1* (*35S::At5g25390;* isolated from the collection of Weiste *et al*., 2007) did not result in an altered hyponastic response upon ethylene (**Fig. 6.2c**), indicating that over-expression of other gene(s) is causal to the *SEE-D* phenotype.

A2-cyclins redundantly control ethylene-induced hyponastic growth

To test if *CYCLINA2;1* (*CYCA2;1*; At5g25380) could be causal for the enhanced petiole

angle in *SEE-D*, we generated plants expressing *CYCA2;1* under control of the constitutive 35S CaMV promoter. Three individual transformants with enhanced expression of *CYCA2;1* were isolated (**Fig. S6.3**) and one of them (Hmz B, further referred to as *35S::CYCA2;1*; **Fig. S6.3**) was used for further studies. The *35S::CYCA2;1* exhibited an enhanced hyponastic growth under ethylene treatment (**Fig. 6.2d**), comparable to *SEE-D.* Other CYCA2 members and various marker genes for specific stages of the cell cycle (based on Yoshizumi *et al*., 2006) were not regulated in *SEE-D* (**Fig. 6.3a**).

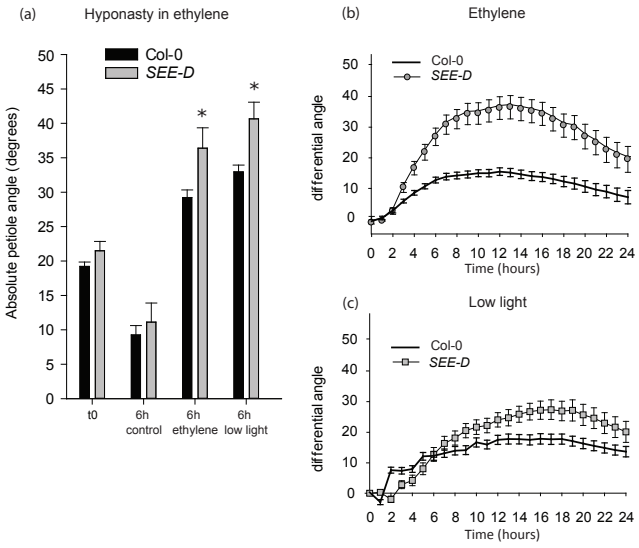

Fig. 6.1. (**a**) Hyponastic response in *SEE-D* and Col-0 at the start of the experiment, after 6h of control/ethylene/low light treatment. (**b**) Kinetics of Col-0 and SEE-D petiole angle in ethylene and (**c**) low light Data points represent average petiole angle ± SE. Asterisks indicate significant differences (P<0.05, n=10-20).

Interestingly, two independent mutant alleles of *cyca2;1* (Yoshizumi *et al.,* 2006) also showed an enhanced hyponastic growth response (**Fig. 6.3b, c**). Possibly, loss of *cyca2-1* is compensated for by an up-regulation of other *CYCA2*s genes in this mutant (Vandepoele *et al.,* 2002; Pillitteri *et al.,* 2007). To confirm the role of CYCA2 in controlling hyponastic growth, we tested the activation-tagged line *INCREASED LEVEL OF POLYPLOIDY1-1D* (*ILP1-1D*), which has reduced expression of all four A2-type cyclin genes (Yoshizumi *et al.,* 2006). Indeed, this line exhibited a substantially reduced hyponastic growth response **(Fig. 6.3d**). In contrast, the *ilp1-2* mutant allele (Yoshizumi *et al.,* 2006), with enhanced expression of all *CYCA2*s showed an increased petiole angle in response to ethylene treatment (**Fig. 6.3e**). To examine if *CYCA2;1* is regulated at a transcriptional level by ethylene and to asses if this corresponds with expression changes in the mitotic marker gene - *CYCB1;1*, we conducted RT-PCR after 3 hours of ethylene treatment using different fragments of a petiole (proximal ad- and abaxial; distal ad- and abaxial). Transcription of both genes was down-regulated in the proximal part of the petiole. In case of *CYCA2;1,* this reduction takes place in both ad- and abaxial sides of the petiole, whereas significant down-regulation of *CYCB1;1* occurs only in the proximal, abaxial side of the petiole (**Fig. 6.4a, b**). Together, our data demonstrate that *CYCA2;1* over-expression likely causes the *SEE-D* phenotype.

CYCA2 proteins are known to control the balance between mitosis and endoreduplication (Imai *et al*., 2006; Yoshizumi *et al*., 2006). It is well known that ethylene can promote endoreduplication events in plant tissues (Gendreau *et al*., 1999; Dan *et al*., 2003) and that increased ploidy levels can account for development of larger cells (Cheniclet *et al*., 2005; Roeder *et al*., 2010). Therefore, we tested if *SEE-D* and/or *35S::CYCA2;1* show increased petiole ploidy levels, but no such differences were observed as compared to wt Col-0 (**Fig. 6.5a**). Furthermore, we separately analysed proximal and distal fragments of wt petioles exposed to ethylene and con-

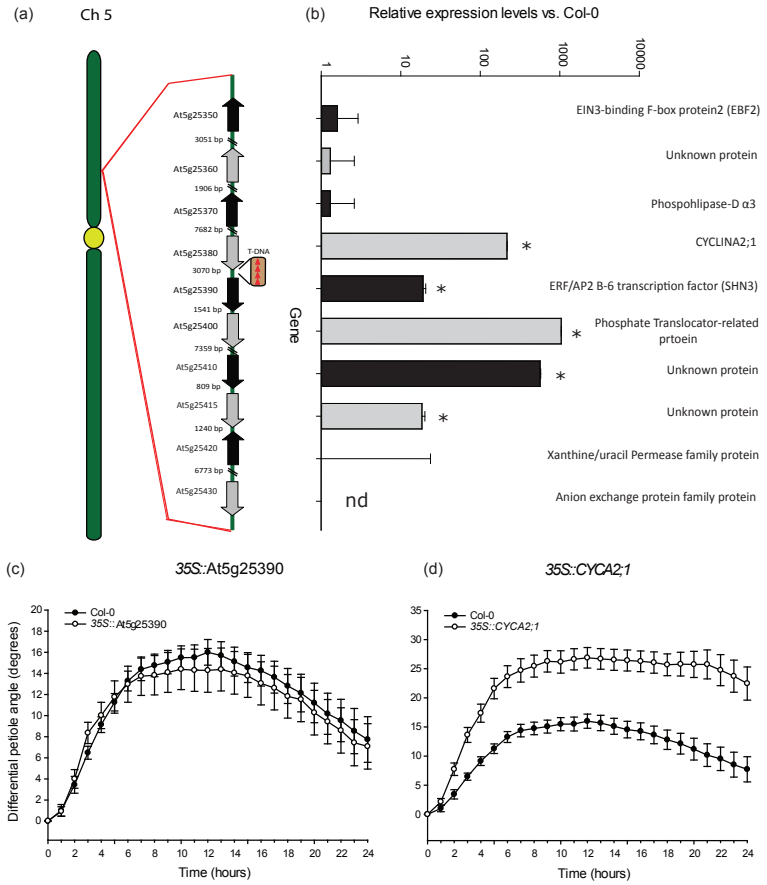

Fig. 6.2. (**a**) Schematic representation of the locus surrounding the T-DNA insertion on chromosome 5 in the *SEE-D* line. Genes (AGI-codes on the left hand side) are represented by arrows indicating the direction of transcription. (**b**) *SEE-D* expression values of genes in the vicinity of the T-DNA insert. Data points represent mean expression values ±SE of the corresponding genes from panel (**a**). Asterisks indicate significant differences compared to transcription in control plants ($P<0.05$, $n\geq4$). (**c-d**) Kinetics of petiole angle in ethylene in (**c**) *35S::At5g2390* and (**d**) *35S::CYCA2;1*. Data points represent average petiole angle ± SE, n=10-20.

trol conditions to verify if ethylene changes the endoreduplication state. Interestingly, this revealed slight differences in DNA content between proximal and distal parts of the petiole, but this was not influenced by ethylene (**Fig. 6.5b**). Therefore, we conclude that enhanced hyponasty in *SEE-D* and *35S::CYCA2;1* is not caused by

(ethylene-mediated) differences in ploidy levels.

35S::CYCA2;1 exhibits wild type-like epidermal cell expansion in ethylene

To test if exaggerated ethylene-induced hyponasty in *35S::CYCA2;1* is due to more pronounced epidermal cell expansion in comparison to wt Col-0, we examined epi-

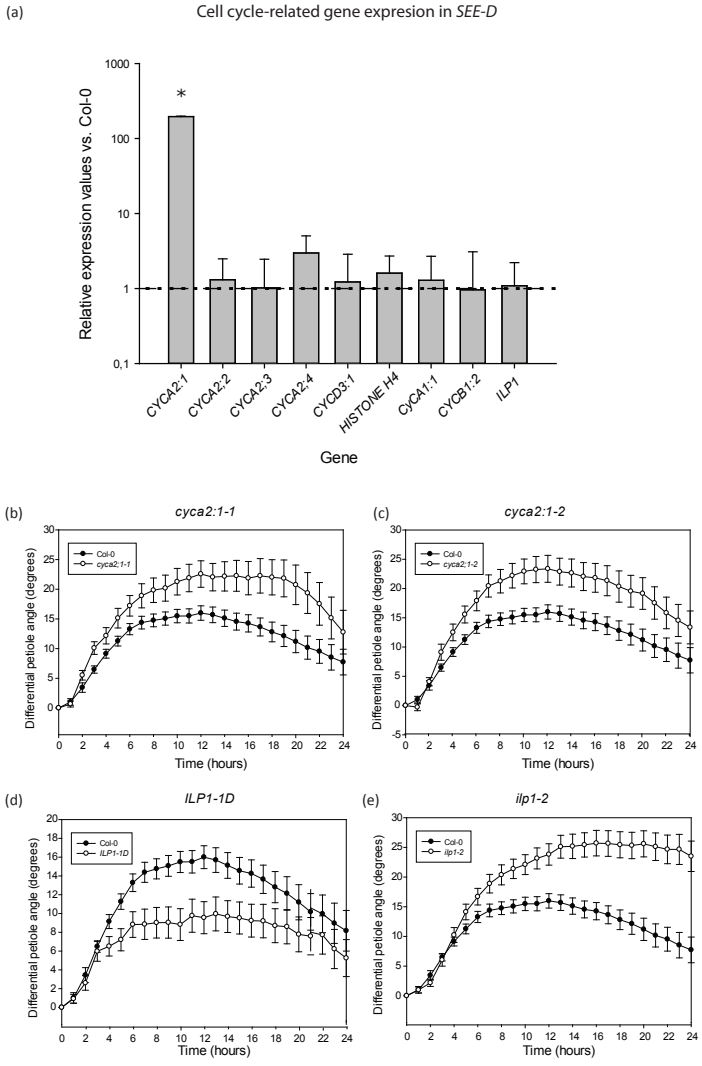

Fig. 6.3. (**a-d**) Kinetics of hyponastic response in (**a**) *cyca2;1-1*, (**b**) *cyca2;1-2*, (**c**) *ILP1-1D* and *ilp1-2*. Data points represent average petiole ±SE, *n*=10-20. (**e**) Expression of cell cycle-related genes in SEE-D. Data points represent mean expression values ± SE. Asterisks indicate significant differences (P<0.05, n≥4).

dermal imprints of ad- and abaxial sides of the *35S::CYCA2;1* petiole in ethylene and control conditions. Interestingly, longitudinal cell expansion in *35S::CYCA2;1* petioles resembles the pattern observed in wt Col-0 when exposed to ethylene (**Fig. 6.6a,** b; for comparison with wt Col-0 see Chapter 2, **Fig. 2.2b, c**). The significant abaxial cell elongation occurs approximately within the first 2 mm of the petiole which

is also observed in Col-0. Additionally, we examined the arrangement of CMTs in the background of *35S::CYCA2;1.* Despite some minor differences in the orientation of CMTs between *35S::CYCA2;1* and Col-0, mostly in ethylene-treated petioles, the overall patterns in both genotypes is highly similar (**Fig. S6.4**). These results show no substantial difference in neither cell expansion nor rearrangements of CMTs between Col-0 and *35S::CYCA2;1.*

Inhibition of cell division is a prerequisite for ethylene-induced petiole angle change

According to the mathematical model presented in Chapter 2, a reduction in cell division at the abaxial side of a petiole contributes to the changes in petiole angle upon ethylene exposure. We predict a reduction of cell division up to 17% in the proximal part of the abaxial side of the petiole. As a consequence, the final predicted petiole angle is 23.1, whereas the observed angle 22.0 degrees (**Fig. 2.6,** for details see Supporting methods **S2.1**). To examine the degree to which the mitotic activity of cells changes in both Col-0 and *35S::CYCA2;1* we calculated the predicted cell division rates in both genotypes upon ethylene and control treatment. The predicted cell division rates are shown in **Fig. 6.7.** Cell division is presented as the percentage of difference between adaxial and abaxial cell division rate. A value of 0 represents a situation where adaxial cell division is equal to abaxial cell division. Positive values indicate more adaxial cell divisions and negative values indicate more abaxial cell divisions. For the wt control treatment our model predicts a bias towards adaxial cell divisions in the proximal part of the petiole. In contrast, this bias is not observed for the *35S::CYCA2;1* line. After the ethylene treatment we predict an enhanced (~40%) bias towards adaxial cell divisions in the wt Col-0. This means that either adaxial cell division is increased or abaxial cell division is decreased. Such an effect is not observed in the *35S::CYCA2;1* line, where the cell division profile after ethylene treatment is very comparable with the cell division profile after the control treatment. In general, the effect of ethylene treatment is predominantly observed

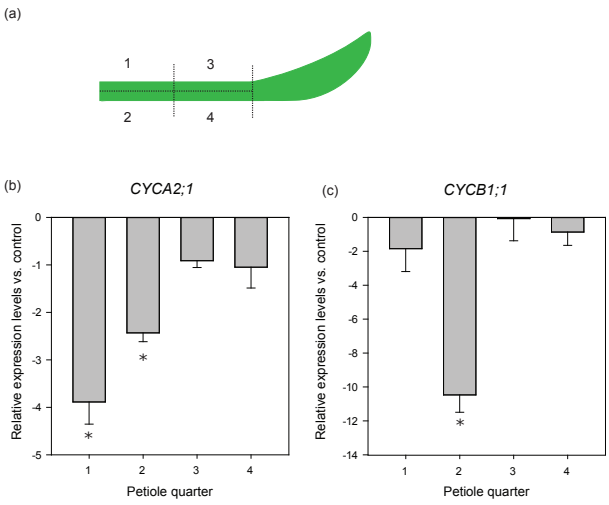

Fig. 6.4. (**a**) Schematic representation of plant material used for gene expression analysis in petiole quarters. (**b-c**). Expression of (**b**) *CYCA2;1* and (**c**) *CYCB1;1* in petiole quarters upon 3h ethylene exposure. Data points represent mean relative expression values ± SE. Asterisks indicate significant differences (P<0.05, n=6).

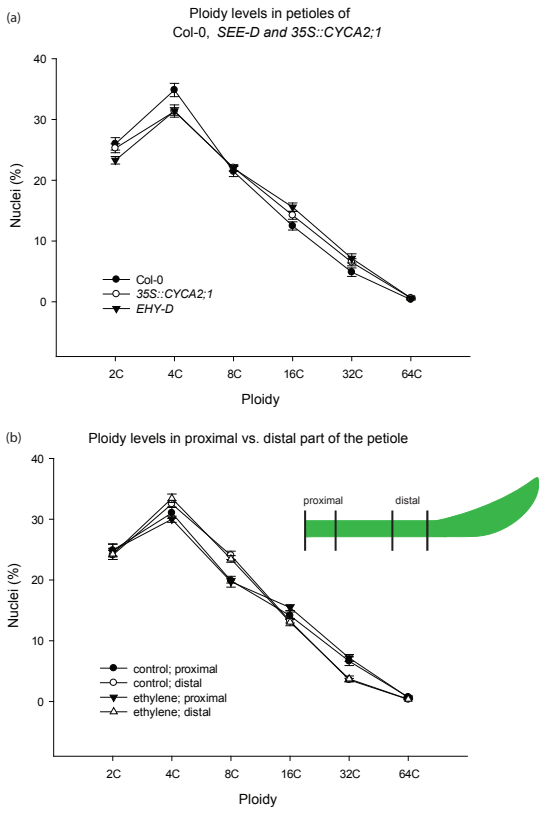

Fig. 6.5. (**a, b**) Ploidy values in (**a**) petioles of Col-0, *SEE-D* and *35S::CYCA2;1* in control conditions; (**b**) in proximal (black symbols) and distal (white symbols) sections of Col-0 petioles in control (circles) and ethylene (triangles) treatment. Data points represent a mean fraction (%) of nuclei ± SE, *n*=6-8.

in the more proximal petiole zone, with hardly any noticeable differences in the more distal part of the petiole.

DISCUSSION

Hyponastic growth is an active process by which a plant repositions its leaves to a more vertical position. Longitudinal cell expansion in a localized zone at the abaxial side of the petiole is a driving force during ethylene-induced hyponasty in *Arabidopsis* (Chapter 2). To identify molecular regulators of this nastic movement, we conducted a forward genetic screen of activation-tagged plants, which led to an identification of *SEE-D*, with enhanced petiole angle in ethylene and low light. Weigel *et al*. (2000) showed that activation-tagged lines often exhibit over-expression of a range of genes in the proximity of the T-DNA. The analysis of gene expression in the vicinity of the T-DNA in *SEE-D* revealed a significant up-regulation of five genes flanking the insertion. Because ERFs are known to control several responses to abiotic stresses (Chapter 5; Karaba *et al*., 2007; Fukao and Bailey-Serres, 2008; Trujillo *et al*., 2008; Abogadallah *et al*., 2011; Fukao *et al*., 2011; Yang *et al*., 2011), *SHN3/WIN1* (*ERF5*) was a likely candidate. However, targeted over-expression of this specific gene did not lead to enhanced hyponastic growth as observed in *SEE-D.* Further analysis of the *35S::CYCA2;1* line demonstrated that increased expression of the plant specific *CYCA2;1* gene does result in enhanced hyponasty in ethylene.

A2-type cyclins are required for cell cycle progression and function as specific regulatory subunits of Cyclin-Dependent Kinase (CDK)-complexes, which control the transition from S-to-G2 *in planta* (Roudier *et al.,* 2000, 2004; Inzé and De Veylder, 2006). They are, among other cyclins, expressed throughout the plant life cycle and required for vascular-differentiation and patterning (Burssens *et al.,* 2000a). As shown by interaction and co-overexpression analyses (Boudolf *et al*., 2009), CYCA2;3 in complex with CDKB1;1, is also involved in G2-to-M transition. Recently, Vanneste *et al*. (2011) demonstrated that individual *CYCA2* genes are often

expressed in an overlapping manner. Other studies indicated that loss of function in one of the A-type cyclins can lead to a (over)compensation of other, highly redundant family members (Fisher and Nurse, 1996; Vandepoele *et al.,* 2002; Pilliterri *et al.,* 2007). This compensation could explain our observation of enhanced hyponasty in single *cyca2;1-1* and *cyca2;1-2* mutants.

To gain more insight into the spatial transcriptional regulation of cell-cycle related genes during hyponasty in ethylene, we examined the expression of *CYCA2;1* together with a mitotic cyclin, *CYCB1;1*, in specific segments of a petiole. Interestingly, the expression of both genes is significantly down-regulated in a part of the petiole where, in ethylene-induced hyponasty, cell elongation occurs (Chapter 2, **Fig. 2.2c**). This suggests that the increased longitudinal cell expansion is associated with a reduction of cell cycle progression in that particular region of a petiole. This is consistent with a recently reported negative effect of ethylene on cell cycle progression during drought stress (Skirycz *et al*., 2011), which results in a growth repression

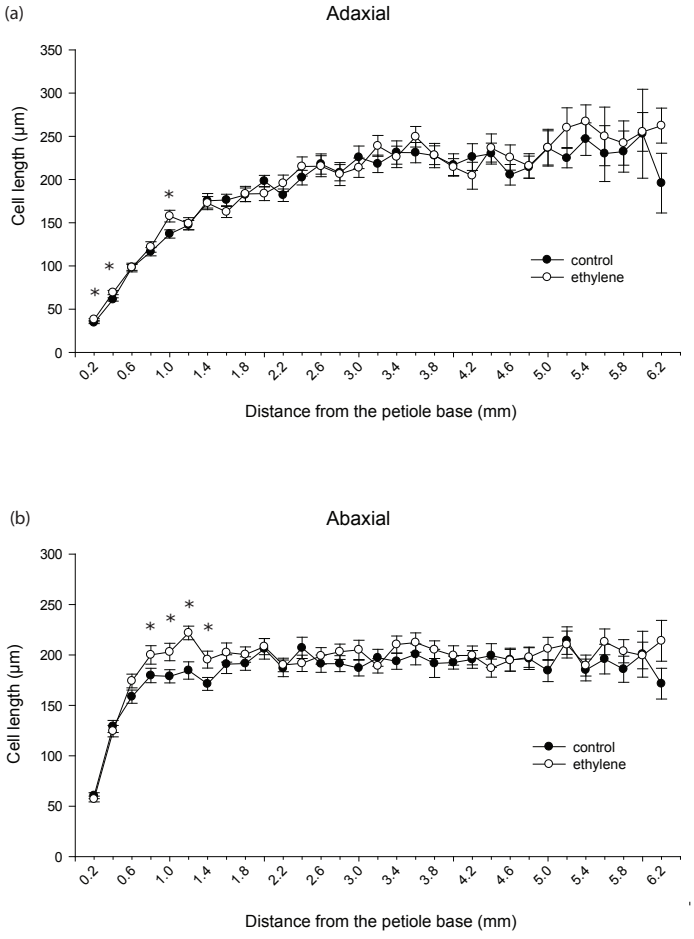

Fig. 6.6. Epidermal cell length for 1 cm petioles of the *35S::CYCA2;1* line at the (**a**) ad- and (**b**) abaxial side in 10h control (black circles) and 10h ethylene (white circles) treatment. Data points represent the mean cell length ± SE of the first 6.2 mm of a petiole. Asterisks indicate significant differences between cell length in ethylene and control conditions (P<0.05) n=13-15.

of early developing leaves in a reversible manner. Likewise, during hyponasty, ethylene-induced inhibition of cell divisions, tentatively through the observed control

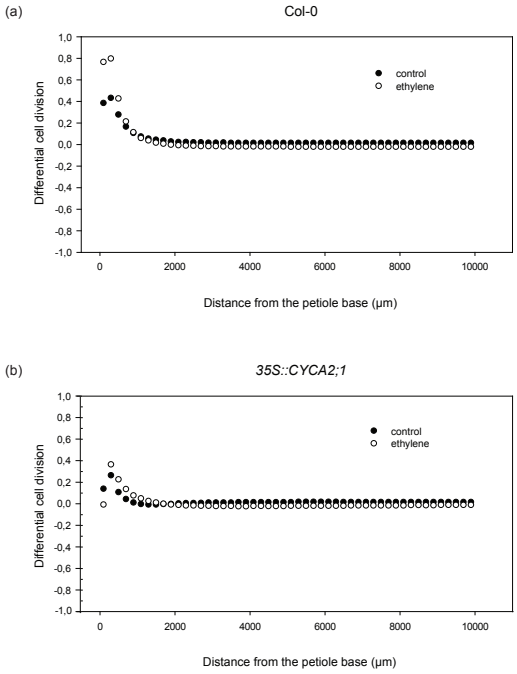

Fig. 6.7. Relative cell division during control and ethylene treatment. Values above 0 indicate that adaxial cell division is predominant; values below 0 indicate that abaxial cell division is predominant.

of cyclins, reduces abaxial petiole growth thereby preventing excessive hyponastic growth.

Although inhibition of cyclins will slow down cell cycle progression and thereby cell divisions, it can in specific instances also result in endoreduplication, a process in which subsequent DNA replication rounds occur without cell division (reviewed in Sugimoto-Shirasu and Roberts, 2003; John and Qi, 2008). Endoreduplication is often associated with larger cells, e.g. in suspensor of *Phaseolus sp.* (Nagl, 1976) or *Brassica oleracea* petals (Kudo and Kimura, 2002) but the exact mechanism of this correlation is unknown. Because changes in expression of A2-type cyclins are known to affect endocycle entry (Burssens *et al.,* 2000a; Dewitte and Murray, 2003; Yu *et al.,* 2003; Yoshizumi *et al*., 2006; Imai *et al.,* 2006; Boudolf *et al.,* 2009), we tested ploidy levels in petioles of *SEE-D* and *35S::CYCA2* lines in comparison to wt Col-0. The results indicate similar constitutive endoreduplication levels. However, because ethylene on its own can induce endoreduplication events in hypocotyls of *Cucumis sativus* (Gendrau *et al.,* 1999; Dan *et al.,* 2003), we also verified the effect of ethylene on ploidy levels in different sections of petioles. We did not observe differences between untreated petioles and 6h ethylene-treated plants and controls. Therefore, it is unlikely that ethylene-induced hyponastic growth is regulated by the effect of *CYCA2;1* via the endocycle. These results are in agreement with Kozuka *et al.* (2005) who studied DNA content in petioles exposed to darkness which leads to both differential petiole growth and non-differential petiole elongation. The authors demonstrated that petiole elongation in the dark is driven by cell expansion and that this process is not correlated with altered ploidy levels in the petiole. Importantly, endoreduplication is likely to drive cell growth (increase in cytoplasmic macromolecular mass) rather than cell expansion (increase in cell volume *via* vacuolation) (Sugimoto-Shirasu and Roberts, 2003). Taken the time-frame of ethylene-induced hyponasty (observed within 2 h after start of ethylene treatment) and previous results (Chapter 2), it is unlikely that macromolecular cell growth would be an important factor during petiole movement, whereas cell expansion can be regulated very rapidly.

35S::CYCA2;1 was found not to have any substantial increase of cell expansion relative to wt Col-0, despite its exaggerated hyponastic response to ethylene. This lack of enhanced cell expansion is consistent with the fact that its CMT reorientation in ethylene is not different from wt Col-0. Therefore, it is likely that enhanced hyponasty in *35S::CYCA2;1* is due to mitotic cell cycle/cell division. Indeed, based on a combination of experimental studies and mathematical modelling, we predicted in Chapter 2 that ethylene-induced hyponasty in wt Col-0 is partly constrained by an ethylene-induced inhibition of cell division rates at the abaxial, proximal zone of the petiole. Similar modelling exercises using the experimental data provided here confirm an increased ratio of adaxial/abaxial cell division rates in ethylene-exposed wt Col-0. The data in **Fig. 6.7** give a clear indication of the influence of ethylene treatment and constitutive *CYCA2;1* expression on cell division rates. For ethylene treatment we observe a relative increase of adaxial cell divisions. Theoretically, this could be caused by an increase in adaxial cell division, a decrease of abaxial cell division or a combination of both. Since a decrease in abaxial *CYCA2;1* expression was measured, the latter scenario is more likely. It is also in line with the prediction of reduced cell division at the abaxial petiole side presented in Chapter 2 (Supporting information). According to our findings, upon a constitutive over-expression of *CYCA2;1* no clear change in in cell division can be observed due to ethylene treatment. In conclusion, this analysis and the analysis discussed in Chapter 2 both indicate that while enhanced cell elongation provides the extra tissue required to bend the petiole upwards, the magnitude of hyponastic growth is controlled by regulating cell division. It appears that ethylene, while triggering hyponastic petiole movement, prevents an excessive response by reducing adaxial cell division rates. It is likely that the switch between mitotic cycle activity and cell expansion are the two major processes regulating hyponasty in ethylene.

The increasing number of studies indicating a dual role of ethylene in plant development continue to lend support to the idea that ethylene is not a straightforward growth inhibitor, but rather inhibits or stimulates growth in a more subtle way that integrates information about environmental conditions and developmental state (reviewed in Pierik *et al.,* 2006). The data presented in this chapter demonstrate that ethylene induces inhibition of the mitotic cell cycle while at the same time promoting longitudinal cell expansion in the exact same proximal region of the abaxial side of a petiole. This fine-tuning appears to be of great importance during hyponastic petiole movement since the lack of cell division inhibition in *35S::CYCA2;1* line leads to increased hyponasty. To our knowledge, this is the first study showing inhibitory and stimulatory functions of ethylene on two growth-control processes simultaneously involved in regulating one response.

Chapter 6

CHAPTER 7

General discussion

Phenotypic plasticity, defined as the ability of an individual genotype to display various phenotypes (Bradshaw, 1965), allows all living organisms to effectively adjust to dynamic environments. The relatively large morphological plasticity of plants in comparison to animals, is related to two major aspects of their development: i) the existence of meristems which throughout a plant's lifetime constantly generate new cells and ii) the organization of a basic body plan which consists of reiterating semi-independent subunits. Paradoxically, the early studies on plant organ movements claimed their alleged resemblance to animal behaviour (reviewed in Whippo and Hangarter, 2009). Modern plant science focuses on different aspects of this phenomenon, namely, the regulatory networks controlling organ repositioning. The occurrence of a physical reorientation of an organ or a part of it is the final result of a number of events tightly regulated on molecular, physiological and cellular levels. The subject of this dissertation is ethylene-induced hyponastic growth in *Arabidopsis thaliana*. Hyponasty consists of an upward organ (in this case – petiole) movement and in natural environments is a part of responses to *e.g*. neighbour proximity, flooding or elevated temperatures. Previous reports have demonstrated that *Arabidopsis* is an ideal model system in studying the genetic and molecular basis of petiole movement (Pierik *et al*., 2005, Millenaar *et al*., 2007, 2009). The functionality of this response has been recently reviewed in Van Zanten *et al*. (2010a). An interplay between several plant hormones – ethylene (ET), abscisic acid (ABA) and auxin during hyponastic growth in *Rumex palustris* and *Arabidopsis* has been mostly elucidated (Cox *et al*., 2003; Benschop *et al*., 2007; Millenaar *et al*., 2007). The aim of the current study was to provide new insights into the molecular regulation of ethylene-induced hyponasty and link it to the developmental alterations that plants follow to modify their phenotypes. The novelties brought about by this project will be further discussed in light of existing knowledge. This will be done by first addressing upstream signalling events in ethylene-induced plasticity, followed by a discussion of the cellular localisation and cell growth processes that contribute to this response.

UPSTREAM SIGNALLING EVENTS

The research presented in Chapter 5 resulted in an identification of several ERF candidates involved in hyponasty. Importantly, our data indicate that their function can be both inhibitory and stimulatory to the response, as different candidate lines display enhanced or decreased petiole angles in ethylene. Furthermore, the expression of two potentially positive regulators of hyponasty, *ERF95* and *ERF112*, increases in the first hour of ethylene treatment. We did not detect significant mRNA reduction of studied ERFs, but this might be due to sensitivity of our technique which could

miss out on down-regulation of already low-abundant transcripts. The involvement of ERFs in abiotic and biotic stress responses has been previously shown for a variety of cases, including submergence responses (Xu *et al*., 2006; Fukao *et al*., 2008, 2011), drought and salt stress (Karaba *et al*., 2007; Trujillo *et al*., 2008; Abogadallah *et al*., 2011). Hattori *et al*. (2009) showed that submergence of some deepwater rice varieties triggers transcriptional up-regulation of the ERF-encoding *SNORKEL* genes which, via gibberellic acid (GA), induce internode elongation. Recent studies proved that the oxygen-sensing mechanism in plants relies on the N-end rule pathway of a targeted proteolysis of the group VII ERFs (Licausi *et al*., 2011, Gibbs *et al*. 2011). Despite their name, not all ERFs are ethylene-inducible and studies show that their involvement ranges from regulation of developmental processes to stress-related responses such as the ones mentioned above. Similar to our observations, antagonistic relationships between closely related ERFs have been previously demonstrated for rice. The master regulator of the quiescence strategy during submergence in some cultivars of rice, *SUBMERGENCE1A-1* (*SUB1A-1*), confers submergence tolerance. Its growth-restricting and energy-reducing role is achieved through limiting mRNA levels of another allele of the same gene, *SUB1C* which, together with gibberellic acid (GA), positively influences internode elongation. Moreover, *SUB1A-1* inhibits ethylene synthesis by a negative feedback mechanism (Fukao *et al*., 2006, Xu *et al*., 2006). In our study, several ERF over-expression lines exhibited elevated ethylene levels. It is likely that similar complex interrelations between ERFs and regulation of endogenous ethylene levels are also taking place during hyponastic growth.

What are the likely downstream components of ERF action in ethylene-induced hyponasty? The antagonizing relationship between ethylene and abscisic acid (ABA) has been reported during submergence-induced hyponasty and petiole elongation in *R. palustris* (Cox *et al*., 2004; Benschop *et al*., 2005). Moreover, internode elongation in the deepwater rice requires a decline in ABA levels and up-regulation of GA (Hoffmann-Benning and Kende, 1992; Kende *et al*., 1998) and a negative effect of ABA in ethylene-induced hyponasty in *Arabidopsis* has been reported (Benschop *et al*., 2007). As shown by studies on development of tobacco seedlings, an ERF protein, TOMATO STRESS RESPONSIVE FACTOR1 (TSR1), positively regulates ABA-related developmental processes. A recent work by Yaish *et al*., 2010 demonstrated the interaction between rice AP2-like transcription factor gene, *OsAP2-39*, and ABA. OsAP2-39 binds to the promoter sequence of a key ABA-biosynthesis gene, *OsNCED-1* (encoding the 9-cis-epoxycarotenoid dioxygenase), indirectly affecting seed germination rates and internode development. In Chapter 4 we show that brassinosteroids (BRs) play a crucial role in induction of hyponasty and that it is likely through their stimulation of cell expansion. Experiments on seed germination strongly suggest that ABA inhibits BR outputs and that this interaction is independent of the BR receptor complex and acts through primary ABA signalling components (Zhang *et al*., 2009). So far, to our knowledge no direct link between ERFs and BRs has been demonstrated, but one cannot exclude an indirect ERF-BR link via ABA signalling.

LOCALISED GROWTH

As presented in Chapter 2, the cellular mechanism driving hyponasty depends on the longitudinal cell expansion of cells in the proximal region of the abaxial side of the petiole. According to our mathematical model, the observed increase in cell size is sufficient to drive hyponasty (Fig. 2.2 and 2.6). The cells examined in this study are likely to follow expansion-related events since their enlargement is coupled with up-regulation of the *EXPANSIN11* gene which is expected to facilitate cell wall loosening (Lee *et al*., 2001). The presented results are consistent with previous observations by Cox *et al*. (2004) which indicated a similar mechanism in petioles of submerged *R. palustris.* An analogous situation was described for tepals of *Tulipa sp*. and *Crocus sp*. in which opening and closing of flowers is driven by cell expansion differences related to their ad- and/or abaxial identity (Wood, 1953). One logical upstream candidate involved in stimulation of cell expansion would be the general growth promoting hormone in above-ground tissues, auxin. Its role in regulating cell expansion has been shown for a tremendous number of biological processes (reviewed in Abel and Theologis, 2010) including organ movements, such as epinasty in *Solanum lycopersicum* (Keller *et al*., 1997). Studies on submergence-induced hyponasty in *R. palustris* also demonstrated a clear involvement of auxin (Cox *et al*., 2004). Previous research has shown that the role of auxin in ethylene-induced hyponasty in *Arabidopsis* remains elusive. The disruption of polar auxin transport (PAT) and use of several PAT-related mutants and mutant combinations did not result in an inhibition of hyponasty in ethylene (Millenaar *et al*., 2009; Van Zanten *et al*., 2009). This led to the speculation that it would not be the long-distance PAT but a local auxin activity which is required for this type of a differential growth. Although the involvement of auxin in ethylene-induced hyponasty is thus still speculative, in this thesis (Chapter 4) evidence is provided for involvement of yet another hormone, brassinosteroid (BR), which shares various molecular targets with auxin (Bao *et al*., 2004; Nemhauser *et al*., 2004; Vert *et al*., 2008). It is especially likely since the mutant line used in our study, which is allelic to *rot3-1*, lacks ethylene-induced cell elongation. *ROT3* has been previously associated with polar cell expansion in *Arabidopsis* leaves and petioles, as reported by Tsuge *et al*. (1996) and Kim *et al*. (1998, 1999). Based on dose-response assays on seedling hypocotyls, we suggest that ethylene might sensitize the tissue for BR action and, therefore, indirectly stimulate cell expansion. A growth-stimulating effect of BR during petiole elongation was also shown in response to light signals (Kozuka *et al*., 2010).

Another aspect highlighted in this project concerns down-regulation of the cell cycle. In Chapter 6, it was demonstrated that the over-expression of *CYCA2;1* leads to enhanced petiole angles in ethylene. It was also shown that, in a wild-type situation, ethylene causes an inhibition of the expression of cell cycle-related genes and that this reduction is required for regulating the magnitude of hyponastic growth. The exact mechanism of this mitotic cycle interplay is not yet known. One might speculate that it could be achieved through the interaction between ERFs and

components of the cell cycle machinery. Such interactions have been reported by, *e.g*. Ikeda *et al*. (2006) who showed that ENHANCER OF SHOOT REGENERATION 2 (ESR2) directly targets CYCLIND1;1 (CYCD1;1), thereby activating cell cycle and promoting shoot regeneration. Moreover, an over-expression of an ERF gene, *BOLITA*, reduces cell proliferation possibly through interaction with *RETINOBLASTOMA-RELATED* (*RBR*) and *CYCLIND* genes (Marsh-Martinez *et al*., 2006). Because BRs have only been reported to maintain regular cell cycle progression (Miyazawa *et al*., 2003; Hacham *et al*., 2011, Gonzalez-Garcia *et al*., 2011), their role in this particular interaction remains ambiguous.

CONCLUSIONS and FUTURE PERSPECTIVES

Experiments from the last decade have significantly contributed to our understanding of the mechanisms driving differential petiole growth. The goal of this thesis was to advance the knowledge on the molecular regulation of hyponasty and examine it from a developmental angle. Not surprisingly, far downstream in the machinery, it employs the regulation of cell expansion and mitotic cell cycle, which ultimately contribute to the (organ) growth of any living organism. One of the remaining challenges is to connect all the known players into a fine network of interactions, especially regarding the upstream ERF regulators. Further research should focus on establishing their precise localisation within a petiole and identification of their direct targets. Another interesting question concerns the ethylene-BR interaction and whether ethylene only modulates tissue sensitivity to BRs or if it simultaneously affects BR biosynthesis.

A major question regarding the cellular aspect of hyponasty still remains: why a particular group of cells expands and whether similar expansion patterns are present in hyponastic responses induced by other stimuli. It could be a matter of sensitivity to an inducing signal together with the developmental potential of responding cells. This point could be experimentally addressed by *e.g.*, a specific and localised inhibition of cell expansion and studying responses of the adjacent cells. Such precise inhibition could result in two possible outcomes: i) either a complete suppression of hyponasty or ii) the maintenance of hyponasty due to neighbouring cells adopting the function in driving petiole movement. The dual role of ethylene as a growth stimulator and growth inhibitor within the same organ contributes to the realisation of subtle processes regulating plant responses to stress. A multidisciplinary approach with detailed genetic and molecular analyses will further contribute to the understanding of plant organ movement phenomena.

REFERENCES

Abel S, Theologis A. 2010. Odyssey of Auxin. *Cold Spring Harbor Perspectives in Biology.*

Abeles FB, Morgan PW, Saltveit ME. 1992. Ethylene in plant biology. *Ethylene in plant biology.* 2nd edition. San Diego USA: Academic Press.

Abeles FB, Rubinstein B. 1964. Regulation of ethylene evolution and leaf abscission by auxin. *Plant Physiol.* **39**: 963-969.

Abogadallah GM, Nada RM, Malinowski R, Quick P. 2011. Overexpression of *HARDY*, an AP2/ERF gene from *Arabidopsis*, improves drought and salt tolerance by reducing transpiration and sodium uptake in transgenic *Trifolium alexandrinum* L. *Planta* **233**: 1265-1276.

Abramoff MD, Magelhaes PJ, Ram SJ. 2004. Image processing with ImageJ. **11**: 36-42.

Aharoni A, Dixit S, Jetter R, Thoenes E, van Arkel G, Pereira A. 2004. The SHINE clade of AP2 domain transcription factors activates wax biosynthesis, alters cuticle properties, and confers drought tolerance when overexpressed in *Arabidopsis*. *Plant Cell* **16**: 2463-2480.

Allen RD. 1969. Mechanism of the Seismonastic Reaction in Mimosa pudica. *Plant Physiol.* **44**: 1101-1107.

Alonso J, Stepanova A, Leisse T, Kim C, Chen H, Shinn P, Stevenson D, Zimmerman J, Barajas P, Cheuk R, Gadrinab C, Heller C, Jeske A, Koesema E, Meyers C, Parker H, Prednis L, Ansari Y, Choy N, Deen H, Geralt M, Hazari N, Hom E, Karnes M, Mulholland C, Ndubaku R, Schmidt I, Guzman P, Aguilar-Henonin L, Schmid M, Weigel D, Carter D, Marchand T, Risseeuw E, Brogden D, Zeko A, Crosby W, Berry C, Ecker J. 2003. Genome-wide Insertional mutagenesis of *Arabidopsis thaliana*. *Science* **301**: 653-657.

Alonso JM, Ecker JR. 2006. Moving forward in reverse: genetic technologies to enable genome-wide phenomic screens in *Arabidopsis*. *Nat. Rev. Genet.* **7**: 524-536.

Altmann T. 1998. Recent advances in brassinosteroid molecular genetics. *Curr. Opin. Plant Biol.* **1**: 378-383.

Altmann T. 1998. A tale of dwarfs and drugs: brassinosteroids to the rescue. *Trends Genet.* **14**: 490-495.

Anker L. 1972. Circumnutation of *Avena* coleoptile, its autonomous nature and its interference with geotropic reaction. *Acta Bot. Neerl.* **21**: 71-76.

Apelbaum A, Burg SP. 1972. Effect of ethylene on cell division and deoxyribonucleic acid synthesis in *Pisum sativum*. *Plant Physiol.* **50**: 117-124.

Apelbaum A, Burg SP. 1971. Altered cell microfibrillar orientation in ethylene-treated *Pisum sativum* stems. *Plant Physiol.* **48**: 648-652.

Arteca RN, Tsai DS, Schlagnhaufer C, Mandava NB. 1983. The effect of brassinosteroid on auxin-induced ethylene production by etiolated mung bean segments. *Physiol. Plantarum* **59**: 539-544.

Asami T, Min Y, Nagata N, Yamagishi K, Takatsuto S, Fujioka S, Murofushi N,

Yamaguchi I, Yoshida S. 2000. Characterization of brassinazole, a triazole-type brassinosteroid biosynthesis inhibitor. *Plant Physiol.* **123**: 93-99.
Bailey-Serres J, Voesenek LACJ. 2008. Flooding stress: Acclimations and genetic diversity. *Annual Review of Plant Biology* **59**: 313-339.
Bajguz A. 2007. Metabolism of brassinosteroids in plants. *Plant Physiol. Biochem.* **45**: 95-107.
Balasubramanian S, Sureshkumar S, Lempe J, Weigel D. 2006. Potent induction of *Arabidopsis thaliana* flowering by elevated growth temperature. *Plos Genetics* **2**: 980-989.
Ballaré CL. 1994. Light gaps: Sensing the light opportunities in highly dynamic canopy environments. In: Caldwell MM, and Pearcy RW, eds. *Exploitation of heterogeneity by plants.* London:Academic Press, 73-110.
Ballaré CL, Sanchez RA, Scopel AL, Casal JJ, Ghersa CM. 1987. Early detection of neighbor plants by phytochrome perception of spectral changes in reflected sunlight. *Plant Cell and Environment* **10**: 551-557.
Ballaré CL, Scopel AL. 1997. Phytochrome signalling in plant canopies: Testing its population-level implications with photoreceptor mutants of *Arabidopsis*. *Funct. Ecol.* **11**: 441-450.
Ballaré CL, Scopel AL, Roush ML, Radosevich SR. 1995. How plants find light in patchy canopies. A comparison between wild-type and phytochrome-B-deficient mutant plants of cucumber. *Funct. Ecol.* **9**: 859-868..
Ballaré CL, Scopel AL, Sanchez RA. 1997. Foraging for light: Photosensory ecology and agricultural implications. *Plant Cell Environ.* **20**: 820-825.
Ballaré CL, Scopel AL, Sanchez RA. 1990. Far-red radiation reflected from adjacent leaves - an early signal of competition in plant canopies. *Science* **247**: 329-332.
Banga M, Bogemann GM, Blom CWPM, Voesenek LACJ. 1997. Flooding resistance of *Rumex* species strongly depends on their response to ethylene: Rapid shoot elongation or foliar senescence. *Physiol. Plantarum* **99**: 415-422.
Banga M, Slaa EJ, Blom CWPM, Voesenek LACJ. 1996. Ethylene biosynthesis and accumulation under drained and submerged conditions - a comparative study of two *Rumex* species. *Plant Physiol.* **112**: 229-237.
Banno H, Ikeda Y, Niu Q, Chua N. 2001. Overexpression of *Arabidopsis ESR1* induces initiation of shoot regeneration. *Plant Cell* **13**: 2609-2618.
Bao F, Shen JJ, Brady SR, Muday GK, Asami T, Yang ZB. 2004. Brassinosteroids interact with auxin to promote lateral root development in *Arabidopsis*. *Plant Physiol.* **134**: 1624-1631.
Barry CS, Giovannoni JJ. 2007. Ethylene and fruit ripening. *J. Plant Growth Regul.* **26**: 143-159.
Baskin TI. 2001. On the alignment of cellulose microfibrils by cortical microtubules: a review and a model. *Protoplasma* **215**: 150-171.
Baskin TI, Wilson JE, Cork A, Williamson RE. 1994. Morphology and microtubule organization in *Arabidopsis* roots exposed to oryzalin or taxol. *Plant Cell Physiol.* **35**: 935-942.

Beaudoin N, Serizet C, Gosti F, Giraudat J. 2000. Interactions between abscisic acid and ethylene signaling cascades. *Plant Cell* **12**: 1103-1115.
Behringer F, Medford J. 1992. A plasmid rescue technique for the recovery of plant DNA disrupted by T-DNA insertion. *Plant Molecular Biology Reporter* **10**: 190-198.
Benschop JJ, Bou J, Peeters AJM, Wagemaker N, Guhl K, Ward D, Hedden P, Moritz T, Voesenek LACJ. 2006. Long-term submergence-induced elongation in *Rumex palustris* requires abscisic acid-dependent biosynthesis of gibberellin. *Plant Physiol.* **141**: 1644-1652.
Benschop JJ, Millenaar FF, Smeets ME, van Zanten M, Voesenek LACJ, Peeters AJM. 2007. Abscisic acid antagonizes ethylene-induced hyponastic growth in *Arabidopsis. Plant Physiol.* **143**: 1013-1023.
Bentley DR. 2006. Whole-genome re-sequencing. *Curr. Opin. Genet. Dev.* **16**: 545-552.
Bleecker A, Estelle M, Somerville C, Kende H. 1988. Insensitivity to ethylene conferred by a dominant mutation in *Arabidopsis thaliana*. *Science* **241**: 1086-1089.
Boniotti M, Griffith M. 2002. "Cross-talk" between cell division cycle and development in plants. *Plant Cell* **14**: 11-16.
Boualem A, Fergany M, Fernandez R, Troadec C, Martin A, Morin H, Sari M, Collin F, Flowers JM, Pitrat M, Purugganan MD, Dogimont C, Bendahmane A. 2008. A conserved mutation in an ethylene biosynthesis enzyme leads to andromonoecy in melons. *Science* **321**: 836-838.
Boudolf V, Lammens T, Boruc J, Van Leene J, Van Den Daele H, Maes S, Van Isterdael G, Russinova E, Kondorosi E, Witters E, De Jaeger G, Inzé D, De Veylder L. 2009. CDKB1;1 forms a functional complex with CYCA2;3 to suppress endocycle onset. *Plant Physiol.* **150**: 1482-1493.
Boyes DC, Zayed AM, Ascenzi R, McCaskill AJ, Hoffman NE, Davis KR, Gorlach J. 2001. Growth stage-based phenotypic analysis of *Arabidopsis*: A model for high throughput functional genomics in plants. *Plant Cell* **13**: 1499-1510.
Braam J. 2005. In touch: plant responses to mechanical stimuli. *New Phytol.* **165**: 373-389.
Bradshaw AD. 1965. Evolutionary significance of phenotypic plasticity in plants. *Advances in Genetics* **12**: 115-155.
Brauner L. 1954. Tropisms and nastic movements. *Annu. Rev. Plant Physiol. Plant Mol. Biol.* **5**: 163-182.
Brenner WG, Romanov GA, Kollmer I, Burkle L, Schmulling T. 2005. Immediate-early and delayed cytokinin response genes of *Arabidopsis thaliana* identified by genome-wide expression profiling reveal novel cytokinin-sensitive processes and suggest cytokinin action through transcriptional cascades. *Plant Journal* **44**: 314-333.
Briggs W, Huala E. 1999. Blue-light photoreceptors in higher plants. *Annu. Rev. Cell Dev. Biol.* **15**: 33-62.
Brown A, Chapman D, Lewis R, Venditti AL. 1990. Circumnutation of sunflower hypocotylsin satelite orbit. *Plant Physiology* **94**: 233-238.
Burg SP. 1973. Ethylene in plant growth. *Proc. Natl. Acad. Sci. U. S. A.* **70**: 591-597.
Burg SP, Burg EA. 1962. Role of ethylene in fruit ripening. *Plant Physiol.* **37**: 179-

189.
Burg S, Burg E. 1966. Auxin-induced ethylene formation - its relation to flowering in pineapple. *Science* **152**: 1269.
Burssens S, Engler JD, Beeckman T, Richard C, Shaul O, Ferreira P, Van Montagu M, Inzé D. 2000. Developmental expression of the *Arabidopsis thaliana* CycA2;1 gene. *Planta* **211**: 623-631.
Burssens S, Himanen K, van de Cotte B, Beeckman T, Van Montagu M, Inzé D, Verbruggen N. 2000. Expression of cell cycle regulatory genes and morphological alterations in response to salt stress in *Arabidopsis thaliana*. *Planta* **211**: 632-640.
Cano-Delgado A, Yin YH, Yu C, Vafeados D, Mora-Garcia S, Cheng JC, Nam KH, Li JM, Chory J. 2004. BRL1 and BRL3 are novel brassinosteroid receptors that function in vascular differentiation in *Arabidopsis*. *Development* **131**: 5341-5351.
Cao H, Chen S. 1993. Brassinosteroid-induced rice lamina joint inclination and its relation to auxin and ethylene. *Plant Physiol.* **102**: 63-63.
Cao Y, Song F, Goodman RM, Zheng Z. 2006. Molecular characterization of four rice genes encoding ethylene-responsive transcriptional factors and their expressions in response to biotic and abiotic stress. *J. Plant Physiol.* **163**: 1167-1178.
Cashmore A, Jarillo J, Wu Y, Liu D. 1999. Cryptochromes: Blue light receptors for plants and animals. *Science* **284**: 760-765.
Catterou M, Dubois F, Schaller H, Aubanelle L, Vilcot B, Sangwan-Norreel BS, Sangwan RS. 2001. Brassinosteroids, microtubules and cell elongation in *Arabidopsis thaliana*. I. Molecular, cellular and physiological characterization of the *Arabidopsis* bull mutant, defective in the delta 7-sterol-C5-desaturation step leading to brassinosteroid biosynthesis. *Planta* **212**: 659-672.
Cheniclet C, Rong W, Causse M, Frangne N, Bolling L, Carde J, Renaudin J. 2005. Cell expansion and endoreduplication show a large genetic variability in pericarp and contribute strongly to tomato fruit growth. *Plant Physiol.* **139**: 1984-1994.
Christie J, Reymond P, Powell G, Bernasconi P, Raibekas A, Liscum E, Briggs W. 1998. *Arabidopsis* NPH1: A flavoprotein with the properties of a photoreceptor for phototropism. *Science* **282**: 1698-1701.
Chuck G, Muszynski M, Kellogg E, Hake S, Schmidt RJ. 2002. The control of spikelet meristem identity by the branched silkless1 gene in maize. *Science* **298**: 1238-1241.
Clouse SD. 2011. Brassinosteroid signal transduction: from receptor kinase activation to transcriptional networks regulating plant development. *Plant Cell* **23**: 1219-1230.
Collings DA, Lill AW, Himmelspach R, Wasteneys GO. 2006. Hypersensitivity to cytoskeletal antagonists demonstrates microtubule-microfilament cross-talk in the control of root elongation in *Arabidopsis thaliana*. *New Phytol.* **170**: 275-290.
Cosgrove DJ. 2005. Growth of the plant cell wall. *Nat. Rev. Mol. Cell Biol.* **6**: 850-861.
Cosgrove DJ. 1989. Characterization of long-term extension of isolated cell walls from growing cucumber hypocotyls. *Planta* **177**: 121-130.
Coté GG. 1995. Signal transduction in leaf movement. *Plant Physiol.* **109**: 729-734.

Cox MC, Benschop JJ, Vreeburg RAM, Wagemakers CAM, Moritz T, Peeters AJM, Voesenek LACJ. 2004. The roles of ethylene, auxin, abscisic acid, and gibberellin in the hyponastic growth of submerged *Rumex palustris* petioles. *Plant Physiol.* **136**: 2948-2960.

Cox MCH, Millenaar FF, van Berkel YEMD, Peeters AJM, Voesenek LACJ. 2003. Plant movement. Submergence-induced petiole elongation in *Rumex palustris* depends on hyponastic growth. *Plant Physiol.* **132**: 282-291.

Crocker W, Knight L. 1908. Effect of illuminating gas and ethylene upon flowering carnations - Contributions from the hull botanical laboratory.. *Bot. Gaz.* **46**: 259-276.

Cronn R, Liston A, Parks M, Gernandt DS, Shen R, Mockler T. 2008. Multiplex sequencing of plant chloroplast genomes using Solexa sequencing-by-synthesis technology. *Nucleic Acids Res.* **36**: e122.

Crowell EF, Gonneau M, Vernhettes S, Hofte H. 2010. Regulation of anisotropic cell expansion in higher plants. *C. R. Biol.* **333**: 320-324.

Czechowski T, Bari RP, Stitt M, Scheible WR, Udvardi MK. 2004. Real-time RT-PCR profiling of over 1400 *Arabidopsis* transcription factors: unprecedented sensitivity reveals novel root- and shoot-specific genes. *Plant Journal* **38**: 366-379.

Da Silva EAA, Toorop PE, Van Lammeren AAM, Hilhorst HWM. 2008. ABA inhibits embryo cell expansion and early cell division events during coffee (*Coffea arabica* 'Rubi') seed germination. *Annals of Botany* **102**: 425-433.

Dan H, Imaseki H, Wasteneys G, Kazama H. 2003. Ethylene stimulates endoreduplication but inhibits cytokinesis in cucumber hypocotyl epidermis. *Plant Physiol.* **133**: 1726-1731.

Darwin C, Darwin F. 1880. *The power of movement in plants.* London: John Murray.

Daxinger L, Hunter B, Sheik M, Jauvion V, Gasciolli V, Vaucheret H, Matzke M, Furner I. 2008. Unexpected silencing effects from T-DNA tags in *Arabidopsis*. *Trends Plant Sci.* **13**: 4-6.

De Grauwe L, Vandenbussche F, Tietz O, Palme K, Van Der Straeten D. 2005. Auxin, ethylene and brassinosteroids: tripartite control of growth in the *Arabidopsis* hypocotyl. *Plant Cell Physiol.* **46**: 827-836.

De Veylder L, Beeckman T, Beemster GTS, Krols L, Terras P, Landrieu I, Van der Schueren E, Maes S, Naudts M, Inzé D. 2001. Functional analysis of cyclin-dependent kinase inhibitors of *Arabidopsis*. *Plant Cell* **13**: 1653-1667.

Deslauriers SD, Larsen PB. 2010. FERONIA Is a Key Modulator of Brassinosteroid and Ethylene Responsiveness in *Arabidopsis* Hypocotyls. *Molecular Plant* **3**: 626-640.

Dewitt TJ, Sih A, Wilson DS. 1998. Costs and limits of phenotypic plasticity. *Trends Ecol. Evol.* **13**: 77-81.

Dewitte W, Murray JAH. 2003. The plant cell cycle. *Annual Review of Plant Biology* **54**: 235-264.

Dinneny J, Yadegari R, Fischer R, Yanofsky M, Weigel D. 2004. The role of JAGGED in shaping lateral organs RID C-1418-2008. *Development* **131**: 1101-1110.

Divi UK, Rahman T, Krishna P. 2010. Brassinosteroid-mediated stress tolerance in *Arabidopsis* shows interactions with abscisic acid, ethylene and salicylic acid pathways. *BMC Plant. Biol.* **10**: 151.

Djakovic-Petrovic T, de Wit M, Voesenek LACJ, Pierik R. 2007. DELLA protein function in growth responses to canopy signals. *Plant J.* **51**: 117-126.
Dolan L. 1997. The role of ethylene in the development of plant form. *J. Exp. Bot.* **48**: 201-210.
Domagalska MA, Sarnowska E, Nagy F, Davis SJ. 2010. Genetic analyses of interactions among gibberellin, abscisic acid, and brassinosteroids in the control of flowering time in *Arabidopsis thaliana*. *PloS One* **5**: e14012.
Donnelly PM, Bonetta D, Tsukaya H, Dengler RE, Dengler NG. 1999. Cell cycling and cell enlargement in developing leaves of *Arabidopsis*. *Dev. Biol.* **215**: 407-419.
Doubt SL. 1917. The response of plants to illuminating gas. *Botanical Gazette* **63**: 209-224.
Edwards ME, Miller JH. 1972. Growth regulation by ethylene in fern gametophytes .2. Inhibition of cell-division. *Am. J. Bot.* **59**: 450-457.
Ehleringer J, Forseth I. 1980. Solar tracking by plants. *Science* **210**: 1094-1098.
Eisinger W, Croner LJ, Taiz L. 1983. Ethylene-induced lateral expansion in etiolated pea stems - kinetics, cell-wall synthesis, and osmotic potential. *Plant Physiol.* **73**: 407-412.
Elliott R, Betzner A, Huttner E, Oakes M, Tucker W, Gerentes D, Perez P, Smyth D. 1996. *AINTEGUMENTA*, an APETALA2-like gene of *Arabidopsis* with pleiotropic roles in ovule development and floral organ growth. *Plant Cell* **8**: 155-168.
Evidente A, Sparapano L, Motta A, Giordano F, Fierro O, Frisullo S. 1996. A phytotoxic pimarane diterpene of *Sphaeropsis sapinea* f sp *Cupressi*, the pathogen of a canker disease of cypress. *Phytochemistry* **42**: 1541-1546.
Feng JX, Liu D, Pan Y, Gong W, Ma LG, Luo JC, Deng XW, Zhu YX. 2005. An annotation update via cDNA sequence analysis and comprehensive profiling of developmental, hormonal or environmental responsiveness of the *Arabidopsis* AP2/EREBP transcription factor gene family. *Plant Mol. Biol.* **59**: 853-868..
Finlayson S, Lee I, Morgan P. 1998. Phytochrome B and the regulation of circadian ethylene production in sorghum. *Plant Physiol.* **116**: 17-25.
Firn RD, Digby J. 1980. The establishment of tropic curvatures in plants. *Annu. Rev. Plant Physiol. Plant Mol. Biol.* **31**: 131-148.
Fisher DL, Nurse P. 1996. A single fission yeast mitotic cyclin B p34(cdc2) kinase promotes both S-phase and mitosis in the absence of G(1) cyclins. *EMBO J.* **15**: 850-860.
Fluhr R, Mattoo AK. 1996. Ethylene - Biosynthesis and perception. *Crit. Rev. Plant Sci.* **15**: 479-523.
Foster R, Mattsson O, Mundy J. 2003. Plants flex their skeletons. *Trends Plant Sci.* **8**: 202-204.
Francis D, Sorrell D. 2001. The interface between the cell cycle and plant growth regulators: a mini review. *Plant Growth Regul.* **33**: 1-12.
Francis D. 2007. The plant cell cycle - 15 years on. *New Phytol.* **174**: 261-278.
Franklin KA. 2009. Light and temperature signal crosstalk in plant development. *Curr. Opin. Plant Biol.* **12**: 63-68.

Franklin KA. 2008. Shade avoidance. *New Phytol.* **179**: 930-944.
Fujita M, Himmelspach R, Hocart CH, Williamson RE, Mansfield SD, Wasteneys GO. 2011. Cortical microtubules optimize cell-wall crystallinity to drive unidirectional growth in *Arabidopsis*. *Plant Journal* **66**: 915-928.
Fukao T, Bailey-Serres J. 2008. Submergence tolerance conferred by Sub1A is mediated by SLR1 and SLRL1 restriction of gibberellin responses in rice. *Proc. Natl. Acad. Sci. U. S. A.* **105**: 16814-16819.
Fukao T, Xu K, Ronald PC, Bailey-Serres J. 2006. A variable cluster of ethylene response factor-like genes regulates metabolic and developmental acclimation responses to submergence in rice(W). *Plant Cell* **18**: 2021-2034.
Fukao T, Yeung E, Bailey-Serres J. 2011. The submergence tolerance regulator sub1a mediates crosstalk between submergence and drought tolerance in rice. *Plant Cell* **23**: 412-427.
Gallego-Bartolome J, Arana MV, Vandenbussche F, Zadnikova P, Minguet EG, Guardiola V, Van der Straeten D, Benkova E, Alabadi D, Blazquez MA. 2011. Hierarchy of hormone action controlling apical hook development in *Arabidopsis*. *Plant Journal* **67**: 622-634.
Gendreau E, Orbovic V, Hofte H, Traas J. 1999. Gibberellin and ethylene control endoreduplication levels in the *Arabidopsis thaliana* hypocotyl. *Planta* **209**: 513-516.
Gendron JM, Wang ZY. 2007. Multiple mechanisms modulate brassinosteroid signaling. *Curr. Opin. Plant Biol.* **10**: 436-441.
Gendron JM, Haque A, Gendron N, Chang T, Asami T, Wang Z. 2008. Chemical genetic dissection of brassinosteroid-ethylene interaction. *Mol. Plant.* **1**: 368-379.
Ghalambor CK, McKay JK, Caroll SP, Reznick DN. 2007. Adaptive versus non-adaptive phenotypic plasticity and the potential for contemporary adaptation in new environments. *Funct. Ecol.* **21**: 394-407.
Gibbs DJ, Lee SC, Isa NM, Gramuglia S, Fukao T, Bassel GW, Correia CS, Corbineau F, Theodoulou FL, Bailey-Serres J, Holdsworth MJ. 2011. Homeostatic response to hypoxia is regulated by the N-end rule pathway in plants. *Nature* **479**: 415-418.
Girardin JPL. 1864. Einfluss des Leuchtgases auf die Promenaden und Strassenbaume. *Agrikultur* **7**: 199-200.
Gniazdowska A, Krasuska U, Bogatek R. 2010. Dormancy removal in apple embryos by nitric oxide or cyanide involves modifications in ethylene biosynthetic pathway. *Planta* **232**: 1397-1407.
Goda H, Sawa S, Asami T, Fujioka S, Shimada Y, Yoshida S. 2004. Comprehensive comparison brassinosteroid-regulated of auxin-regulated and brassinosteroid-regulated genes in *Arabidopsis*. *Plant Physiol.* **134**: 1555-1573.
Goda H, Shimada Y, Asami T, Fujioka S, Yoshida S. 2002. Microarray analysis of brassinosteroid-regulated genes in *Arabidopsis*. *Plant Physiol.* **130**: 1319-1334.
Gonzalez-Garcia M, Vilarrasa-Blasi J, Zhiponova M, Divol F, Mora-Garcia S, Russinova E, Cano-Delgado AI. 2011. Brassinosteroids control meristem size by promoting cell cycle progression in *Arabidopsis* roots. *Development* **138**: 849-859.
Grandjean O, Vernoux T, Laufs P, Belcram K, Mizukami Y, Traas J. 2004. *In vivo* analysis of cell division, cell growth, and differentiation at the shoot apical meristem

in *Arabidopsis*. *Plant Cell* **16**: 74-87.
Gray W, Ostin A, Sandberg G, Romano C, Estelle M. 1998. High temperature promotes auxin-mediated hypocotyl elongation in *Arabidopsis*. *Proc. Natl. Acad. Sci. U. S. A.* **95**: 7197-7202.
Grimoldi A, Insausti P, Roitman G, Soriano A. 1999. Responses to flooding intensity in *Leontodon taraxacoides*. *New Phytol.* **141**: 119-128.
Grove MD, Spencer GF, Rohwedder WK, Mandava N, Worley JF, Warthen JD, Steffens GL, Flippenanderson JL, Cook JC. 1979. Brassinolide, a plant growth-promoting steroid isolated from brassica-napus pollen. *Nature* **281**: 216-217.
Gu YQ, Yang C, Thara VK, Zhou J, Martin GB. 2000. Pti4 is induced by ethylene and salicylic acid, and its product is phosphorylated by the Pto kinase. *Plant Cell* **12**: 771-785.
Guan H, Kang D, Fan M, Chen Z, Qu LJ. 2009. Overexpression of a new putative membrane protein gene *AtMRB1* results in organ size enlargement in *Arabidopsis*. *J. Integr. Plant. Biol.* **51**: 130-139.
Guo H, Li L, Ye H, Yu X, Algreen A, Yin Y. 2009. Three related receptor-like kinases are required for optimal cell elongation in *Arabidopsis thaliana*. *Proc. Natl. Acad. Sci. U. S. A.* **106**: 7648-7653.
Gushwa N, Hayashi D, Kemper A, Abram B, Taylor J, Upton J, Tay C, Fiedler S, Pullen S, Miller L, Tallman G. 2003. Thermotolerant guard cell protoplasts of tree tobacco do not require exogenous hormones to survive in culture and are blocked from reentering the cell cycle at the G1-to-S transition. *Plant Physiol.* **132**: 1925-1940.
Gutierrez R, Lindeboom JJ, Paredez AR, Emons AMC, Ehrhardt DW. 2009. *Arabidopsis* cortical microtubules position cellulose synthase delivery to the plasma membrane and interact with cellulose synthase trafficking compartments. *Nat. Cell Biol.* **11**: 797-806.
Guzman P, Ecker J. 1990. Exploiting the triple response of *Arabidopsis* to identify ethylene related mutants. *Plant Cell* **2**: 513-523.
Hacham Y, Holland N, Butterfield C, Ubeda-Tomas S, Bennett MJ, Chory J, Savaldi-Goldstein S. 2011. Brassinosteroid perception in the epidermis controls root meristem size. *Development* **138**: 839-848..
Halliday KJ. 2004. Plant hormones: the interplay of brassinosteroids and auxin. *Curr. Biol.* **14**: R1008-1010.
Hamant O, Heisler MG, Jonsson H, Krupinski P, Uyttewaal M, Bokov P, Corson F, Sahlin P, Boudaoud A, Meyerowitz EM, Couder Y, Traas J. 2008. Developmental patterning by mechanical signals in *Arabidopsis*. *Science* **322**: 1650-1655.
Hangarter RP. 1997. Gravity, light and plant form. *Plant Cell and Environment* **20**: 796-800.
Hardham AR, Gunning BE. 1978. Structure of cortical microtubule arrays in plant cells. *J. Cell Biol.* **77**: 14-34.
Hart JW. 1990. *Plant tropisms and other growth movements.* London: Unwin Hyman.
Harvey EM. 1915. Some Effects of Ethylene on the Metabolism of Plants. *Bot. Gaz.*

60: 193-214.
Hattori Y, Nagai K, Furukawa S, Song X, Kawano R, Sakakibara H, Wu J, Matsumoto T, Yoshimura A, Kitano H, Matsuoka M, Mori H, Ashikari M. 2009. The ethylene response factors SNORKEL1 and SNORKEL2 allow rice to adapt to deep water. *Nature* **460**:
Haubrick LL, Assmann SM. 2006. Brassinosteroids and plant function: some clues, more puzzles. *Plant. Cell. Environ.* **29**: 446-457.
Haupt W, Feinleib ME. 1979. Physiology of movements*. Enclyclopedia of plant physiology.* Berlin New York: Springer-Verlag.
Hayashi H, Czaja I, Lubenow H, Schell J, Walden R. 1992. Activation of a plant gene by T-dna tagging: auxin-independent growth *in vitro*. *Science* **258**: 1350-1353.
Hayashi T, Maclachlan G. 1984. Pea xyloglucan and cellulose .3. Metabolism during lateral expansion of pea epicotyl cells. *Plant Physiol.* **76**: 739-742.
Hayes A. 1977. Developmental aspects of leaf blade hyponasty. *Botanical Gazette* **138**: 52-55.
Hays D, Reid D, Yeung E, Pharis R. 2000. Role of ethylene in cotyledon development of microspore-derived embryos of *Brassica napus*. *J. Exp. Bot.* **51**: 1851-1859.
He JX, Fujioka S, Li TC, Kang SG, Seto H, Takatsuto S, Yoshida S, Jang JC. 2003. Sterols regulate development and gene expression in *Arabidopsis*. *Plant Physiol.* **131**: 1258-1269.
He JX, Gendron JM, Sun Y, Gampala SSL, Gendron N, Sun CQ, Wang ZY. 2005. BZR1 is a transcriptional repressor with dual roles in brassinosteroid homeostasis and growth responses. *Science* **307**: 1634-1638.
He Z, Wang ZY, Li J, Zhu Q, Lamb C, Ronald P, Chory J. 2000. Perception of brassinosteroids by the extracellular domain of the receptor kinase BRI1. *Science* **288**: 2360-2363.
Hemerly A, Bergounioux C, Vanmontagu M, Inzé D, Ferreira P. 1992. Genes regulating the plant cell cycle - isolation of a mitotic-like cyclin from *Arabidopsis-thaliana*. *Proc. Natl. Acad. Sci. U. S. A.* **89**: 3295-3299.
Heydarian Z, Sasidharan R, Cox MC, Pierik R, Voesenek LACJ, Peeters AJM. 2010. A kinetic analysis of hyponastic growth and petiole elongation upon ethylene exposure in Rumex palustris. *Ann. Bot.* **106**: 429-435.
Himmelspach R, Nick P. 2001. Gravitropic microtubule reorientation can be uncoupled from growth. *Planta* **212**: 184-189.
Hirota A, Kato T, Fukaki H, Aida M, Tasaka M. 2007. The auxin-regulated AP2/EREBP gene *PUCHI* is required for morphogenesis in the early lateral root primordium of *Arabidopsis*. *Plant Cell* **19**: 2156-2168.
Hodick D, Sievers A. 1989. On the mechanism of trap closure of venus flytrap (*Dionaea-muscipula ellis*). *Planta* **179**: 32-42.
Hoffmannbenning S, Kende H. 1992. On the role of abscisic-acid and gibberellin in the regulation of growth in rice. *Plant Physiol.* **99**: 1156-1161.
Hong Z, Ueguchi-Tanaka M, Umemura K, Uozu S, Fujioka S, Takatsuto S, Yoshida S, Ashikari M, Kitano H, Matsuoka M. 2003. A rice brassinosteroid-deficient

mutant, ebisu dwarf (d2), is caused by a loss of function of a new member of cytochrome P450. *Plant Cell* **15**: 2900-2910.
Hu Y, Bao F, Li J. 2000. Promotive effect of brassinosteroids on cell division involves a distinct CycD3-induction pathway in *Arabidopsis*. *Plant J.* **24**: 693-701.
Huber H. 1996. Plasticity of internodes and petioles in prostrate and erect *Potentilla* species. *Funct. Ecol.* **10**: 401-409.
Huck N, Moore JM, Federer M, Grossniklaus U. 2003. The *Arabidopsis* mutant *feronia* disrupts the female gametophytic control of pollen tube reception. *Development* **130**: 2149-2159.
Hush JM, Overall L. 1996. Cortical microtubule reorientation in higher plants: Dynamics and regulation. *Journal of Microscopy-Oxford* **181**: 129-139.
Hutchings MJ, de Kroon H. 1994. Foraging in plants: The role of morphological plasticity in resource acquisition. In: Begon M, andFitter AH, eds. *Advances in ecological research.* london:Academic Press, 159-238.
Iijima T, Sibaoka T. 1985. Membrane-potentials in excitable cells of *Aldrovanda vesiculosa* trap lobes. *Plant Cell Physiol.* **26**: 1-13.
Iino M. 2006. Toward understanding the ecological functions of tropisms: interactions among and effects of light o.n tropisms - Commentary. *Curr. Opin. Plant Biol.* **9**: 89-93.
Ikeda Y, Banno H, Niu Q, Howell SH, Chua N. 2006. The *ENHANCER OFSHOOT REGENERATION2* gene in *Arabidopsis* regulates *CUP-SHAPED COTYLEDON1* at the transcriptional level and controls cotyledon development. *Plant Cell Physiol.* **47**: 1443-1456.
Imai KK, Ohashi Y, Tsuge T, Yoshizumi T, Matsui M, Oka A, Aoyama T. 2006. The A-type cyclin CYCA2;3 is a key regulator of ploidy levels in *Arabidopsis* endoreduplication. *Plant Cell* **18**: 382-396.
Inada S, Shimmen T. 2000. Regulation of elongation growth by gibberellin in root segments of *Lemna minor*. *Plant Cell Physiol.* **41**: 932-939.
Ingemarson B, Eklund L, Eliasson L. 1991. Ethylene effects on cambial activity and cell wall formation in hypocotyls of *Picea abies* seedlings. *Physiol. Plantarum* **82**: 219-224.
Insausti P, Grimoldi A, Chaneton E, Vasellati V. 2001. Flooding induces a suite of adaptive plastic responses in the grass *Paspalum dilatatum*. *New Phytol.* **152**: 291-299.
Inzé D, De Veylder L. 2006. Cell cycle regulation in plant development. *Annu. Rev. Genet.* **40**: 77-105.
Ivanchenko MG, Muday GK, Dubrovsky JG. 2008. Ethylene-auxin interactions regulate lateral root initiation and emergence in *Arabidopsis thaliana*. *Plant Journal* **55**: 335-347.
Jackson MB. 1985. Ethylene and responses of plants to soil waterlogging and submergence. *Annu. Rev. Plant Physiol. Plant Mol. Biol.* **36**: 145-174.
Jackson MB. 1979. Is the diageotropic tomato ethylene deficient. *Physiol. Plantarum* **46**: 347-351.
Jackson MB, Campbell DJ. 1976. Waterlogging and petiole epinasty in tomato - role

of ethylene and low oxygen. *New Phytol.* **76**: 21-29.
Jaffe MJ. 1970. On heliotropism in tendrils of *Pisum sativum* - a response to infrared irradiation. *Planta* **92**: 146-151.
Jaffe MJ, Takahashi H, Biro RL. 1985. A pea mutant for the study of hydrotropism in roots. *Science* **230**: 445-447.
Jaffe M. 1972. Physiological studies on pea tendrils .8. Relationship of circumnutation to contact coiling - with a description of a laboratory intervalometer using integrated digital circuits. *Physiol. Plantarum* **26**: 73-80.
Jeffrey P, Ruso A, Polyak K, Gibbs E, Hurwitz J, Massague J, Pavletich N. 1995. Mechanism of CDK activation revealed by the structure of a cyclinA-CDK2 complex. *Nature* **376**: 313-320.
John PCL, Qi R. 2008. Cell division and endoreduplication: doubtful engines of vegetative growth. *Trends Plant Sci.* **13**: 121-127.
Johnson Flanagan A, Spencer M. 1994. Ethylene production during development of mustard (*Brassica juncea*) and canola (*Brassica napus*) seed. *Plant Physiol.* **106**: 601-606.
Johnsson A. 1979. Circumnutation. in *Physiology of movements.* In: Haupt W, and Feinleib ME, eds. *Physiology of movements. encyclopedia of plant physiology.* Berlin - New York:Springer-Verlag, 627-646.
Johnsson A, Solheim BGB, Iversen T. 2009. Gravity amplifies and microgravity decreases circumnutations in *Arabidopsis thaliana* stems: results from a space experiment. *New Phytol.* **182**: 621-629.
Jones RA, Elabd SO. 1989. Prevention of salt-induced epinasty by alpha-aminooxyacetic acid and cobalt. *Plant Growth Regul.* **8**: 315-323.
Jusaitis M. 1986. Rooting response of mung bean cuttings to 1-aminocyclopropane-1-carboxylic acid and inhibitors of ethylene biosynthesis. *Scientia Horticulturae* **29**: 77-85.
Kagale S, Divi UK, Krochko JE, Keller WA, Krishna P. 2007. Brassinosteroid confers tolerance in *Arabidopsis thaliana* and *Brassica napus* to a range of abiotic stresses. *Planta* **225**: 353-364.
Kang BG. 1979. Epinasty. Pages 647-667 In: Haupt W, and Felnleib ME, eds. *Encyclopedia of plant physiology. plant movements.* Berlin:Springer-Verlag, 647-667.
Kang B, Wang H, Nam KH, Li J, Li J. 2010. Activation-tagged suppressors of a weak brassinosteroid receptor mutant. *Mol. Plant.* **3**: 260-268.
Karaba A, Dixit S, Greco R, Aharoni A, Trijatmiko KR, Marsch-Martinez N, Krishnan A, Nataraja KN, Udayakumar M, Pereira A. 2007. Improvement of water use efficiency in rice by expression of *HARDY*, an *Arabidopsis* drought and salt tolerance gene. *Proc. Natl. Acad. Sci. U. S. A.* **104**: 15270-15275.
Kardailsky I, Shukla V, Ahn J, Dagenais N, Christensen S, Nguyen J, Chory J, Harrison M, Weigel D. 1999. Activation tagging of the floral inducer FT. *Science* **286**: 1962-1965.
Karimi M, Inzé D, Depicker A. 2002. GATEWAY™ vectors for *Agrobacterium*-mediated plant transformation. *Trends Plant Sci.* **7**: 193-195.
Karlova R, de Vries SC. 2006. Advances in understanding brassinosteroid signal-

ing. *Sci. STKE* **2006**: pe36.
Kawase M. 1974. Role of ethylene in induction of flooding damage in sunflower. *Physiol. Plantarum* **31**: 29-38.
Kazama H, Dan H, Imaseki H, Wasteneys GO. 2004. Transient exposure to ethylene stimulates cell division and alters the fate and polarity of hypocotyl epidermal cells. *Plant Physiol.* **134**: 1614-1623.
Keller C, VanVolkenburgh E. 1997. Auxin-induced epinasty of tobacco leaf tissues - A nonethylene-mediated response. *Plant Physiol.* **113**: 603-610.
Kende H, van der Knaap E, Cho HT. 1998. Deepwater rice: A model plant to study stem elongation. *Plant Physiol.* **118**: 1105-1110.
Keuskamp DH, Pollmann S, Voesenek LACJ, Peeters AJM, Pierik R. 2010. Auxin transport through PIN-FORMED3 (PIN3) controls shade avoidance and fitness during competition. *Proc. Natl. Acad. Sci. U. S. A.* **107**: 22740-22744.
Keuskamp DH, Sasidharan R, Vos I, Peeters AJM, Voesenek LACJ, Pierik R. 2011. Blue-light-mediated shade avoidance requires combined auxin and brassinosteroid action in *Arabidopsis* seedlings. *Plant Journal* **67**: 208-217.
Khripach V, Zhabinskii V. 2007. Labeled brassinosteroids for biochemical studies. *Chem. Rec.* **7**: 265-274.
Kim GT, Fujioka S, Kozuka T, Tax FE, Takatsuto S, Yoshida S, Tsukaya H. 2005. CYP90C1 and CYP90D1 are involved in different steps in the brassinosteroid biosynthesis pathway in *Arabidopsis thaliana*. *Plant J.* **41**: 710-721.
Kim GT, Tsukaya H, Saito Y, Uchimiya H. 1999. Changes in the shapes of leaves and flowers upon overexpression of cytochrome P450 in *Arabidopsis*. *Proc. Natl. Acad. Sci. U. S. A.* **96**: 9433-9437.
Kim GT, Tsukaya H, Uchimiya H. 1998. The *ROTUNDIFOLIA3* gene of *Arabidopsis thaliana* encodes a new member of the cytochrome P-450 family that is required for the regulated polar elongation of leaf cells. *Genes Dev.* **12**: 2381-2391.
Kim HB, Kwon M, Ryu H, Fujioka S, Takatsuto S, Yoshida S, An CS, Lee I, Hwang I, Choe S. 2006. The regulation of *DWARF4* expression is likely a critical mechanism in maintaining the homeostasis of bioactive brassinosteroids in *Arabidopsis*. *Plant Physiol.* **140**: 548-557.
Kim S, Mollet J, Dong J, Zhang K, Park S, Lord E. 2003. Chemocyanin, a small basic protein from the lily stigma, induces pollen tube chemotropism. *Proc. Natl. Acad. Sci. U. S. A.* **100**: 16125-16130.
Kim TW, Chang SC, Lee JS, Hwang B, Takatsuto S, Yokota T, Kim SK. 2004. Cytochrome P450-catalyzed brassinosteroid pathway activation through synthesis of castasterone and brassinolide in *Phaseolus vulgaris*. *Phytochemistry* **65**: 679-689.
Kim TW, Wang ZY. 2010. Brassinosteroid signal transduction from receptor kinases to transcription factors. *Annu. Rev. Plant. Biol.* **61**: 681-704.
King D. 1997. The functional significance of leaf angle in *Eucalyptus*. *Aust. J. Bot.* **45**: 619-639.
Kitazawa D, Hatakeda Y, Kamada M, Fujii N, Miyazawa Y, Hoshino A, Iida S, Fukaki H, Morita M, Tasaka M, Suge H, Takahashi H. 2005. Shoot circumnutation and winding movements require gravisensing cells. *Proc. Natl. Acad. Sci. U. S. A.* **102**:

18742-18747.
Klahre U, Noguchi T, Fujioka S, Takatsuto S, Yokota T, Nomura T, Yoshida S, Chua NH. 1998. The *Arabidopsis DIMINUTO/DWARF1* gene encodes a protein involved in steroid synthesis. *Plant Cell* **10**: 1677-1690.
Knight L, Crocker W. 1913. Toxicity of smoke - contributions from the hull botanical laboratory. *Bot. Gaz.* **55**: 0337-0371.
Koini MA, Alvey L, Allen T, Tilley CA, Harberd NP, Whitelam GC, Franklin KA. 2009. High temperature-medated adaptations in plant architecture require the bHLH transcription factor PIF4. *Curr. Biol.* **19**: 408-413.
Konings H, Jackson MB. 1979. Relationship between rates of ethylene production by roots and the promoting or inhibiting effects of exogenous ethylene and water on root elongation. *Zeitschrift Fur Pflanzenphysiologie* **92**: 385-397.
Koornneef M, Bentsink L, Hilhorst H. 2002. Seed dormancy and germination. *Curr. Opin. Plant Biol.* **5**: 33-36.
Kovtun Y, Chiu WL, Tena G, Sheen J. 2000. Functional analysis of oxidative stress-activated mitogen-activated protein kinase cascade in plants. *Proc. Natl. Acad. Sci. U. S. A.* **97**: 2940-2945.
Kozuka T, Horiguchi G, Kim GT, Ohgishi M, Sakai T, Tsukaya H. 2005. The different growth responses of the *Arabidopsis thaliana* leaf blade and the petiole during shade avoidance are regulated by Photoreceptors and sugar. *Plant and Cell Physiology* **46**: 213-223.
Kozuka T, Kobayashi J, Horiguchi G, Demura T, Sakakibara H, Tsukaya H, Nagatani A. 2010. Involvement of auxin and brassinosteroid in the regulation of petiole elongation under the shade. *Plant Physiol.* **153**: 1608-1618.
Krishna P. 2003. Brassinosteroid-mediated stress responses. *J. Plant Growth Regul.* **22**: 289-297.
Kudo N, Kimura Y. 2002. Nuclear DNA endoreduplication during petal development in cabbage: relationship between ploidy levels and cell size. *J. Exp. Bot.* **53**: 1017-1023.
Kuppusamy KT, Chen AY, Nemhauser JL. 2009. Steroids are required for epidermal cell fate establishment in *Arabidopsis* roots. *Proc. Natl. Acad. Sci. U. S. A.* **106**: 8073-8076.
Lalande M. 1990. A reversible arrest point in the late G1 phase of the mammalian cell cycle. *Exp. Cell Res.* **186**: 332-339.
Lambers H, Chapin III FS, Pons T. 1998. Growth and allocation. Environmental influences. New York:Springer-Verlag, 320-351.
Lang JM, Eisinger WR, Green PB. 1982. Effects of ethylene on the orientation of microtubules and cellulose microfibrils of pea epicotyl cells with polylamellate cell walls. *Protoplasma* **110**: 5-14.
Le J, Vandenbussche F, De Cnodder T, Van Der Straeten D, Verbelen JP. 2005. Cell elongation and microtubule behavior in the *Arabidopsis* hypocotyl: Responses to ethylene and auxin. *J. Plant Growth Regul.* **24**: 166-178.
Lee Y, Choi D, Kende H. 2001. Expansins: ever-expanding numbers and functions. *Curr. Opin. Plant Biol.* **4**: 527-532.

Lee YK, Kim GT, Kim IJ, Park J, Kwak SS, Choi G, Chung WI. 2006. *LONGIFOLIA1* and *LONGIFOLIA2*, two homologous genes, regulate longitudinal cell elongation in *Arabidopsis*. *Development* **133**: 4305-4314.
Lehman A, Black R, Ecker J. 1996. *HOOKLESS1*, an ethylene response gene, is required for differential cell elongation in the *Arabidopsis* hypocotyl. *Cell* **85**: 183-194.
Lewis DR, Negi S, Sukumar P, Muday GK. 2011. Ethylene inhibits lateral root development, increases IAA transport and expression of PIN3 and PIN7 auxin efflux carriers. *Development* **138**: 3485-3495.
Li J. 2010. Regulation of the nuclear activities of brassinosteroid signaling. *Curr. Opin. Plant Biol.* **13**: 540-547.
Li J, Lease KA, Tax FE, Walker JC. 2001. BRS1, a serine carboxypeptidase, regulates BRI1 signaling in *Arabidopsis thaliana*. *Proc. Natl. Acad. Sci. U. S. A.* **98**: 5916-5921.
Li J, Jiang J, Qian Q, Xu Y, Zhang C, Xiao J, Du C, Luo W, Zou G, Chen M, Huang Y, Feng Y, Cheng Z, Yuan M, Chong K. 2011. Mutation of rice *BC12/GDD1*, which encodes a kinesin-like protein that binds to a GA biosynthesis gene promoter, leads to dwarfism with impaired cell elongation. *Plant Cell* **23**: 628-640.
Li L, Xu J, Xu ZH, Xue HW. 2005. Brassinosteroids stimulate plant tropisms through modulation of polar auxin transport in Brassica and *Arabidopsis*. *Plant Cell* **17**: 2738-2753.
Li Y, Darley CP, Ongaro V, Fleming A, Schipper O, Baldauf SL, McQueen-Mason SJ. 2002. Plant expansins are a complex multigene family with an ancient evolutionary origin. *Plant Physiol.* **128**: 854-864.
Li ZC, Durachko DM, Cosgrove DJ. 1993. An oat coleoptile wall protein that induces wall extension *in vitro* and that is antigenically related to a similar protein from cucumber hypocotyls. *Planta* **191**: 349-356.
Li Z, Zhang L, Yu Y, Quan R, Zhang Z, Zhang H, Huang R. 2011. The ethylene response factor AtERF11 that is transcriptionally modulated by the bZIP transcription factor HY5 is a crucial repressor for ethylene biosynthesis in *Arabidopsis*. *Plant J.* **68**: 88-99.
Lin Z, Arciga-Reyes L, Zhong S, Alexander L, Hackett R, Wilson I, Grierson D. 2008. SlTPR1, a tomato tetratricopeptide repeat protein, interacts with the ethylene receptors NR and LeETR1, modulating ethylene and auxin responses and development. *J. Exp. Bot.* **59**: 4271-4287.
Lin Z, Zhong S, Grierson D. 2009. Recent advances in ethylene research. *J. Exp. Bot.* **60**: 3311-3336.
Lippincott JA, Lippincott BB. 1968. Effect of auxin antagonists on auxin-induced leaf hyponasty. *Am. J. Bot.* **55**: 731..
Liu JH, Mukherjee I, Reid DM. 1990. Adventitious rooting in hypocotyls of sunflower (*Helianthus annuus*) seedlings .3. The role of ethylene. *Physiol. Plantarum* **78**: 268-276.
Liu YD, Zhang SQ. 2004. Phosphorylation of 1-aminocyclopropane-1-carboxylic acid synthase by MPK6, a stress-responsive mitogen-activated protein kinase, induces ethylene biosynthesis in *Arabidopsis*. *Plant Cell* **16**: 3386-3399.
Liu YG, Mitsukawa N, Oosumi T, Whittier RF. 1995. Efficient isolation and map-

ping of A*rabidopsis thaliana* T-DNA insert junctions by thermal asymmetric interlaced PCR. *Plant Journal* **8**: 457-463.
Liu YG, Whittier RF. 1995. Thermal asymmetric interlaced PCR - automatable amplification and sequencing of insert end fragments from P1 and YAC clones for chromosome walking. *Genomics* **25**: 674-681.
Livak KJ, Schmittgen TD. 2001. Analysis of relative gene expression data using real-time quantitative PCR and the $^{2\Delta\Delta CT}$ Method. *Methods* **25**: 402-408.
Llop-Tous I, Barry CS, Grierson D. 2000. Regulation of ethylene biosynthesis in response to pollination in tomato flowers. *Plant Physiol.* **123**: 971-978.
Love J, Bjorklund S, Vahala J, Hertzberg M, Kangasjarvi J, Sundberg B. 2009. Ethylene is an endogenous stimulator of cell division in the cambial meristem of *Populus. Proc. Natl. Acad. Sci. U. S. A.* **106**: 5984-5989.
Mandal A, Lang V, Orczyk W, Palva ET. 1993. Improved efficiency for t-dna-mediated transformation and plasmid rescue in *Arabidopsis thaliana*. *Theor. Appl. Genet.* **86**: 621-628.
Mangelsdorf DJ, Thummel C, Beato M, Herrlich P, Schutz G, Umesono K, Blumberg B, Kastner P, Mark M, Chambon P, Evans RM. 1995. The nuclear receptor superfamily - the 2nd decade. *Cell* **83**: 835-839.
Manuel Perez-Perez J, Candela H, Robles P, Lopez-Torrejon G, del Pozo JC, Luis Micol J. 2010. A role for AUXIN RESISTANT3 in the coordination of leaf growth. *Plant Cell Physiol.* **51**: 1661-1673.
Marcinkowska E, Wiedlocha A. 2002. Steroid signal transduction activated at the cell membrane: from plants to animals. *Acta Biochim. Pol.* **49**: 735-745.
Mariconti L, Pellegrini B, Cantoni R, Stevens R, Bergounioux C, Cella R, Albani D. 2002. The E2F family of transcription factors from *Arabidopsis thaliana* - novel and conserved components of the retinoblastoma/E2F pathway in plants. *J. Biol. Chem.* **277**: 9911-9919.
Marsch-Martinez N, Greco R, Becker JD, Dixit S, Bergervoet JHW, Karaba A, de Folter S, Pereira A. 2006. *BOLITA*, an *Arabidopsis* AP2/ERF-like transcription factor that affects cell expansion and proliferation/differentiation pathways. *Plant Mol. Biol.* **62**: 825-843.
Mase H, Hashiba M, Matsuo N, Banno H. 2007. Expression patterns of *Arabidopsis* VIII-b subgroup genes during *in vitro* shoot regeneration and effects of their overexpression on shoot regeneration efficiency. *Plant Biotechnology* **24**: 481-186.
Mathur J, Molnar G, Fujioka S, Takatsuto S, Sakurai A, Yokota T, Adam G, Voigt B, Nagy F, Maas C, Schell J, Koncz C, Szekeres M. 1998. Transcription of the *Arabidopsis* CPD gene, encoding a steroidogenic cytochrome P450, is negatively controlled by brassinosteroids. *Plant J.* **14**: 593-602.
Mayer WE, Flach D, Raju MVS, Starrach N, Wiech E. 1985. Mechanics of circadian pulvini movements in *Phaseolus coccineus.* l - Shape and arrangement of motor cells, micellation of motor cell walls, and bulk moduli of extensibility epsilonbars. *Planta* **163**: 381-390.
McElver J, Tzafrir I, Aux G, Rogers R, Ashby C, Smith K, Thomas C, Schetter A, Zhou Q, Cushman MA, Tossberg J, Nickle T, Levin JZ, Law M, Meinke D, Patton D.

2001. Insertional mutagenesis of genes required for seed development in *Arabidopsis thaliana*. *Genetics* **159**: 1751-1763.
McMurray A, Miller C. 1968. Cucumber sex expression modified by 2-chloroethanephosphonic acid. *Science* **162**: 1397-1398.
McQueen-Mason S, Durachko DM, Cosgrove DJ. 1992. 2 endogenous proteins that induce cell-wall extension in plants. *Plant Cell* **4**: 1425-1433.
Medina E, Sobrado M, Herrera R. 1978. Significance of leaf orientation for leaf temperature in an amazonian sclerophyll vegetation. *Radiat. Environ. Biophys.* **15**: 131-140.
Menges M, de Jager SM, Gruissem W, Murray JAH. 2005. Global analysis of the core cell cycle regulators of *Arabidopsis* identifies novel genes, reveals multiple and highly specific profiles of expression and provides a coherent model for plant cell cycle control. *Plant Journal* **41**: 546-566.
Menges M, Murray JA. 2002. Synchronous *Arabidopsis* suspension cultures for analysis of cell cycle gene activity. *Plant J.* **30**: 203-212.
Metraux J, Kende H. 1983. The role of ethylene in the growth-response of submerged deep-water rice. *Plant Physiol.* **72**: 441-446.
Michielse CB, Rep M. 2009. Pathogen profile update: *Fusarium oxysporum*. *Mol. Plant Pathol.* **10**: 311-324.
Millar AJ, Carre IA, Strayer CA, Chua NH, Kay SA. 1995. Circadian clock mutants in *Arabidopsis* identified by luciferase imaging. *Science* **267**: 1161-1163.
Millenaar FF, Cox MCH, van Berkel YEM, Welschen RAM, Pierik R, Voesenek LACJ, Peeters AJM. 2005. Ethylene-induced differential growth of petioles in *Arabidopsis*. Analyzing natural variation, response kinetics, and regulation. *Plant Physiol.* **137**: 998-1008.
Millenaar FF, van Zanten M, Cox MCH, Pierik R, Voesenek LACJ, Peeters AJM. 2009. Differential petiole growth in *Arabidopsis thaliana*: photocontrol and hormonal regulation. *New Phytol.* **184**: 141-152.
Mitchell J, Mandava N, Worley J, Plimmer J, Smith M. 1970. Brassins - a new family of plant hormones from rape pollen. *Nature* **225**: 1065-1066.
Miyazawa Y, Nakajima N, Abe T, Sakai A, Fujioka S, Kawano S, Kuroiwa T, Yoshida S. 2003. Activation of cell proliferation by brassinolide application in tobacco BY-2 cells: effects of brassinolide on cell multiplication, cell cycle-related gene expression, and organellar DNA contents. *J. Exp. Bot.* **54**: 2669-2678.
Mommer L, Pons T, Wolters-Arts M, Venema J, Visser E. 2005. Submergence-induced morphological, anatomical, and biochemical responses in a terrestrial species affect gas diffusion resistance and photosynthetic performance. *Plant Physiol.* **139**: 497-508.
Morejohn LC, Bureau TE, Molè-Bajer J, Bajer AS, Fosket DE. 1987. Oryzalin, a dinitroaniline herbicide, binds to plant tubulin and inhibits microtubule polymerization in vitro. *Planta* **172**: 252-264.
Morelli G, Ruberti I. 2000. Shade avoidance responses. Driving auxin along lateral routes. *Plant Physiol.* **122**: 621-626.
Morgan DC, Smith H. 1979. A systematic relationship between phytochrome-con-

trolled development and species habitat, for plants grown in simulated natural radiation. *Planta* **145**: 253-258.
Morgan PW, Drew MC. 1997. Ethylene and plant responses to stress. *Physiol. Plantarum* **100**: 620-630.
Morita MT, Tasaka M. 2004. Gravity sensing and signaling. *Curr. Opin. Plant Biol.* **7**: 712-718.
Morozova O, Marra MA. 2008. Applications of next-generation sequencing technologies in functional genomics. *Genomics* **92**: 255-264.
Mullen JL, Weinig C, Hangarter RP. 2006. Shade avoidance and the regulation of leaf inclination in *Arabidopsis*. *Plant Cell and Environment* **29**: 1099-1106.
Murray AW, Kirschner MW. 1989. Cyclin synthesis drives the early embryonic cell cycle. *Nature* **339**: 275-280.
Musgrave A, Jackson MB, Ling E. 1972. *Callitriche* stem elongation is controlled by ethylene and gibberellin. *Nature-New Biology* **238**: 93-96.
Mussig C, Altmann T. 2001. Brassinosteroid signaling in plants. *Trends Endocrinol. Metab.* **12**: 398-402.
Mussig C, Lisso J, Coll-Garcia D, Altmann T. 2006. Molecular analysis of brassinosteroid action. *Plant. Biol. (Stuttg)* **8**: 291-296.
Nafati M, Cheniclet C, Hernould M, Do PT, Fernie AR, Chevalier C, Gevaudant F. 2011. The specific overexpression of a cyclin-dependent kinase inhibitor in tomato fruit mesocarp cells uncouples endoreduplication and cell growth. *Plant Journal* **65**: 543-556.
Nagano AJ, Fukazawa M, Hayashi M, Ikeuchi M, Tsukaya H, Nishimura M, Hara-Nishimura I. 2008. AtMap1: a DNA microarray for genomic deletion mapping in *Arabidopsis thaliana*. *Plant J.* **56**: 1058-1065.
Nagata N, Asami T, Yoshida S. 2001. Brassinazole, an inhibitor of brassinosteroid biosynthesis, inhibits development of secondary xylem in cress plants (*Lepidium sativum*). *Plant Cell Physiol.* **42**: 1006-1011.
Nagata N, Min YK, Nakano T, Asami T, Yoshida S. 2000. Treatment of dark-grown *Arabidopsis thaliana* with a brassinosteroid-biosynthesis inhibitor, brassinazole, induces some characteristics of light-grown plants. *Planta* **211**: 781-790.
Nagl W. 1976. DNA endoreduplication and polyteny understood as evolutionary strategies. *Nature* **261**: 614-615. 10.1038/261614a0.
Nakamura A, Higuchi K, Goda H, Fujiwara MT, Sawa S, Koshiba T, Shimada Y, Yoshida S. 2003. Brassinolide induces *IAA5*, *IAA19*, and DR5, a synthetic auxin response element in *Arabidopsis*, implying a cross talk point of brassinosteroid and auxin signaling. *Plant Physiol.* **133**: 1843-1853.
Nakamura A, Nakajima N, Goda H, Shimada Y, Hayashi K, Nozaki H, Asami T, Yoshida S, Fujioka S. 2006. *Arabidopsis Aux/IAA* genes are involved in brassinosteroid-mediated growth responses in a manner dependent on organ type. *Plant J.* **45**: 193-205.
Nakano T, Suzuki K, Ohtsuki N, Tsujimoto Y, Fujimura T, Shinshi H. 2006. Identification of genes of the plant specific transcription factor families cooperatively regulated by ethylene and jasmonate in *Arabidopsis thaliana*. *J. Plant Res.* **119**: 407-413.

Nakatsuka A, Murachi S, Okunishi H, Shiomi S, Nakano R, Kubo Y, Inaba A. 1998. Differential expression and internal feedback regulation of 1-aminocyclopropane-1-carboxylate synthase, 1-aminocyclopropane-1-carboxylate oxidase, and ethylene receptor genes in tomato fruit during development and ripening. *Plant Physiol.* **118**: 1295-1305.

Nakatsuka A, Shiomi S, Kubo Y, Inaba A. 1997. Expression and internal feedback regulation of ACC synthase and ACC oxidase genes in ripening tomato fruit. *Plant and Cell Physiology* **38**: 1103-1110.

Nakaya M, Tsukaya H, Murakami N, Kato M. 2002. Brassinosteroids control the proliferation of leaf cells of *Arabidopsis thaliana*. *Plant Cell Physiol.* **43**: 239-244.

Nakazawa M, Ichikawa T, Ishikawa A, Kobayashi H, Tsuhara Y, Kawashima M, Suzuki K, Muto S, Matsui M. 2003. Activation tagging, a novel tool to dissect the functions of a gene family. *The Plant Journal* **34**: 741-750.

Neff MM, Nguyen SM, Malancharuvil EJ, Fujioka S, Noguchi T, Seto H, Tsubuki M, Honda T, Takatsuto S, Yoshida S, Chory J. 1999. *BAS1*: A gene regulating brassinosteroid levels and light responsiveness in *Arabidopsis*. *Proc. Natl. Acad. Sci. U. S. A.* **96**: 15316-15323.

Neff M, Fankhauser C, Chory J. 2000. Light: an indicator of time and place. *Genes Dev.* **14**: 257-271.

Negi S, Ivanchenko MG, Muday GK. 2008. Ethylene regulates lateral root formation and auxin transport in *Arabidopsis thaliana*. *Plant Journal* **55**: 175-187.

Neljubow D. 1901. Uber die horizontale nutation der stengel von *Pisum sativum* und einiger anderen Pflanzen. *Pflanzen Beih. Bot. Zentralb* **10**: 128-139.

Nemhauser JL, Mockler TC, Chory J. 2004. Interdependency of brassinosteroid and auxin signaling in *Arabidopsis*. *Plos Biology* **2**: 1460-1471.

Newell-Price J, Clark AJL, King P. 2000. DNA methylation and silencing of gene expression. *Trends in Endocrinology and Metabolism* **11**: 142-148.

Nishiuchi T, Suzuki K, Kitajima S, Sato F, Shinshi H. 2002. Wounding activates immediate early transcription of genes for ERFs in tobacco plants. *Plant Mol. Biol.* **49**: 473-482.

Noguchi T, Fujioka S, Choe S, Takatsuto S, Tax FE, Yoshida S, Feldmann KA. 2000. Biosynthetic pathways of brassinolide in *Arabidopsis*. *Plant Physiol.* **124**: 201-209.

Noguchi T, Fujioka S, Choe S, Takatsuto S, Yoshida S, Yuan H, Feldmann KA, Tax FE. 1999. Brassinosteroid-insensitive dwarf mutants of *Arabidopsis* accumulate brassinosteroids. *Plant Physiol.* **121**: 743-752.

Noguchi T, Fujioka S, Takatsuto S, Sakurai A, Yoshida S, Li J, Chory J. 1999. *Arabidopsis* det2 is defective in the conversion of (24R)-24-methylcholest-4-En-3-one to (24R)-24-methyl-5alpha-cholestan-3-one in brassinosteroid biosynthesis. *Plant Physiol.* **120**: 833-840.

Oh MH, Clouse SD, Huber SC. 2009. Tyrosine phosphorylation in brassinosteroid signaling. *Plant. Signal. Behav.* **4**: 1182-1185.

Ohmetakagi M, Shinshi H. 1995. Ethylene-inducible DNA-binding proteins that interact with an ethylene-responsive element. *Plant Cell* **7**: 173-182.

Ohme-Takagi M, Suzuki K, Shinshi H. 2000. Regulation of ethylene-*i*nduced tran-

scription of defense genes. *Plant and Cell Physiology* **41**: 1187-1192.
Ohnishi T, Szatmari AM, Watanabe B, Fujita S, Bancos S, Koncz C, Lafos M, Shibata K, Yokota T, Sakata K, Szekeres M, Mizutani M. 2006. C-23 hydroxylation by *Arabidopsis* CYP90C1 and CYP90D1 reveals a novel shortcut in brassinosteroid biosynthesis. *Plant Cell* **18**: 3275-3288.
Ohno R, Kadota Y, Fujii S, Sekine M, Umeda M, Kuchitsu K. 2011. Cryptogein-induced cell cycle arrest at G2 phase is associated with inhibition of cyclin-dependent kinases, suppression of expression of cell cycle-related genes and protein degradation in synchronized tobacco BY-2 cells. *Plant Cell Physiol.* **52**: 922-932.
Ostergaard L, Yanofsky M. 2004. Establishing gene function by mutagenesis in *Arabidopsis thaliana*. *Plant J.* **39**: 682-696.
Palatnik J, Allen E, Wu X, Schommer C, Schwab R, Carrington J, Weigel D. 2003. Control of leaf morphogenesis by microRNAs. *Nature* **425**: 257-263.
Paredez AR, Somerville CR, Ehrhardt DW. 2006. Visualization of cellulose synthase demonstrates functional association with microtubules. *Science* **312**: 1491-1495.
Pauwels L, Morreel K, De Witte E, Lammertyn F, Van Montagu M, Boerjan W, Inzé D, Goossens A. 2008. Mapping methyl jasmonate-mediated transcriptional reprogramming of metabolism and cell cycle progression in cultured *Arabidopsis* cells. *Proc. Natl. Acad. Sci. U. S. A.* **105**: 1380-1385.
Peeters AJM, Cox MCH, Benschop JJ, Vreeburg RAM, Bou J, Voesenek LACJ. 2002. Submergence research using *Rumex palustris* as a model; looking back and going forward. *J. Exp. Bot.* **53**: 391-398.
Pierik R, Millenaar FF, Peeters AJM, Voesenek LACJ. 2005. New perspectives in flooding research: The use of shade avoidance and *Arabidopsis thaliana*. *Ann. Bot.* **96**: 533-540.
Pierik R, Tholen D, Poorter H, Visser EJW, Voesenek LA. 2006. The Janus face of ethylene: growth inhibition and stimulation. *Trends Plant Sci.* **11**: 176-183.
Pierik R, Visser EJW, De Kroon H, Voesenek LACJ. 2003. Ethylene is required in tobacco to successfully compete with proximate neighbours. *Plant Cell and Environment* **26**: 1229-1234.
Pierik R, Whitelam GC, Voesenek LACJ, de Kroon H, Visser EJW. 2004. Canopy studies on ethylene-insensitive tobacco identify ethylene as a novel element in blue light and plant-plant signalling. *Plant J.* **38**: 310-319. x.
Pierik R, Djakovic-Petrovic T, Keuskamp DH, De Wit M, Voesenek LACJ. 2009. Auxin and ethylene regulate elongation responses to neighbor proximity signals independent of gibberellin and DELLA proteins in *Arabidopsis*. *Plant Physiol.* **149**: 1701-1712.
Pierik R, Sasidharan R, Voesenek LACJ. 2007. Growth control by ethylene: adjusting phenotypes to the environment. *J. Plant Growth Regul.* **26**: 188-200.
Pillitteri LJ, Bemis SM, Shpak ED, Torii KU. 2007. Haploinsufficiency after successive loss of signaling reveals a role for *ERECTA*-family genes in *Arabidopsis* ovule development. *Development* **134**: 3099-3109.
Polko J, Voesenek L, Peeters A, Pierik R. 2011. Petiole hyponasty: an ethylene-

driven, adaptive response to changes in the environment. *AoB Plants* doi: 10.1093/aobpla/plr031.

Polko JK, van Zanten M, van Rooij JA, Marée AFM, Voesenek LACJ, Peeters AJM, Pierik R. 2012. Ethylene-induced differential petiole growth in *Arabidopsis thaliana* involves local microtubule reorientation and cell expansion. *New Phytol.* **193**: 339-348.

Poorter H, Lambers H. 1986. Growth and competitive ability of a highly plastic and a marginally plastic genotype of *Plantago major* in a fluctuating environment. *Physiol. Plantarum* **67**: 217-222.

Pratt H, Biale J. 1944. Relation of the production of an active etranation to respiration in the avocudo fruit. *Plant Physiol.* **19**: 519-528.

Pre M, Atallah M, Champion A, De Vos M, Pieterse CMJ, Memelink J. 2008. The AP2/ERF domain transcription factor ORA59 integrates jasmonic acid and ethylene signals in plant defense. *Plant Physiol.* **147**: 1347-1357.

Prichard JM, Forseth IN. 1988. Photosynthetic responses of two heliotropic legumes from contrasting habitats. *Plant, Cell Environ.* **11**: 591-601.

Quail MA, Kozarewa I, Smith F, Scally A, Stephens PJ, Durbin R, Swerdlow H, Turner DJ. 2008. A large genome center's improvements to the Illumina sequencing system. *Nature Methods* **5**: 1005-1010.

Quail P, Boylan M, Parks B, Short T, Xu Y, Wagner D. 1995. Phytochromes - photosensory perception and signal-transduction. *Science* **268**: 675-680.

Rao S, Vardhini B, Sujatha E, Anuradha S. 2002. Brassinosteroids - a new class of phytohormones. *Curr. Sci.* **82**: 1239-1245.

Rayle D, Cleland R. 1970. Enhancement of wall loosening and elongation by acid solutions. *Plant Physiol.* **46**: 250-253.

Raz V, Ecker J. 1999. Regulation of differential growth in the apical hook of *Arabidopsis*. *Development* **126**: 3661-3668.

Renaudin JP, Doonan JH, Freeman D, Hashimoto J, Hirt H, Inzé D, Jacobs T, Kouchi H, Rouze P, Sauter M, Savoure A, Sorrell DA, Sundaresan V, Murray JA. 1996. Plant cyclins: a unified nomenclature for plant A-, B- and D-type cyclins based on sequence organization. *Plant Mol. Biol.* **32**: 1003-1018.

Richard C, Granier C, Inzé D, De Veylder L. 2001. Analysis of cell division parameters and cell cycle gene expression during the cultivation of *Arabidopsis thaliana* cell suspensions. *J. Exp. Bot.* **52**: 1625-1633.

Richard C, Lescot M, Inzé D, De Veylder L. 2002. Effect of auxin, cytokinin, and sucrose on cell cycle gene expression in *Arabidopsis thaliana* cell suspension cultures. *Plant Cell Tissue and Organ Culture* **69**: 167-176.

Ridge I, Amarasinghe I. 1984. Ethylene and growth control in the fringed waterlily (*Nymphoides peltata*) - stimulation of cell division and interaction with buoyant tension in petioles. *Plant Growth Regulation* **2**: 235-249.

Roberts IN, Lloyd CW, Roberts K. 1985. Ethylene-induced microtubule reorientations: mediation by helical arrays. *Planta* **164**: 439-447.

Roeder AHK, Chickarmane V, Cunha A, Obara B, Manjunath BS, Meyerowitz EM.

2010. Variability in the control of cell division underlies sepal epidermal patterning in *Arabidopsis thaliana*. *PLoS. Biol.* **8**: e1000367.
Romberger JA, Hejnowicz Z, Hill JF. 1993. *Plant structure: Function and development.* Berlin: Springer-Verlag.
Rosso MG, Li Y, Strizhov N, Reiss B, Dekker K, Weisshaar B. 2003. An *Arabidopsis thaliana* T-DNA mutagenized population (GABI-Kat) for flanking sequence tag-based reverse genetics. *Plant Mol. Biol.* **53**: 247-259.
Roudier F, Fedorova E, Gyorgyey J, Feher A, Brown S, Kondorosi A, Kondorosi E. 2000. Cell cycle function of a *Medicago sativa* A2-type cyclin interacting with a PSTAIRE-
Ruiz-Sanchez MC, Domingo R, Torrecillas A, Perez-Pastor A. 2000. Water stress preconditioning to improve drought resistance in young apricot plants. *Plant Science* **156**: 245-251.
Ruzicka K, Ljung K, Vanneste S, Podhorska R, Beeckman T, Friml J, Benkova E. 2007. Ethylene regulates root growth through effects on auxin biosynthesis and transport-dependent auxin distribution. *Plant Cell* **19**: 2197-2212.
Sakuma Y, Liu Q, Dubouzet JG, Abe H, Shinozaki K, Yamaguchi-Shinozaki K. 2002. DNA-binding specificity of the ERF/AP2 domain of *Arabidopsis* DREBs, transcription factors involved in dehydration- and cold-inducible gene expression. *Biochem. Biophys. Res. Commun.* **290**: 998-1009.
Sakurai A, Fujioka S. 1997. Studies on biosynthesis of brassinosteroids. *Biosci. Biotechnol. Biochem.* **61**: 757-762.
Sampedro J, Cosgrove DJ. 2005. The expansin superfamily. *Genome Biol.* **6**: 242.
Sanchezbravo J, Ortuno AM, Perezgilabert M, Acosta M, Sabater F. 1992. Modification by ethylene of the cell growth pattern in different tissues of etiolated lupine hypocotyls. *Plant Physiol.* **98**: 1121-1127.
Sasidharan R, Chinnappa CC, Staal M, Elzenga JTM, Yokoyama R, Nishitani K, Voesenek LACJ, Pierik R. 2010. Light quality-mediated petiole elongation in *Arabidopsis* during shade avoidance involves cell wall modification by xyloglucan endotransglucosylase/hydrolases. *Plant Physiol.* **154**: 978-990.
Sasidharan R, Chinnappa CC, Voesenek LACJ, Pierik R. 2008. The regulation of cell wall extensibility during shade avoidance: a study using two contrasting ecotypes of *Stellaria longipes*. *Plant Physiol.* **148**: 1557-1569.
Satter RL, Geballe GT, Applewhite PB, Galston AW. 1974. Potassium flux and leaf movement in *Samanea saman* .1. Rhythmic Movement. *J. Gen. Physiol.* **64**: 413-430.
Satter RL, Gorton HL, Vogelmann TC. 1990. *The pulvinus: Motor organ for leaf movement.* Rockville, Maryland: American Society of Plant Physiologists.
Savaldi-Goldstein S, Peto C, Chory J. 2007. The epidermis both drives and restricts plant shoot growth. *Nature* **446**: 199-202.
Schaller H. 2003. The role of sterols in plant growth and development. *Prog. Lipid Res.* **42**: 163-175.
Schlagnhaufer C, Arteca R. 1985. Brassinosteroid-induced epinasty in tomato plants. *Plant Physiol.* **78**: 300-303.
Schlichting CD. 1986. The evolution of phenotypic plasticity in plants. *Annu. Rev.*

Ecol. Syst. **17**: 667-693.
Schmitt J. 1997. Is photomorphogenic shade avoidance adaptive? Perspectives from population biology. *Plant Cell and Environment* **20**: 826-830.
Schneider K, Wells B, Dolan L, Roberts K. 1997. Structural and genetic analysis of epidermal cell differentiation in *Arabidopsis* primary roots. *Development* **124**: 1789-1798.
Schubert D, Lechtenberg B, Forsbach A, Gils M, Bahadur S, Schmidt R. 2004. Silencing in *Arabidopsis* T-DNA transformants: The predominant role of a gene-specific RNA sensing mechanism versus position effects. *Plant Cell* **16**: 2561-2572.
Schumacher K, Vafeados D, McCarthy M, Sze H, Wilkins T, Chory J. 1999. The *Arabidopsis det3* mutant reveals a central role for the vacuolar H(+)-ATPase in plant growth and development. *Genes Dev.* **13**: 3259-3270.
Shaul O, Mironov V, Burssens S, VanMontagu M, Inzé D. 1996. Two *Arabidopsis* cyclin promoters mediate distinctive transcriptional oscillation in synchronized tobacco BY-2 cells. *Proc. Natl. Acad. Sci. U. S. A.* **93**: 4868-4872.
Shi Y, Zhu S, Mao X, Feng J, Qin Y, Zhang L, Cheng J, Wei L, Wang Z, Zhu Y. 2006. Transcriptome profiling, molecular biological, and physiological studies reveal a major role for ethylene in cotton fiber cell elongation. *Plant Cell* **18**: 651-664.
Shibaoka H. 1994. Plant hormone-induced changes in the orientation of cortical microtubules - alterations in the cross-linking between microtubules and the plasma-membrane. *Annu. Rev. Plant Physiol. Plant Mol. Biol.* **45**: 527-544.
Shimada Y, Goda H, Nakamura A, Takatsuto S, Fujioka S, Yoshida S. 2003. Organ-specific expression of brassinosteroid-biosynthetic genes and distribution of endogenous brassinosteroids in *Arabidopsis*. *Plant Physiol.* **131**: 287-297.
Shropshire W. 1979. Stimulus perception. in *physiology of movements.*In: Haupt W., andFeinlieb M. E., eds. *Encyclopedia of plant physiology.* Berlin - New York: Springer-Verlag, 10-41.
Sibaoka T. 1991. Rapid plant movements triggered by action-potentials. *Botanical Magazine-Tokyo* **104**: 73-95. 10.1007/BF02493405.
Sibaoka T. 1962. Excitable Cells in Mimosa. *Science* **137**: 226.
Singer T, Burke E. 2003. High-throughput TAIL-PCR as a tool to identify DNA flanking insertions. *Methods Mol. Biol.* **236**: 241-72.
Skirycz A, Claeys H, De Bodt S, Oikawa A, Shinoda S, Andriankaja M, Maleux K, Eloy NB, Coppens F, Yoo S, Saito K, Inzé D. 2011. Pause-and-stop: the effects of osmotic stress on cell proliferation during early leaf development in *Arabidopsis* and a role for ethylene signaling in cell cycle arrest. *Plant Cell* **23**: 1876-1888.
Smalle J, Haegman M, Kurepa J, VanMontagu M, VanderStraeten D. 1997. Ethylene can stimulate *Arabidopsis* hypocotyl elongation in the light. *Proc. Natl. Acad. Sci. U. S. A.* **94**: 2756-2761.
Smalle J, VanderStraeten D. 1997. Ethylene and vegetative development. *Physiol. Plantarum* **100**: 593-605.
Smith H. 2000. Phytochromes and light signal perception by plants - an emerging synthesis. *Nature* **407**: 585-591.

Smith H, Whitelam G. 1997. The shade avoidance syndrome: Multiple responses mediated by multiple phytochromes. *Plant Cell and Environment* **20**: 840-844.
Soga K, Yamaguchi A, Kotake T, Wakabayashi K, Hoson T. 2010. 1-aminocyclopropane-1-carboxylic acid (ACC)-induced reorientation of cortical microtubules is accompanied by a transient increase in the transcript levels of gamma-tubulin complex and katanin genes in azuki bean epicotyls. *J. Plant Physiol.* **167**: 1165-1171.
Solano R, Stepanova A, Chao QM, Ecker JR. 1998. Nuclear events in ethylene signaling: a transcriptional cascade mediated by ETHYLENE-INSENSITIVE3 and ETHYLENE-RESPONSE-FACTOR1. *Genes Dev.* **12**: 3703-3714.
Song L, Zhou XY, Li L, Xue LJ, Yang X, Xue HW. 2009. Genome-wide analysis revealed the complex regulatory network of brassinosteroid effects in photomorphogenesis. *Mol. Plant.* **2**: 755-772.
Steber CM, McCourt P. 2001. A role for brassinosteroids in germination in *Arabidopsis*. *Plant Physiol.* **125**: 763-769.
Steen DA, Chadwick AV. 1981. Ethylene effects in pea stem tissue : evidence of microtubule mediation. *Plant Physiol.* **67**: 460-466.
Stepanova AN, Hoyt JM, Hamilton AA, Alonso JM. 2005. A link between ethylene and auxin uncovered by the characterization of two root-specific ethylene-insensitive mutants in *Arabidopsis*. *Plant Cell* **17**: 2230-2242.
Stepanova AN, Alonso JM. 2009. Ethylene signaling and response: where different regulatory modules meet. *Curr. Opin. Plant Biol.* **12**: 548-555.
Stewart E, Freebairn.HT. 1969. Ethylene, seed germination, and epinasty. *Plant Physiol.* **44**: 955-958.
Stift M, Luttikhuizen PC, Visser EJW, van Tienderen PH. 2008. Different flooding responses in *Rorippa amphibia* and *Rorippa sylvestris*, and their modes of expression in F-1 hybrids. *New Phytol.* **180**: 229-239.
Stolarz M. 2009. Circumnutation as a visible plant action and reaction: physiological, cellular and molecular basis for circumnutations. *Plant Signaling & Behavior* **4**: 380-387.
Strader LC, Chen GL, Bartel B. 2010. Ethylene directs auxin to control root cell expansion. *Plant Journal* **64**: 874-884.
Street J, Baldwin J, Mueller T. 1992. Influence of growth stage on rice (*Oryza sativa*) tolerance to triclopyr. *Weed Technol.* **6**: 930-933.
Sugimoto K, Himmelspach R, Williamson RE, Wasteneys GO. 2003. Mutation or drug-dependent microtubule disruption causes radial swelling without altering parallel cellulose microfibril deposition in *Arabidopsis* root cells. *Plant Cell* **15**: 1414-1429.
Sugimoto-Shirasu K, Roberts K. 2003. "Big it up": endoreduplication and cell-size control in plants. *Curr. Opin. Plant Biol.* **6**: 544-553.
Sultan SE. 2000. Phenotypic plasticity for plant development, function and life history. *Trends Plant Sci.* **5**: 537-542.
Summers JE, Voesenek LACJ, Blom CWPM, Lewis MJ, Jackson MB. 1996. Potamogeton pectinatus is constitutively incapable of synthesizing ethylene and lacks

1-aminocyclopropane-1-carboxylic acid oxidase. *Plant Physiol.* **111**: 901-908.
Suzuki H, Kim S, Takahashi N, Yokota T. 1993. Metabolism of castasterone and brassinolide in mung bean explant. *Phytochemistry* **33**: 1361-1367.
Suzuki K, Nishiuchi T, Nakayama Y, Ito M, Shinshi H. 2006. Elicitor-induced down-regulation of cell cycle-related genes in tobacco cells. *Plant Cell and Environment* **29**: 183-191.
Suzuki K, Suzuki N, Ohme-Takagi M, Shinshi H. 1998. Immediate early induction of mRNAs for ethylene-responsive transcription factors in tobacco leaf strips after cutting. *Plant Journal* **15**: 657-665.
Suzuki S, Ono R, Narita T, Pask AJ, Shaw G, Wang C, Kohda T, Alsop AE, Graves JAM, Kohara Y, Ishino F, Renfree MB, Kaneko-Ishino T. 2007. Retrotransposon silencing by DNA methylation can drive mammalian genomic imprinting. *Plos Genetics* **3**: e55.
Swarup R, Perry P, Hagenbeek D, Van Der Straeten D, Beemster GTS, Sandberg G, Bhalerao R, Ljung K, Bennett MJ. 2007. Ethylene upregulates auxin biosynthesis in *Arabidopsis* seedlings to enhance inhibition of root cell elongation. *Plant Cell* **19**: 2186-2196.
Swiatek A, Lenjou M, Van Bockstaele D, Inzé D, Van Onckelen H. 2002. Differential effect of jasmonic acid and abscisic acid on cell cycle progression in tobacco BY-2 cells. *Plant Physiol.* **128**: 201-211.
Symons G, Davies C, Shavrukov Y, Dry I, Reid J, Thomas M. 2006. Grapes on steroids. Brassinosteroids are involved in grape berry ripening. *Plant Physiol.* **140**: 150-158.
Symons GM, Ross JJ, Jager CE, Reid JB. 2008. Brassinosteroid transport. *J. Exp. Bot.* **59**: 17-24.
Szekeres M, Nemeth K, Koncz-Kalman Z, Mathur J, Kauschmann A, Altmann T, Redei GP, Nagy F, Schell J, Koncz C. 1996. Brassinosteroids rescue the deficiency of CYP90, a cytochrome P450, controlling cell elongation and de-etiolation in *Arabidopsis*. *Cell* **85**: 171-182.
Takahashi H. 1997. Hydrotropism: The current state of our knowledge. *J. Plant Res.* **110**: 163-169.
Tanaka K, Asami T, Yoshida S, Nakamura Y, Matsuo T, Okamoto S. 2005. Brassinosteroid homeostasis in *Arabidopsis* is ensured by feedback expressions of multiple genes involved in its metabolism. *Plant Physiol.* **138**: 1117-1125.
Tao Y, Ferrer J, Ljung K, Pojer F, Hong F, Long JA, Li L, Moreno JE, Bowman ME, Ivans LJ, Cheng Y, Lim J, Zhao Y, Ballaré CL, Sandberg G, Noel JP, Chory J. 2008. Rapid synthesis of auxin via a new tryptophan-dependent pathway is required for shade avoidance in plants. *Cell* **133**: 164-176.
Tholen D, Voesenek L, Poorter H. 2004. Ethylene insensitivity does not increase leaf area or relative growth rate in *Arabidopsis*, *Nicotiana tabacum*, and *Petunia* x *hybrida*. *Plant Physiol.* **134**: 1803-1812.
Thomas H, Ougham H, Wagstaff C, Stead A. 2003. Defining senescence and death. *J. Exp. Bot.* **54**: 1127-1132.

Trujillo LE, Sotolongo M, Menendez C, Ochogavia ME, Coll Y, Hernandez I, Borras-Hidalgo O, Thomma BPHJ, Vera P, Hernandez L. 2008. SodERF3, a novel sugarcane ethylene responsive factor (ERF), enhances salt and drought tolerance when overexpressed in tobacco plants. *Plant and Cell Physiology* **49**: 512-525.

Tsang DL, Edmond C, Harrington JL, Nuehse TS. 2011. Cell wall integrity controls root elongation via a general 1-aminocyclopropane-1-carboxylic acid-dependent, ethylene-independent pathway. *Plant Physiol.* **156**: 596-604.

Tsao TH. 1949. A study of chemotropism of pollen tubes invitro. *Plant Physiol.* **24**: 494-504.

Tsuge T, Tsukaya H, Uchimiya H. 1996. Two independent and polarized processes of cell elongation regulate leaf blade expansion in *Arabidopsis thaliana* (L) Heynh. *Development* **122**: 1589-1600.

Tsukaya H. 2002. The leaf index: heteroblasty, natural variation, and the genetic control of polar processes of leaf expansion. *Plant Cell Physiol.* **43**: 372-378.

Tsukaya H, Horiguchi G. 2005. Leaf morphogenesis. *Tanpakushitsu Kakusan Koso* **50**: 627-632.

Tsukaya H, Kozuka T, Kim GT. 2002. Genetic control of petiole length in *Arabidopsis thaliana*. *Plant Cell Physiol.* **43**: 1221-1228.

Ueda K, Matsuyama T, Hashimoto T. 1999. Visualization of microtubules in living cells of transgenic *Arabidopsis thaliana*. *Protoplasma* **206**: 201-206.

Uehlein N, Kaldenhoff R. 2008. Aquaporins and plant leaf movements. *Ann. Bot.* **101**: 1-4. 10

Van der Graaff E, Den Dulk-Ras A, Hooykaas P, Keller B. 2000. Activation tagging of the *LEAFY PETIOLE* gene affects leaf petiole development in *Arabidopsis thaliana*. *Development* **127**: 4971-4980.

Van Kleunen M, Fischer M. 2005. Constraints on the evolution of adaptive phenotypic plasticity in plants. *New Phytol.* **166**: 49-60.

Van Zanten M, Pons TL, Janssen JAM, Voesenek LACJ, Peeters AJM. 2010. On the relevance and control of leaf angle. *Crit. Rev. Plant Sci.* **29**: 300-316.

Van Zanten M, Millenaar FF, Cox MCH, Pierik R, Voesenek LACJ, Peeters AJM. 2009a. Auxin perception and polar auxin transport are not always a prerequisite for differential growth. *Plant Signal Behav* **4**: 899-901.

Van Zanten M, Voesenek LACJ, Peeters AJM, Millenaar FF. 2009b. Hormone- and light-mediated regulation of heat-induced differential petiole growth in *Arabidopsis*. *Plant Physiol.* **151**: 1446-1458.

Vandepoele K, Raes J, De Veylder L, Rouze P, Rombauts S, Inzé D. 2002. Genome-wide analysis of core cell cycle genes in *Arabidopsis*. *Plant Cell* **14**: 903-916.

Vanneste S, Coppens F, Lee E, Donner TJ, Xie Z, Van Isterdael G, Dhondt S, De Winter F, De Rybel B, Vuylsteke M, De Veylder L, Friml J, Inzé D, Grotewold E, Scarpella E, Sack F, Beemster GTS, Beeckman T. 2011. Developmental regulation of CYCA2s contributes to tissue-specific proliferation in *Arabidopsis*. *EMBO J.* **30**: 3430-3441.

Vashisht D, Hesselink A, Pierik R, Ammerlaan JMH, Bailey-Serres J, Visser EJW,

Pedersen O, van Zanten M, Vreugdenhil D, Jamar DCL, Voesenek LACJ, Sasidharan R. 2011. Natural variation of submergence tolerance among *Arabidopsis thaliana* accessions. *New Phytol.* **190**: 299-310.

Vasseur F, Pantin F, Vile D. 2011. Changes in light intensity reveal a major role for carbon balance in *Arabidopsis* responses to high temperature. *Plant Cell and Environment* **34**: 1563-1576.

Verkest A, Manes C, Vercruysse S, Maes S, Van der Schueren E, Beeckman T, Genschik P, Kuiper M, Inzé D, De Veylder L. 2005. The cyclin-dependent kinase inhibitor KRP2 controls the onset of the endoreduplication cycle during *Arabidopsis* leaf development through inhibition of mitotic CDKA;1 kinase complexes. *Plant Cell* **17**: 1723-1736.

Vert G, Chory J. 2006. Downstream nuclear events in brassinosteroid signalling. *Nature* **441**: 96-100.

Vert G, Nemhauser JL, Geldner N, Hong F, Chory J. 2005. Molecular mechanisms of steroid hormone signaling in plants. *Annu. Rev. Cell Dev. Biol.* **21**: 177-201.

Vert G, Walcher CL, Chory J, Nemhauser JL. 2008. Integration of auxin and brassinosteroid pathways by Auxin Response Factor 2. *Proc. Natl. Acad. Sci. U. S. A.* **105**: 9829-9834.

Vesely J, Havlicek L, Strnad M, Blow JJ, Donelladeana A, Pinna L, Letham DS, Kato J, Detivaud L, Leclerc S, Meijer L. 1994. Inhibition of Cyclin-Dependent Kinases by Purine Analogs. *European Journal of Biochemistry* **224**: 771-786.

Voesenek LACJ, Banga AM, Thier RH, Mudde CM, Harren FJM, Barendse GWM, Blom CWPM. 1993. Submergence-induced ethylene synthesis, entrapment, and growth in 2 plant species with contrasting flooding resistances. *Plant Physiol.* **103**: 783-791.

Voesenek LACJ, Blom CWPM. 1989. Growth-responses of *Rumex* species in relation to submergence and ethylene. *Plant Cell and Environment* **12**: 433-439.

Voesenek LACJ, Colmer TD, Pierik R, Millenaar FF, Peeters AJM. 2006. How plants cope with complete submergence. *New Phytol.* **170**: 213-226.

Vreeburg RAM, Benschop JJ, Peeters AJM, Colmer TD, Ammerlaan JMH, Staal M, Elzenga TM, Staals RHJ, Darley CP, McQueen-Mason SJ, Voesenek LACJ. 2005. Ethylene regulates fast apoplastic acidification and expansin a transcription during submergence-induced petiole elongation in *Rumex palustris*. *Plant J.* **43**: 597-610.

Vriezen WH, De Graaf B, Mariani C, Voesenek LACJ. 2000. Submergence induces expansin gene expression in flooding-tolerant *Rumex palustris* and not in flooding-intolerant *R. acetosa*. *Planta* **210**: 956-963.

Waggoner P, Dimond A. 1954. Nonspecificity of the triple response for ethylene. *Science* **119**: 123-124.

Walley JW, Coughlan S, Hudson ME, Covington MF, Kaspi R, Banu G, Harmer SL, Dehesh K. 2007. Mechanical stress induces biotic and abiotic stress responses via a novel cis-element. *Plos Genetics* **3**: 1800-1812.

Wang D, Zhang C, Hearn DJ, Kang I, Punwani JA, Skaggs MI, Drews GN, Schumaker KS, Yadegari R. 2010. Identification of transcription factor genes expressed in the *Arabidopsis* female gametophyte. *BMC Plant Biology* **10**: 110.

Wang D, Li F, Duan Q, Han T, Xu Z, Bai S. 2010. Ethylene perception is involved in female cucumber flower development. *Plant Journal* **61**: 862-872.
Wang H, Qi QG, Schorr P, Cutler AJ, Crosby WL, Fowke LC. 1998. ICK1, a cyclin-dependent protein kinase inhibitor from *Arabidopsis thaliana* interacts with both Cdc2a and CycD3, and its expression is induced by abscisic acid. *Plant Journal* **15**: 501
Wang X, Chory J. 2006. Brassinosteroids regulate dissociation of BKI1, a negative regulator of BRI1 signaling, from the plasma membrane. *Science* **313**: 1118-1122. 1
Ward JM, Smith AM, Shah PK, Galanti SE, Yi HK, Demianski AJ, van der Graaff E, Keller B, Neff MM. 2006. A new role for the *Arabidopsis* AP2 transcription factor, LEAFY PETIOLE, in gibberellin-induced germination is revealed by the misexpression of a homologous gene, *SOB2/DRN-LIKE*. *Plant Cell* **18**: 29-39.
Wasteneys GO, Williamson RE. 1993. Cortical microtubule organization and internodal cell maturation in *Chara corallina*. *Bot. Acta* **106**: 136-142.
Wei W, Qi X, Wang L, Zhang Y, Hua W, Li D, Lv H, Zhang X. 2011. Characterization of the sesame (*Sesamum indicum* L.) global transcriptome using Illumina paired-end sequencing and development of EST-SSR markers. *BMC Genomics* **12**: 451..
Weigel D, Ahn JH, Blazquez MA, Borevitz JO, Christensen SK, Fankhauser C, Ferrandiz C, Kardailsky I, Malancharuvil EJ, Neff MM, Nguyen JT, Sato S, Wang ZY, Xia Y, Dixon RA, Harrison MJ, Lamb CJ, Yanofsky MF, Chory J. 2000. Activation tagging in *Arabidopsis*. *Plant Physiol.* **122**: 1003-1013.
Weiste C, Iven T, Fischer U, Onate-Sanchez L, Droege-Laser W. 2007. In planta ORFeome analysis by large-scale over-expression of GATEWAY (R)-compatible cDNA clones: screening of ERF transcription factors involved in abiotic stress defense. *Plant Journal* **52**: 382-390.
West G, Inzé D, Beemster G. 2004. Cell cycle modulation in the response of the primary root of *Arabidopsis* to salt stress. *Plant Physiol.* **135**: 1050-1058.
Whippo CW, Hangarter RP. 2009. The "sensational" power of movement in plants: a darwinian system for studying the evolution of behavior. *Am. J. Bot.* **96**: 2115-2127.
Whittington AT, Vugrek O, Wei KJ, Hasenbein NG, Sugimoto K, Rashbrooke MC, Wasteneys GO. 2001. MOR1 is essential for organizing cortical microtubules in plants. *Nature* **411**: 610-613.
Wiesler B, Wang Q, Nick P. 2002. The stability of cortical microtubules depends on their orientation. *Plant J.* **32**: 1023-1032.
Williams-Carrier R, Stiffler N, Belcher S, Kroeger T, Stern DB, Monde R, Coalter R, Barkan A. 2010. Use of Illumina sequencing to identify transposon insertions underlying mutant phenotypes in high-copy Mutator lines of maize. *Plant Journal* **63**: 167-177.
Wilms FHA, Derksen J. 1988. Reorganization of cortical microtubules during cell differentiation in tobacco explants. *Protoplasma* **146**: 127-132.
Wood WML. 1953. Thermonasty in tulip and crocus flowers. *J. Exp. Bot.* **4**: 65-77.
Xie L, Yang C, Wang X. 2011. Brassinosteroids can regulate cellulose biosynthesis by controlling the expression of CESA genes in *Arabidopsis*. *J. Exp. Bot.* **62**: 4495-4506.

Xu K, Xu X, Fukao T, Canlas P, Maghirang-Rodriguez R, Heuer S, Ismail AM, Bailey-Serres J, Ronald PC, Mackill DJ. 2006. Sub1A is an ethylene-response-factor-like gene that confers submergence tolerance to rice. *Nature* **442**: 705-708.

Yaish MW, El-Kereamy A, Zhu T, Beatty PH, Good AG, Bi Y, Rothstein SJ. 2010. The APETALA-2-like transcription factor OsAP2-39 controls key interactions between abscisic acid and gibberellin in rice. *PLoS Genetics* **6**.

Yamamoto S, Suzuki K, Shinshi H. 1999. Elicitor-responsive, ethylene-independent activation of GCC box-mediated transcription that is regulated by both protein phosphorylation and dephosphorylation in cultured tobacco cells. *Plant J.* **20**: 571-579.

Yang C, Hsu F, Li J, Wang N, Shih M. 2011. The AP2/ERF transcription factor AtERF73/HRE1 modulates ethylene responses during hypoxia in *Arabidopsis*. *Plant Physiol.* **156**: 202-212.

Yin Y, Vafeados D, Tao Y, Yoshida S, Asami T, Chory J. 2005. A new class of transcription factors mediates brassinosteroid-regulated gene expression in *Arabidopsis*. *Cell* **120**: 249-259.

Yoshizumi T, Tsumoto Y, Takiguchi T, Nagata N, Yamamoto YY, Kawashima M, Ichikawa T, Nakazawa M, Yamamoto N, Matsui M. 2006. Increased level of polyploidy1, a conserved repressor of *CYCLINA2* transcription, controls endoreduplication in *Arabidopsis*. *Plant Cell* **18**: 2452-2468.

Yu Y, Steinmetz A, Meyer D, Brown S, Shen WH. 2003. The tobacco A-type cyclin, *Nicta;CYCA3;2*, at the nexus of cell division and differentiation. *Plant Cell* **15**: 2763-2777.

Yuan M, Shaw PJ, Warn RM, Lloyd CW. 1994. Dynamic reorientation of cortical microtubules, from transverse to longitudinal, in living plant cells. *Proc. Natl. Acad. Sci. U. S. A.* **91**: 6050-6053.

Zacarias L, Reid M. 1990. Role of growth-regulators in the senescence of *Arabidopsis-thaliana* leaves. *Physiol. Plantarum* **80**: 549-554.

Zhang H, Yang Y, Zhang Z, Chen J, Wang X, Huang R. 2008. Expression of the ethylene response factor gene *TSRF1* enhances abscisic acid responses during seedling development in tobacco. *Planta* **228**: 777-787.

Zhang L, Li Z, Quan R, Li G, Wang R, Huang R. 2011. An AP2 domain-containing gene, ESE1, targeted by the ethylene signaling component EIN3 Is important for the salt response in *Arabidopsis*. *Plant Physiol.* **157**: 854-865.

Zhang S, Cai Z, Wang X. 2009. The primary signaling outputs of brassinosteroids are regulated by abscisic acid signaling. *Proc. Natl. Acad. Sci. U. S. A.* **106**: 4543-4548.

Zhang Z, Huang R. 2010. Enhanced tolerance to freezing in tobacco and tomato overexpressing transcription factor *TERF2/LeERF2* is modulated by ethylene biosynthesis. *Plant Mol. Biol.* **73**: 241-249.

Zhang Z, Zhang H, Quan R, Wang X, Huang R. 2009. Transcriptional regulation of the ethylene response factor LeERF2 in the expression of ethylene biosynthesis genes controls ethylene production in tomato and tobacco. *Plant Physiol.* **150**: 365-377.

Zhang Z, Ramirez J, Reboutier D, Brault M, Trouverie J, Pennarun A, Amiar Z,

Biligui B, Galagovsky L, Rona J. 2005. Brassinosteroids regulate plasma membrane anion channels in addition to proton pumps during expansion of *Arabidopsis thaliana* cells. *Plant Cell Physiol.* **46**: 1494-1504.
Zhao Q, Guo H. 2011. Paradigms and paradox in the ethylene signaling pathway and interaction network. *Mol. Plant.* **4**: 626-634.

References

SUPPORTING INFORMATION

Chapter 2

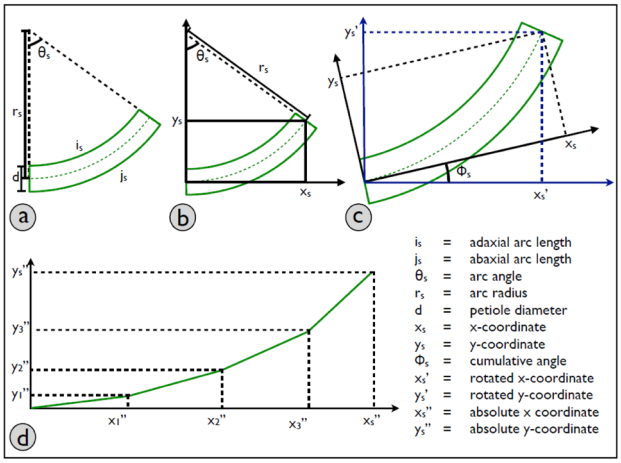

Fig. S2.1 To reconstruct petiole shape, it was divided into small sections (*s*). (**a**) Each section is represented by an arc. From the ad- and abaxial section length and the petiole diameter, the radius and angle of the arc can be calculated (Eq. 1, 2). (**b**) The arc angle and radius are used to calculate the x and y coordinates at the end of the arc (Eq. 3, 4). (**c**) These coordinates are rotated (Eq. 6,7) to account for the cumulative angle (Eq. 5) of all previous sections as well as the angle at which the petiole emerges from the shoot. (**d**) The absolute coordinates (Eq. 8, 9) of each section can be used to draw the shape of the petiole.

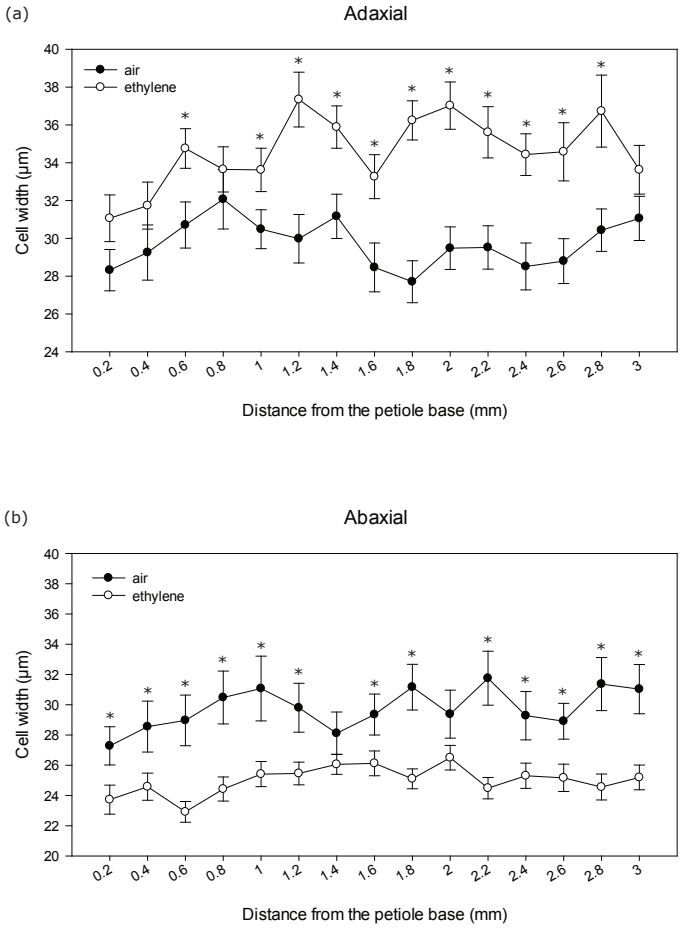

Fig. S2.2 Epidermal cell width of first 3 mm of a 1cm petiole. Data points represent the means ±SE of cell width at the adaxial (**a**) and abaxial (**b**) side of the petiole after 10h of ethylene and control treatment. Asterisks indicate significant differences relative to the cell width of control treated petioles (P<0.05); n=5

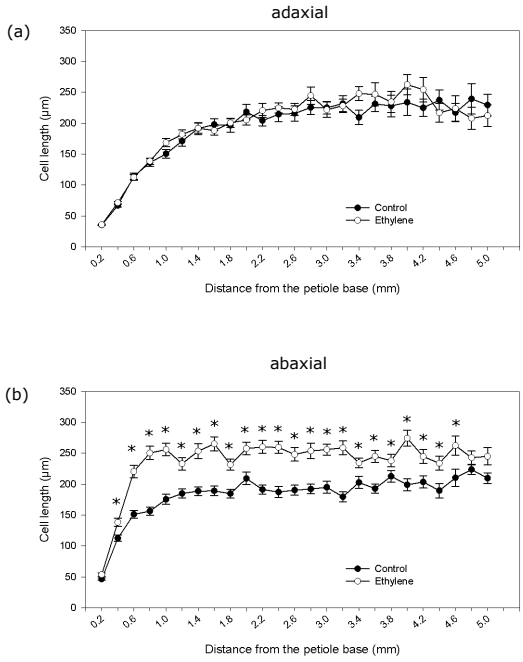

Fig. S2.3 Epidermal cell length of a 5mm petiole. Data points represent the means ±SE of cell lengths at the adaxial (**a**) and abaxial (**b**) side of the petiole after 10h of ethylene and control treatment. Asterisks indicate significant differences relative to the cell lengths of control treated petioles (P<0.05); n=12¬–20.

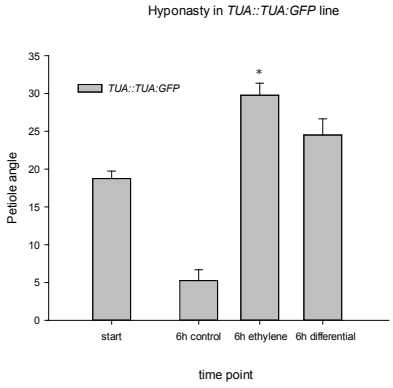

Fig. S2.4 Petiole angle of *35S::TUA:GFP* line at the start of the experiment, after 6h in control conditions and in ethylene (means ±SE). Asterisk indicates significant difference relative to the control treatment (P<0.05); n=5.

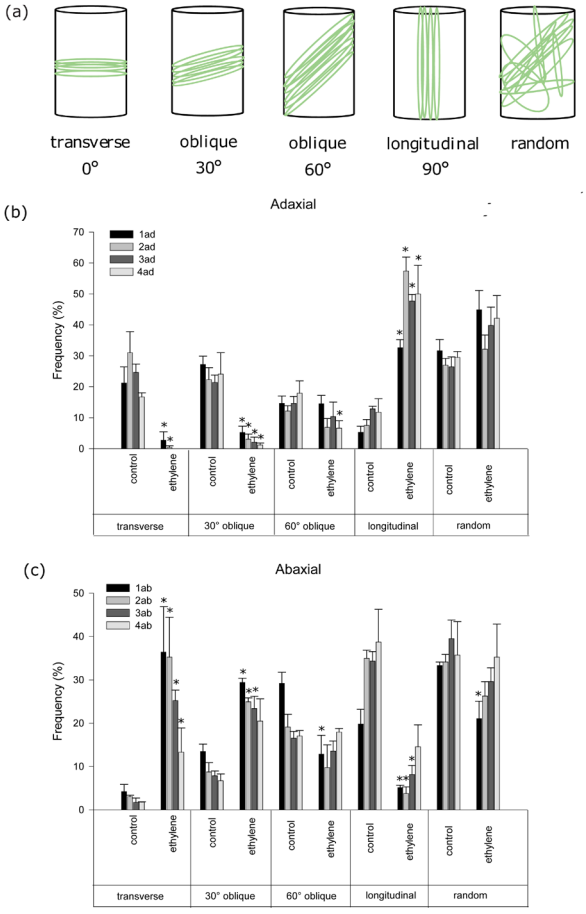

Fig. S2.5 Orientation of CMTs in petiole epidermal cells changes upon ethylene treatment. (**a**) Schematic illustration of classes of different CMT orientations that have been scored in this study: transverse to the long cell axis (0°), oblique (30°), oblique (60°), longitudinal (90°) and random. (**b**) The full coverage of different CMT orientation in ethylene and control conditions described in this study. Data points refer to the average number (n=3) of areas representing categories of CMT arrangement ± SE. Asterisks indicate significant differences (P<0.05) between the frequency in control and ethylene treated plants.

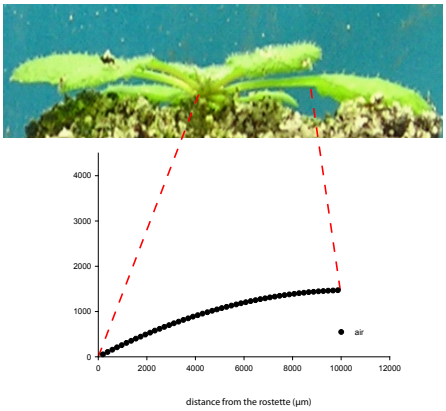

Fig. S2.6 The observed petiole shape after air treatment is described with a second degree polynomial equation (eq. 10).

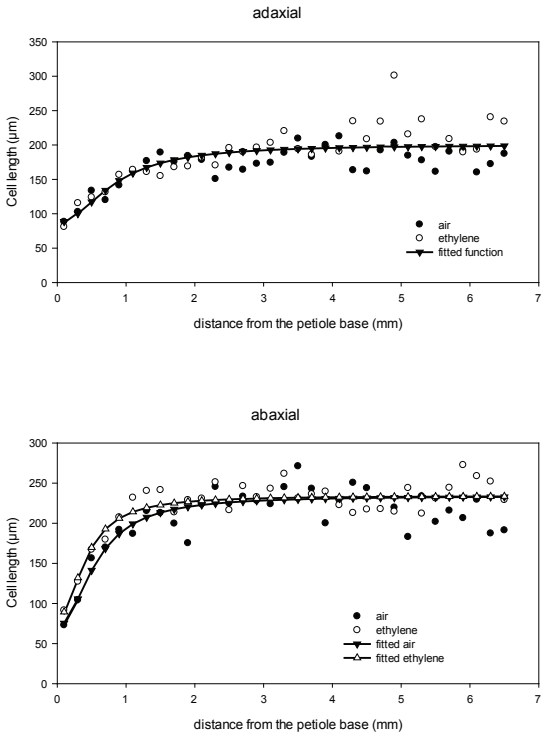

Fig. S2.7 For the model, the observed cell lengths are fitted using using Eq.11. The adaxial cell lengths were fitted as one dataset, while for the abaxial side the air and ethylene datasets were fitted separately.

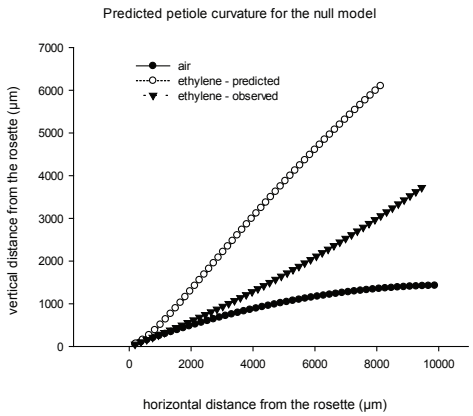

Fig. S2.8 For the null-hypothesis of no changes in cell division rate, both the predicted petiole curvature and the petiole elongation are an overestimate of the observed values.

Methods S2.1

Calibration of the model

To link observed changes in cell length under ethylene treatment to the observed changes in petiole shape, we use the observed petiole shape under air treatment as a reference shape. To calculate the ad- and abaxial length of each section, the observed petiole shape is described as a second-degree polynomial equation which was fitted to match the observed initial and final petiole angle (**Fig. S2.6**):

$$f(x) = ax^2 + bx \qquad (10)$$

Giving a = $-1.27*10^{-5}$ μm^{-1} and b = 0.27. To gage the accuracy of the predicted petiole shape, the function was also fitted to the observed petiole shape after ethylene treatment, giving a = $1.30*10^{-5}$ μm^{-1} and b = 0.27.

By integrating along this curve, the x and y coordinates at the end of each 200 µm section were determined, and, by inverting equations (1) and (2), the effective corresponding ad- and abaxial arc length, radius and angle were calculated. In the next step, the average number of cells spanning along both the ad- and abaxial side of each section was calculated, using the measured cell length data for the air treatment. Note that while the arc length along the centre of the petiole is exactly 200 µm, this is not true for the adaxial and abaxial arc lengths and . Consequently, the spatial 200 µm intervals over which adaxial and abaxial mean cell length are measured do not map directly to the petiole segments , and therefore a weighted contribution has to be used to calculate the average cell length within a segment, based upon multiple measurement blocks. Also note that these weighted contributions differ between the adaxial and abaxial side, because both have a different build-up of total length along the curve.

Assuming no difference in total cell number and using the measured cell length data, the average number of cells per section could then straightforwardly be used to predict the change in ad- and abaxial section length due to the ethylene treatment, by calculating the change in cell length in each segment. Due to the small section size, the cell length data is relatively noisy. Since the cumulative angle of a section depends on the curvature of all previous sections (Eq. 5), this not only can influence the local petiole shape but also the overall petiole shape. To prevent strong effects on the predicted petiole shape due to irregularities in cell length, we smoothed the measured cell lengths by fitting the following function to the data (**Fig. S2.7**):

$$f(x) = a - \frac{b}{1+\frac{x^2}{c^2}} \qquad (11)$$

Because at the adaxial side only one significant difference in cell length was found between the air and ethylene treatment, both sets of adaxial cell length data were fitted using the same function, giving a=200.14μm, b=113.23μm, c=834.29μm. At the abaxial side, however, ethylene treatment caused significantly enhanced cell elongation, although the differences were mainly found at the proximal part of the petiole. This has been captured by fitting the data to two separate functions, but with the same maximal cell length, giving a=234.06μm, b=163.60μm, c=572.60μm for the air treatment and a=234.06μm, b=152.63μm, c= 426.50μm for the ethylene treatment.

Predicted petiole shape assuming no differential cell division

We first assumed that ethylene treatment causes only differential cell elongation, with no effect on the cell division rate. The corresponding predicted petiole shape is compared with the observed petiole shape after ethylene treatment in **Fig. S2.8**. There are two clear discrepancies between the predicted and observed petiole shape. First, the petiole curves much stronger upwards: The predicted final petiole angle is 36.9 degrees, compared to the observed 22.0 degrees. Second, the predicted petiole elongation due to the ethylene treatment is higher than observed by Millenaar *et al.,* 2005. The model predicts a petiole elongation of 2.5 % as opposed to the observed 1.8 %.

Predicted petiole shape assuming reduced abaxial cell division

From the above analysis we can conclude that abaxial cell elongation is indeed the driving force behind hyponastic growth. However, the large discrepancy between predicted and observed petiole shape shows that the changes in cell elongation alone cannot accurately explain the observed changes in petiole shape. Clearly, the model overestimates the total abaxial length of all petiole sections together as derived from the cell length measurements, which gives rise to both an overestimation of the hyponastic growth and the petiole elongation. Since the petiole length is a function of both cell length and cell number, we therefore conclude that the ethylene treatment not only causes enhanced cell elongation, but that this coincides with re-

duced cell division. To predict the petiole shape taking the reduced cell division into account, we reduced the average number of cells per section weighted with respect to the observed increase in petiole elongation, i.e. we assumed that, for each section, reduced cell division is correlated with cell expansion, and that hence segments which present less cell expansion also undergo a smaller reduction in cell division. The total reduction in cell division was adjusted to fit the predicted petiole length to the observed petiole length after ethylene treatment. This method predicts a reduction in cell division of up to 17% for the most proximal parts of the petiole, where cell elongation is highest. Since we now fit the petiole length to its observed value, we can no longer use it as a proxy to gage the accuracy of the model. The petiole shape itself, however, is still predicted without using the observed petiole curvature. **Fig.2.6** shows that the model now correctly predicts the final petiole shape after ethylene treatment. The final predicted angle is 23.1 degrees compared with the observed 22.0 degrees. Moreover, the local petiole curvature is also correctly predicted, both the upward curvature at the proximal part of the petiole and the straightness at the distal part of the petiole match the observations.

References:

Millenaar FF, Cox MC, van Berkel YE, Welschen RA, Pierik R, Voesenek LA, Peeters AJM. 2005. Ethylene-induced differential growth of petioles in *Arabidopsis.* Analyzing natural variation, response kinetics, and regulation. *Plant Physiology* **137:** 998-1008.

Chapter 3

SUPPORTING TABLES

Table S3.1. Primer sequences used for the RT-Q-PCR of genes flanking T-DNA insertions.

Gene	Forward primer	Reverse primer
At4g36280	GGCGGGAGATTACTTTGTGA	AGAATGCCAACGCTCTGAGT
At4g36290	TGGGATCAGAAAATGCATGA	TCTCGGAGCCGTATATCCAC
At4g36350	TGGTGATGTGAAACCGAAAA	AACGGTGAATGTAGGGCTTG
At4g36360	ACAGAATCGGCAGCAAGAGT	CAAAGGCAGAACCTGAAAGC
At4g36370	GCGGTGTCGATGATGACATA	GCTCGAGAAAATTTAGACGAAAA
At4g36380	AGATTTCGTCAGCGGAAAGA	CCAAAGGGTGTGAAGCAAAT
At4g36390	AGCGCAGAAGTCATTTTCGT	CCAACCTCGCGGATTATAGA
At4g36400	ACCCTTTGTTTTCGTCGTTG	ACGGATTAGACGCAAACCAC
At4g36410	AGTTCATGGAGTGGCAAACC	TTGTCTTTCGGCTTTTGCTT
At4g36420	CGTGTCCAAAATCGTCAATG	TTGTTCTTGCTCATGCTCCA
At4g36430	GGCTGCTTCCTTGTTGAGAC	ACTACCGGAGAGAGCGACAA

At2g19990	GACCATTCGGCGAGAATCTA	CCCGGAGGATCATAGCTACA
At2g20000	GGGAACACAAATGGCTCAGT	CCTCATATGCAGCCCAAAGT
At2g20010	GGGGAAGTTCCTTCCTCAAG	ACGGCAGCAGAGTCTTGAAT
At2g20020	TCCTATTCCGTGGCAGAAAC	CATGAGCTCTCGTCCTTTCC
At2g20030	CGATCAGAGACCGACAGTGA	TCAAGCCCTTGTTTCAATCC
At2g20050	ATCCTCGAGATGCTTGTGCT	CATCCAAAGGTGGAAGGAGA
At2g20060	GCCTAAAACCTTCACCACCA	TCCAAAAGTGCGAAAAATCC
At2g20070	GATCCGATGTGTCCTGGAGT	CAATCAAGCAGTTGGTGGAA
At2g20080	GCCACAGAGAGGTCTTGGAG	CTTGGATTCCAGCTCATGGT
At2g20100	TTTGGCAAGACTGACACAGC	TTTTGATTGTCCGTCGATGA
At2g20110	TCCACATGGTGGACGAGATA	CCAAGCATTTGCAGTTCTCA
At1g60000	GGTGCAAGTGCTGTTCTTGA	TCTAGCCCCAACCACATCTC
At1g60010	TCCTTTGCCGGAGAAGAATA	TCCCTCACGTAAAACCCAAA
At1g60020	AGAAGCTCCTCAACCGTGAA	TGAGTCGCACCACTATCGAG
At1g60030	TCGGTCTTCATGGGCTTATC	AAACAGGCACACACCACAAA
At1g60040	ATCTCCATGTTTGGCCTCAG	ATCCATTCCCGTGTAAGCTG
At1g60050	ACCCTTCCTCACGAAACCTT	TCCAAATGGAGATGGAGAGC
At1g60060	AAATGAGCTCCGGAGAAGGT	GGAGAAGCGTTGATGAAAGG
At1g60070	TTGTCACCAACTCGCTGAAG	TCCAGCGACGTCATACTCAG
At1g60080	GCTTGGATGGGTTATCTGGA	CAGCTCTTGATGGCTGATGA
At1g60090	ACCCAAAGAGCCCAAGATTT	TTTGAGCACACCACCAATGT
At1g60095	AAGTGGAAAAGCGTGAGCAT	ACTTGACGAATGCGATACCC

Table S3.2. Position coordinates and sequences of paired-reads from *Arabidopsis* and T-DNA genome. (a-b) breakpoint 1 is located on chromosome 4 and has **15** supporting paired reads (a) *Arabidopsis* (b) T-DNA. (c-d) breakpoint 2 is located on chromosome 2 and has **4** supporting paired reads (c) *Arabidopsis* (d) T-DNA. (e-f) breakpoint 3 is located on chromosome 1 and has **4** supporting paired reads (e) *Arabidopsis* (f) T-DNA. (g) other potential breakpoints with only one supporting paired-read.

(a)

	POS	**DIR**	**READ**
1	17189364	+	GGCGTTAATACAAATCGTCCTGCTCTGACAGCCGTCCACTCTGTTTTCTT
2	17189571	+	TTAAAATCTCCTCACAAGACAAACATCTAATCTAACGGTCCACAGACGTC
3	17189669	+	TGCACATCAATACGTACCACGAGTTTGGCTAGAGCGACGGGGTTGTCACT
4	17189698	+	TAGAGCGACGGGGTTGTCACTTAAGAATTTGACAGCCAAGGTCATCGCCG
5	17189714	+	TCACTTAAGAATTTGACAGCCAAGGTCATCGCCGTTGGCATTGTTTCCTC
6	17189714	+	TCACTTAAGAATTTGACAGCCAAGGTCATCGCCGTTGGCATTGTTTCCTC

7	17189745	+	CCGTTGGCATTGTTTCCTCTCCGGGTATCATCATCTCAACGATCTTTCCG
8	17189858	-	GAGGAGAGACAAGTGGCGATGACAACGACGTCTCCGGCAAATGACGTGGG
9	17189938	-	TTAGTGTGTAAATACTAGGGTTTAATACTTCAATCATGCAGGCGAAAGAG
10	17189944	-	ATTTTGTTAGTGTGTAAATACTAGGGTTTAATACTTCAATCATGCAGGCG
11	17189952	-	CTGATTTCATTTTGTTAGTGTGTAAATACTAGGGTTTAATACTTCAATCA
12	17189959	-	TCAATATCTGATTTCATTTTGTTAGTGTGTAAATACTAGGGTTTAATACT
13	17189993	-	AAGGTAAAATATTTCCTTATAATACATGAGCATATCAATATCTGATTTCA
14	17190041	-	ATTTGTATCCCCATCAAATTCCCTGGCACTAGACTCTACAAATCCTTAAA
15	17190107	-	AGCACATCTCCTGGTGAAGATATGAACATTCTCAAACTTGAGTTCGAAGA

(b)

	POS	**DIR**	**READ**
1	7753	-	GGTAATTACTCTTTCTTTTCCTCCATATTGACCATCATACTCATTGCTGA
2	7863	-	CTTGCTTTCGCCTATAAATACGACGGATCGTACTTTTCCGTTTTATCAAA
3	7727	-	ATTGACCATCATACTCATTGCTGATCCATGTAGATTTCCCGGACATGAAG
4	7781	-	ATCTACATTTTTGAATTGAAAAAAAATTGGTAATTACTCTTTCTTTTCCT
5	7771	-	TTGAATTGAAAAAAAATTGGTAATTACTCTTTCTTTTCCTCCATATTGAC
6	7778	-	TACATTTCTGAATTGAAAAAAAATTGGTAATTACTCTTTCTTTTCCTCCA
7	7786	-	CGGACATCTACATTTTTGAATTGAAAAAAAAATTGTAAATAATTTTTTCT
8	8071	-	GTGACGACAAATCGTTGGGCGGGTCCAGGGCGAATTTTGAGACAACATGT
9	8028	-	AACATGTCGAGGCTCAGCAGGACCTGCAGGCATGCAAGCTTATCGATATC
10	7746	-	ACTCTTTCTTTTCCTCCATATTGACCATCATACTCATTGCTGATCCATGT
11	7762	-	AAAAAAATTGGTAATTACTCTTTCTTTTCCTCCATATTGACCATCATACT
12	7768	-	AATTGAAAAAAAATTGGTAATTACTCTTTCTTTTCCTCCATATTGACCAT
13	7936	-	TCATCTAAGCCCCCATTTGGACGTGAATGTAGACACGTCGAAATAAAGAT
14	7894	-	ATAAAGATTTCCGAATTAGAATAATTTGTTTATTGCTTTCGCCTATAAAT
15	7850	-	ATAAATACGACGGATCGTAATTTGTCGTTTTATCAAAATGTACTTTCATT

(c)

	POS	**DIR**	**READ**
1	8650997	+	TGAGCAAATTTTCTTTATCTTTCAAATGCACGAGCCCAATCTCACTACAG
2	8651019	+	CAAATGCACGAGCCCAATCTCACTACAGTCTGTTGTACTCAAGCATGTTG
3	8651461	-	TATGACAATCTTGAAATCGGAACAGAAGTCTCCATAGACAAGCATGAAGG
4	8651477	-	TGGAATCACTAACGAGTATGACAATCTTGAAATCGGAACAGAAGTCTCCA

(d)

	POS	DIR	READ
1	4225	+	AGCAAGTGGATTGATGTGATATCTAGATCCGAAACTATCAGTGTTTGAAT
2	4228	+	AAGTGGATTGATGTGATATCTAGATCCGAAACTATCAGTGTTTGAATGGT

3	4216	+	CGTCTTCAAAGCAAGTGGATTGATGTGATATCTAGATCCGAAACTATCAG
4	4224	+	AAGCAAGCGGATTGATGTGATATCTAGATCCGAAACTATCAGTGTTTGAA

(e)

	POS	DIR	READ
1	7764	-	GAAAAAAAATTGGTAATTACTCTTTCTTTTCCTCCATATTGACCATCATA
2	8081	-	AACCTTGACAGTGACGACAAATCGTTGGGCGGGTCCAGGGCGAATTTTGC

(f)

	POS	DIR	READ
1	22137215	+	ATTAATGAAGTCTAATTCATTTCTTAAGTTAATTTTTAAAAATATTAAAC
2	22137338	+	TATTCTCCAAAATCATTAAAGATGAATTTAAAGTCGCAAATCACATTACG

(g)

Chr1	17678800	-	GAGTCAGAATTACCTTTCAAGGATAAGTATCAGTCATTAGTGCCACACTA
TDNA	2611	+	CTGCGCGTAACCACCACACCCGCCGCGCTTAATGCGCCGCTACAGGGCTG
Chr1	29052364	-	TCACTACCGTCTTTACCCTGAAATTTATTTTATGAAGTATACGCTAATCA
TDNA	9031	+	GGAGCCCAGTCCCGTCCGCTGGTGGCGGGGGGAGACGCTCACGGTTGACT
Chr2	3261127	-	GAGTCGATCCCGACTTGGGAAGCAAGGGTCTCGGAGTTCAGGAAGCAGTT
TDNA	1497	-	TGACACCACGATGCCTGTAGCAATGGCAACAACGTTGCGCAAACTATTAA
Chr2	12247295	+	ACCAGAGTCGTCTCATAAACGCTACTGCCATTTTAGAAGATCTAATCTTG
TDNA	9921	+	AAATGCCAATTTCTCAGACCTACCTCGGCTCTGCGAAGGCCCCCGCTGGT
Chr3	1877464	-	ATATTAGCCTAATATATACACAAAATATTCGATTTATGATGAAATTTGNA
TDNA	9734	-	GAGTCAGTTTTTATTTTTCTACTACTTTGGTCGTTTATTTCGGCGTGTAG
Chr5	16110755	-	TTTCTGGGTTTTTTCTAATTCTTCCATTTTCGTAGATATTTTGTGGGTTT
TDNA	9973	-	CCTTCTCGTTGAGGTCGGTCGCGCCATGTCGGATGAAATAAAAACTTTTG
Chr5	23194947	+	CTCAAAACTCCCATTGTCGAGAACCTGCAGGTTACTGTTATAAACTTTCT
TDNA	8520	+	TTCAGCACAATATATTGTTTTCATTTTAATATTGTACATATAAGTAGTAG

Chapter 4

Table S4.1 Primer sequences used for RT-Q-PCR.

Gene	Forward primer	Reverse primer
BR6OX	CCCAACCATGATGAAAGACC	TCTCAAGATCATCCCAACCAC
ROT3	AGATTTCGTCAGCGGAAAGA	CCAAAGGGTGTGAAGCAAAT
β-TUB-6	ATAGCTCCCCGAGGTCTCTC	TCCATCTCGTCCATTCCTTC

Chapter 5

Table S5.1 Primer sequences used for the RT-Q-PCR.

Gene	Forward primer	Reverse primer
ERF95 (At3g23220)	GGAGATTCGCGACTCAGCTA	CCTCTATATCCCGACGACGA
ERF112 (At2g33710)	ATTCCAGTGCCAACTTGTCC	GCGCCTAAAATGATCAAAGC
ROT3 (At4g36380)	AGATTTCGTCAGCGGAAAGA	CCAAAGGGTGTGAAGCAAAT
β-TUB-6 (At5g12250)	ATAGCTCCCCGAGGTCTCTC	TCCATCTCGTCCATTCCTTC

Chapter 6

Supporting figures

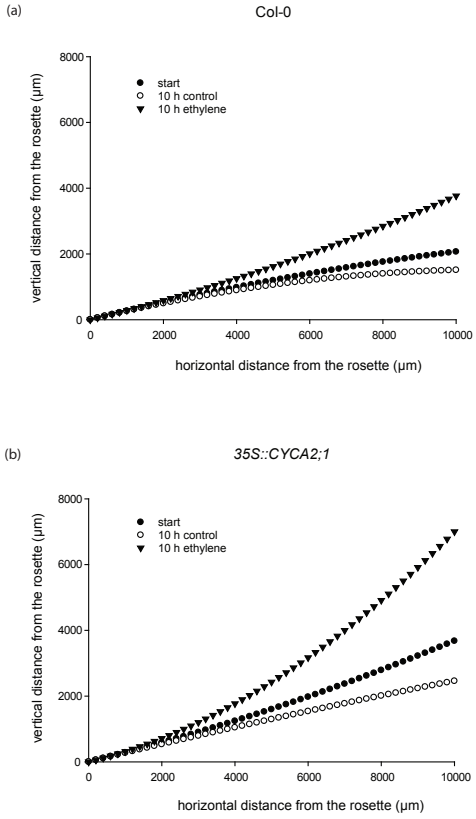

Fig. S6.1. Extrapolated petiole shape. The measured initial and final petiole angles were used to extrapolate petiole shape using the function: $f(x)=ax^2+bx$.

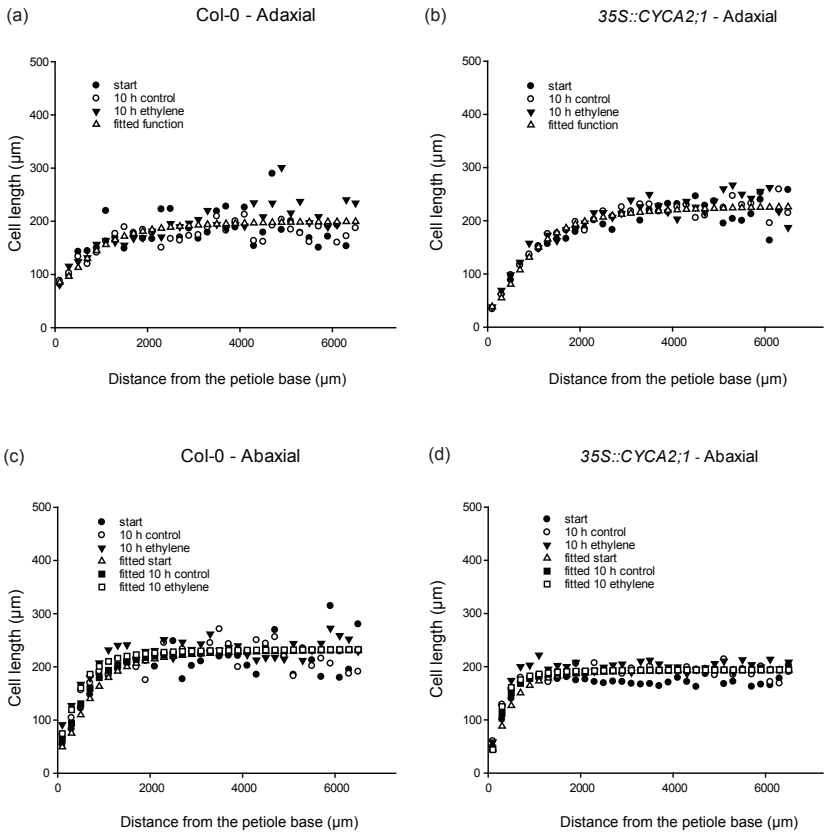

Fig. S6.2. Extrapolated cell length. The cell length data was used to describe the cell length along the petiole with the function: $f(x) = a\text{-}b/(1+(x^2/c^2))$. Abaxial cell lengths were fitted concurrently; adaxial cell lengths were fitted separately but with the same maximal cell length.

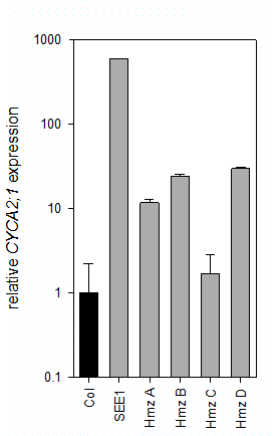

Fig. S6.3. Quantitative RT-Q-PCR analysis of *CYCA2;1* expression in four independent *35S::CYCA2;1* transformants and *SEE1-1D*. Expression levels were assayed in homozygous plants (gray bars) ($n \geq 4$ ±SE). Transgenic line Hmz B was further characterized and is referred to as *35S::CYCA2;1*.

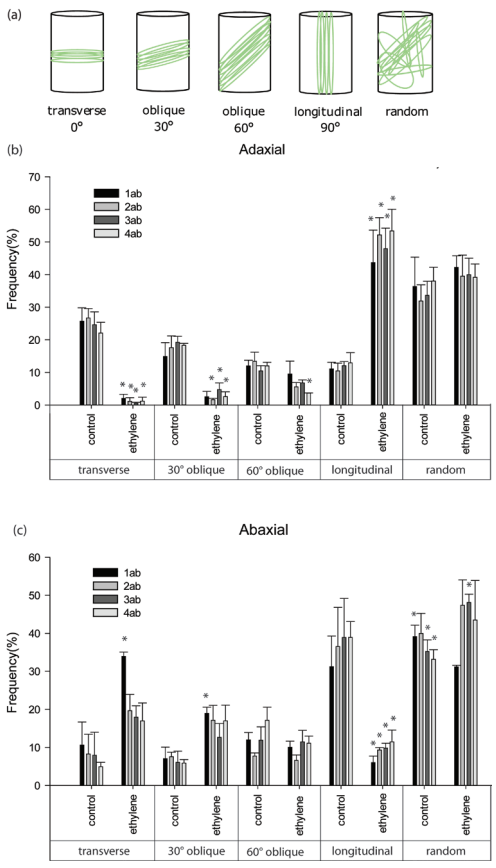

Fig S6.4. (**a**) Schematic illustration of CMT orientation types. (**b-c**) Orientation of CMTs in petiole epidermal cells upon ethylene treatment at the (a) adaxial and (**b**) abaxial side of a petiole. Data points refer to the average number (n = 3) of areas representing categories of CMT arrangement ± SE. Asterisks indicate significant differences (P < 0.05) between the frequency in control and ethylene treated plants.

Supporting tables

Gene/AGI code	Forward primer	Reverse primer
At5g12250	ATAGCTCCCCGAGGTCTCTC	TCCATCTCGTCCATTCCTTC
At5g25350	CTTTCACGGTGTCCTGGAAT	GTGGGCAGCTCCTGATAGAG
At5g25360	AAGCCAAGCGTATCAGAGGA	CAGAGGTTCAATCCGTGGTT
At5g25370	ATTCAATTTATGCGGCAAGG	CGGTGTAGACGTGGAAGGAT
At5g25380-a	ATCAGTTCCCACCACCAAAA	CCGCGAAATAGTTGGCTAAG
At5g25380-b	AGCGTGTTGCTAGACCGAGT	TTCTTTACCACCTCGCTTGC
At5g25390	GGGTCAAAAACGAGTCCAAA	CGCCATTTGATCATCTTCCT
At5g25400	CCTTGGATTGTCGTGGAGTT	CAGAGGTTTTCCCAACCAAA
At5g25410	TGGAGACCCAAAGGAATCAG	TTGGCAAATGTCAAACTCCA
At5g25415	CATGAACCAGAGACCAGCAA	GAAGGATCTGAGAGGCAACG

At5g25420	TGATCGCTTCGGCTTCTTAT	AGCAATCGACAGAGGGCTTA
At5g25430	CCTATGGCCGGGATATTTTT	CCGCGTCGTAGAATTCATCT
CYCA2;2/At5g11300	TGTATGTGTTGGCCGTAATG	TGGTGTCTCTTGCATGCTTA
CYCA2;3/At1g15570	CTCTATGCCCCTGAAATCCA	ACCTCCACAAGCAATCAAC
CYCA2;4/At1g80370	CAAAGCCTCCGATCTCAAAG	CTTGTCCGGTAGCTCTCCAG
HISTONE H4/ At2g28740	CCAAGCCTGCGATCCGAAGATTGGC	CGCTACCGCAAACTGAACGCCAAACCC
CYCA1;1/At1g44110	CGATGACGAAGAAACGAGCA	TGGCATTAACGCAAACACTTG
CYCD3;1/At4g34160	GCCACCGTCTCCTCCTCTCTGTAAT	GCCCATGGCAGATGCAAAATCGGCT
CYCA2;1/At5g23580	CGCTTCAGCGGTTTTCTTAG	ATCCTCCATTGCAAGTACCG
ILP1/At1g17210	AGCTTGCCAAGAAGGCATTG	TCATCAACGACGCAGTCAGA
CYCB1;1/At1g16330	CGAGACGCCCCCACTACTTAGACTT	CGGGTTTAGCTCGAATCGGACATGC

Table S6.2. Parameters used to profile cell division rates.

	Length	Thickness	Initial angle	Final angle	Petiole shape		Cell length - adaxial			Cell length - abaxial		
					$f(x)= a^{2} + b\,x$		$g\,x\ = a\ \frac{b}{+\frac{x}{c}}$					
					a	b	a	b	c	a	b	c
Col-0 start	10000 µm	700 µm	15.7 °	12.0 °	-6.5 * 10^{-6}	0.27	201.3	117.6	870.3	233.3	187.8	694.0
Col-0 10 h control	-	700 µm	15.7 °	8.2 °	-1.2 * 10^{-5}	0.27	201.3	117.6	870.3	233.3	174.4	598.4
Col-0 10 h ethylene	-	700 µm	15.7 °	22.7 °	1.1 * 10^{-6}	0.27	201.3	117.6	870.3	233.3	167.1	439.7
35S::CYCA2;1 start	10000 µm	700 µm	15.7 °	21.2 °	9.7 * 10^{-6}	0.27	229.6	193.5	915.4	194.3	156.7	435.1
35S::CYCA2;1 10 h control	-	700 µm	15.7 °	14.2 °	-2.5 * 10^{-6}	0.27	229.6	193.5	915.4	194.3	164.0	300.1
35S::CYCA2;1 10 h ethylene	-	700 µm	15.7 °	40.3 °	4.4 * 10^{-5}	0.27	229.6	193.5	915.4	194.3	176.2	241.3

Supporting boxes

Box S6.1: Deriving number of cells from petiole shape and cell lengths

The number of cells along the adaxial and abaxial side of a petiole can be derived from the equations describing petiole shape, and adaxial and abaxial cell length (eq. 1-3).

To obtain spatial resolution, the petiole is divided into 50 sections (s) of equal arc length.

The final coordinates of the section are transformed such that they are relative to the coordinates of the starting points of the section (eq. 4 and 5) and rotated with the derivative of the function describing the petiole shape at the starting x-coordinate of the section (eq. 6-8).

These transformed coordinates can be used to calculate the radius (eq. 9) and arc length (eq. 10) of an arc describing the section.

Together with the thickness of the petole (d), these give the length along the adaxial and abaxial side of the section (eq. 11 and 12).

Finally, the number of cells is given by the adaxial and abaxial section length divided by the average cell length over the section length (eq. 13 and 14)

$$f(x) = ax^2 + bx \quad (1)$$

$$g(x) = \mathrm{a} - \frac{\mathrm{b}}{1 + \frac{x^2}{c^2}} \quad (2)$$

$$h(x) = \mathrm{a} - \frac{\mathrm{b}}{1 + \frac{x^2}{c^2}} \quad (3)$$

$$x'_s = x_s - \sum_{t=1}^{s-1} x_t \quad (4)$$

$$y' = y_s - \sum_{t=1}^{s-1} y_t \quad (5)$$

$$\phi_s = f'(x_{s-1}) \quad (6)$$

$$x''_s = cos(\phi_s) \cdot x'_s + \sin(\phi_s) \cdot y'_s \quad (7)$$

$$y''_s = -sin(\phi_s) \cdot x'_s + \cos(\phi_s) \cdot y'_s \quad (8)$$

$$r_s = \frac{(x''_s)^2}{(2 * y''_s)} + \frac{y''_s}{2} \quad (9)$$

$$\theta_s = atan\left(\frac{x''_s}{r_s - y''_s}\right) \quad (10)$$

$$i_s = \left(r_s - \frac{d}{2}\right) * \theta_s \quad (11)$$

$$j_s = \left(r_s + \frac{d}{2}\right) * \theta_s \quad (12)$$

$$n_s = \frac{i_s - i_{s-1}}{\int_{x=i_{s-1}}^{x=i_s} g(x)} \quad (13)$$

$$m_s = \frac{j_s - j_{s-1}}{\int_{x=j_{s-1}}^{x=j_s} g(x)} \quad (14)$$

Box S6.2: Profiling cell division along petiole

Differential cell division (adaxial vs. Abaxial) can be calculated using the number of cells along the adaxial (n_s) and abaxial (m_s) side of the petiole, derived from the data from the control treatment, the function describing petiole shape (eq. 1) and the functions adaxial and abaxial cell length (eq. 2 and 3).

The adaxial and abaxial section length are obtained by solving equation 4 and 5 for x, where d_s and e_s are cell division rates.

The adaxial and abaxial section length are used to compute an arc describing the section (eq. 6 and 7). These can be used to calculate coordinates for the section (eq. 8 and 9), which are rotated according to the angle of the function describing petiole shape at the starting x coordinate of the section (eq. 10 - 12). Finally, the absolute coordinates of the section are calculated taking previous sections into account (eq. 13 and 14).

The difference between the reconstructed petiole shape abd the observed petiole shape (eq. 15) is minimised by adjusting adaxial (d_s)or abaxial cell divisions (e_s).

Because this method does not take petiole elongation into account, the cell division rates are represented as the difference between adaxial and abaxial cell division (eq. 16).

$$f(x) = ax^2 + bx \quad (1)$$

$$g(x) = \mathrm{a} - \frac{\mathrm{b}}{1 + \frac{x^2}{c^2}} \quad (2)$$

$$h(x) = \mathrm{a} - \frac{\mathrm{b}}{1 + \frac{x^2}{c^2}} \quad (3)$$

$$\frac{i_s - i_{s-1}}{\int_{x=i_{s-1}}^{x=i_s} g(x)} = n_s * d_s \quad (4)$$

$$\frac{j_s - j_{s-1}}{\int_{x=i_{s-1}}^{x=i_s} h(x)} = m_s * e_s \quad (5)$$

$$r_s = \frac{d \cdot (i_s + j_s)}{j_s - i_s} \quad (6)$$

$$\phi_s = f'(x_{s-1}) \quad (7)$$

$$x_s = r_s \cdot sin(\theta_s) \quad (8)$$

$$y_s = r_s - r_s \cdot cos(\theta_s) \quad (9)$$

$$\phi_s = f'(x_{s-1}) \quad (10)$$

$$x'_s = cos(\phi_s) \cdot x_s - sin(\phi_s) \cdot y_s \quad (11)$$

$$y'_s = sin(\phi_s) \cdot x_s + cos(\phi_s) \cdot y_s \quad (12)$$

$$x''_s = \sum_{t=1}^{s} x'_t \quad (13)$$

$$y''_s = \sum_{t=1}^{s} y'_t \quad (14)$$

$$\Delta_{shape} = (y_s - f(x_s))^2 \quad (15)$$

$$\Delta_{division} = d_s - e_s \quad (16)$$

SAMENVATTING IN HET NEDERLANDS

(Summary in Dutch)

Fenotypische plasticiteit, dat wil zeggen het vermogen van een individueel genotype om verschillende fenotypes aan te nemen, stelt levende organismen in staat om zich effectief aan te passen aan hun dynamische omgeving. De relatief sterk fenotypische plasticiteit van planten ten opzichte van dieren, heeft te maken met twee aspecten van hun ontwikkeling: i) de aanwezigheid van meristemen die een plant in staat stellen constant nieuwe cellen aan te maken, en ii) de opbouw van planten die bestaat uit zich herhalende eenheden. Desondanks benadrukten de vroegste studies naar plantbewegingen voornamelijk de ogenschijnlijke gelijkenis met dierlijk gedrag. De moderne plantenwetenschap richt zich echter voornamelijk op de regulatienetwerken die ten grondslag liggen aan levensprocessen, zo ook aan bewegingen van plantenorganen. De fysieke heroriëntatie van, delen van, plantenorganen is het gevolg van een scala aan regulatiestappen op moleculair, fysiologisch en cellulair niveau. Het onderwerp van dit proefschrift is ethyleen-geïnduceerde hyponastische groei in *Arabidopsis thaliana* (zandraket).

Hyponastische groei is een opwaartse beweging van een orgaan (in dit geval een petiool ofwel bladsteel) waardoor bladeren in een meer verticale positie komen te staan. Verschillende, veelal stressvolle, omgevingsvariabelen kunnen hyponastische groei veroorzaken. Onderzoek aan semi-aquatische plantensoorten heeft laten zien dat planten door een combinatie van hyponastische groei en verhoogde petioolstrekking, bladeren aan een overstroming kunnen ontsnappen. Bodemoverstroming, alsmede volledige overstroming bëinvloeden de bladhoeken in verschillende soorten zoals *Rumex palustris*, *Leontodon taraxoides*, *Paspalum dilatatum* or *Rorippa sylvestris*. Ofschoon vroegere studies zich vooral richtten op soorten die van nature voorkomen in frequent overstroomde gebieden, laten recente experimenten zien dat het bestuderen van hyponastie in *Arabidopsis thaliana* van grote waarde kan zijn in het ontrafelen van de mechanismen van overstromingsgeïnduceerde hyponastie. Het gasvormige plantenhormoon ethyleen vervult een centrale functie in het complexe regulatienetwerk van hyponastie. De diffusie van dit gas vanuit de plant naar buiten wordt ernstig beperkt onder water, waardoor het zich in overstroomde planten passief ophoopt tot hoge concentraties. Deze ethyleenophoping is cruciaal voor hyponastie en voor niet-differentiële, lineaire strekking van petiolen en internodiën. Hyponastie wordt gestimuleerd door twee andere plantenhormonen auxine (indol azijnzuur, IAA) en gibberelline zuur (GA), die worden geactiveerd door ethyleen. Een vierde hormoon, abscisine zuur (ABA) remt juist hyponastie en wordt door hoge ethyleen concentraties afgebroken en verminderd aangemaakt. Als gevolg van deze ABA daling kan GA juist in concentratie toenemen en stimuleert vervolgens de hyponastie. De hoogste snelheid van opwaartse bladbeweging correspondeert met een toegenomen zijwaartse verdeling van IAA in de petiolen. Deze hormonen werken ook tijdens niet-differentiële ethyleen-geïnduceerde petioolstrekking, maar deze

twee processen zijn niet direct gekoppeld via hormoonregulatie.

Een tweede omgevingsfactor die hyponastie veroorzaakt in plantensoorten zoals *R. palustris* en *A. thaliana* is beschaduwing. Wanneer planten in dichte vegetatie elkaar beschaduwen is petiool hyponastie een succesvolle strategie om aan de schaduw te ontsnappen. De ontdekking van de rood:verrood (R:FR) ratio als het primaire signaal om nabije vegetatie op te merken, zelfs al voordat er werkelijk beschaduwing plaatsvindt, en daarop te reageren met schaduw mijdende reacties (shade avoidance responses) is uitgebreid bestudeerd. Fotoreceptor eiwitten (fytochromen) nemen het licht waar. De fytochromen zijn specifiek gevoelig voor de R:FR ratio, terwijl cryptochromen en fototropines blauw licht waarnemen. In dichte vegetaties van *Nicotiana tabacum* is aangetoond dat ook het waarnemen van het gasvormige plantenhormoon ethyleen een belangrijke rol speelt in de competitie om licht. Ethyleen concentraties in de atmosfeer binnen deze vegetaties waren vier keer verhoogd ten opzichte van normaal en ethyleen-ongevoelige planten bleken vertraagde shade avoidance reacties te vertonen vergeleken met controle planten. Auxine and auxine transport spelen eveneens een zeer belangrijke rol in deze shade avoidance reacties, waarbij auxine veelal synergistisch met brassinosteroïden (BRs) werkt. Regulatie van DELLA eiwitten door GA draagt ook bij aan shade avoidance reacties en deze regulatie lijkt onafhankelijk te zijn van auxine en ethyleen. Eerdere studies hebben aangetoond dat licht perceptie sterk interacteert met de waarneming van temperatuur , waarbij plantenhormonen en transcriptionele regulatoren de knooppunten van deze interacties vormen. Hoge temperatuur en schaduw leveren vergelijkbare reacties op, zoals hypocotylstrekking en versnelde bloei. Hogere temperaturen leiden ook tot hyponastie, waarbij ethyleen een negatieve regulator is. De bladhoek blijkt sterk gecorreleerd te zijn aan de bladtemperatuur en verhoogde bladhoeken beïnvloeden de koelcapaciteit van de bladeren.

Zoals eerder genoemd is ethyleen van de belangrijke regulatoren van hyponastische groei in reactie op veranderende omgevingscondities en toediening van ethyleen zelf kan de reacties nabootsen van planten die onder water staan of beschaduwd worden. Ethyleen-geïnduceerde hyponastie is derhalve een bruikbaar systeem om het regulatienetwerk te onderzoeken dat deze veranderingen in de ontwikkeling van petiolen reguleert. Het doel van deze studie was om inzicht verkrijgen in de moleculaire regulatie van ethyleen-geïnduceerde hyponastie in *A. thaliana*, en deze inzichten te verbinden de aanpassingen in de ontwikkeling van planten om zo hun fenotype aan te passen. In **hoofdstuk 2** worden de morfologische aanpassingen tijdens hyponastie beschrijven. Op basis van een gedetailleerde analyse van epidermis cellen tijdens een behandeling met ethyleen wordt aangetoond dat longitudinale cel expansie optreedt in een specifieke zone van cellen aan de abaxiale zijde van de petiool. In deze zone treedt ook voornamelijk transverse oriëntatie op van microtubuli (CMT: cortical microtubules), hetgeen longitudinale cel expansie faciliteert. Op basis van cellengte data is een mathematisch model opgesteld dat nauwkeurig de gevonden hyponastie voorspelt. De daarop volgende hoofdstukken maken gebruik van genetische selectieprocedures (screen) op basis van twee trans-

gene populaties. Het methodische **hoofdstuk 3** beschrijft een nieuwe DNA basevolgorde analyse techniek (Ilumina sequencing) om de locatie van T-DNA inserties op het chromosoom terug te vinden in een zogenaamde activation-tagging populatie. Deze identificatie kan namelijk problematisch zijn met conventionele methodes. In de activation-tagging screen werden vier kandidaat lijnen geselecteerd met afwijkende petioolhoeken in controle-, ethyleen- en/of laag licht condities. Het genomische DNA van deze vier lijnen werd gemengd en met behulp van Illumina sequencing kon van drie van de vier lijnen de precieze locatie van de T-DNA insertie worden vastgesteld. Een van de kandidaten vertoonde een verlaagde petioolhoek onder alle condities, werd *ddd1* genoemd, en in meer detail bestudeerd in **hoofdstuk 4**. Het fenotype van *ddd1* correspondeert met een T-DNA insertie in de intragene regio van het ROTUNDIFOLIA3 (ROT3) gen, hetgeen codeert voor een enzym in de biosynthese van BRs. De observatie dat de typische ethyleen-geïnduceerde lokale cel expansie niet optreedt in *ddd1*, leidde vervolgens tot de hypothese dat er een interactie is tussen ethyleen, BRs en cel expansie. Dit werd aangetoond doordat planten met geremde BR biosynthese een verminderde hyponastische groei vertoonden. Tevens werden duidelijk effecten van ethyleen op de transcriptie van BR-gerelateerde genen gevonden. Geconcludeerd wordt dat BRs een belangrijke rol spelen in de longitudinale cel expansie in de abaxiale zone van petiolen tijdens het optreden van hyponastie. **Hoofdstuk 5** beschrijft de invloed van Ethyleen Respons Factoren (ERFs) op hyponastische groei. ERFs zijn onderdeel van een grote familie van transcriptiefactoren die betrokken zijn bij veel verschillende biologische processen. ERFs reguleren reacties op biotische (bijvoorbeeld pathogenen) en abiotische (bijvoorbeeld droogte, zout en overstroming) stressen. Met behulp van een zgn. forward genetic screen werden kandidaat ERFs gezocht die een rol van betekenis spelen tijdens ethyleen-geïnduceerde hyponastie. Van de subset van kandidaat ERF genen die tot overexpressie gebracht waren werd vervolgens de ethyleenproductie gemeten en de expressie van verschillende ERF genen in ethyleen behandelde controleplanten werd onderzocht. Op basis van deze data kunnen vervolgstudies worden opgezet om de precieze rol van ERFs bij de regulatie van ethyleen-geïnduceerde hyponastie te onderzoeken. **Hoofdstuk 6** beschrijft de rol van de cel cyclus gedurende de regulatie van hyponastie. Overexpressie van het cel cyclus gen *CYCLINA2;1* stimuleert hyponastische groei. Verdere studies aan de cel cyclus laten zien dat ethyleen de transcriptie van cel cyclus genen reguleert aan de adaxiale zijde van de petiool, waardoor celdeling wordt geremd. Gecombineerd met resultaten uit hoofdstuk 2 laten deze bevindingen zien dat ethyleen een duale functie vervult in de regulatie van hyponastie: het stimuleert cel expansie aan de abaxiale zijde en remt celdeling aan adaxiale zijde.

Dit proefschrift heeft tot doel om de moleculaire regulatie van hyponastische groei verder op te helderen. Vervolgonderzoek zou zich kunnen richten op het vaststellen van de exacte rol en localisatie van ERFs in de petiool alsmede het vinden van de directe doelgenen/doeleiwitten. Verder staat de vraag nog open of ethyleen BRs reguleert op het niveau van biosynthese of uitsluitend op het niveau van gevoeligheid. Een laatste, maar zeer belangrijke vraag die beantwoord moet worden is waarom

een specifieke groep cellen t.o.v. de overige cellen, versneld groeit in ethyleen en of vergelijkbare patronen optreden wanneer hyponastie wordt geïnduceerd door een ander signaal dan ethyleen.

ACKNOWLEDGEMENTS

I'm glad in every thesis there is a chapter that everyone wants to read and you can put all the data you want without being too selective J. I would like to thank all the wonderful people I've come across not only in the academic world but in all kinds of situations during my stay in the the Netherlands.
Theo and Frank, I believe you had a substantial impact on my scientific life. Coming from the traditional, hierarchic university world, I learned it's even better when hard work is combined with lots of fun (and 3 pm tea breaksJ). Thanks, Rens, for "taking me under your wings", teaching me you "can't compare apples to pears" and making sure things work as easy as "two fingers in a nose". Ton, thank you for your patience (especially regarding the molecular work and teaching me how to work with my lovely students… I can't say I got an 8 on that one! ;)). You recognised I needed a lot of freedom and trusted I would develop into some sort of a scientific animal. I hope I haven't let you down! Ronald, thanks for being Ronald. I haven't been the easiest one to work with but you always gave me what I needed at a time, a cocktail of supervision and friendship! I envy all your future PhD's already and I sincerely hope all your future dreams come true and we'll get to work together soon. Pushki, if I were to do the psychoanalysis of all the great memories we created, I'm afraid they would have to invent a new term for our syndrome ;). I missed you every time you went on your long journeys, I missed you when you graduated. We truly had a blast together! Rashmi and Mieke, it is the hardest to thank the ones who are your closest friends. What could I possibly write? You know pretty well how much I love you… All our adventures (and, believe me, I remember more than you can imagine ;)) will stay with me till we become three grannies doing the hyponasty dance (or a "walker race", like we agreed) when no one can see. Woutas, you're the youngest in our team but surely, the sharpest (at least in finding peculiar connections between words, items and people). You're a bit crazy but it's more than okay, keep it this way and don't forget you have a job in my super cool guest house as a multifunctional worker. Just, please, do something about your hair - I don't want you to scare the German tourists. Dus… Pushki, Mieke, Mimi and Woutas - thank you from the most proximal parts of my heartJ!

Martijn, we both are pretty stubborn creatures but I was happy to realise how nicely we join our forces! Obviously, without your input the thesis would look different. Thanks for all the energy, discussions, brainstorming, persistence on getting things doneJ and being constantly ready to go. That week we spent harvesting petiole quarters paid off more than what we might have expected! Good luck with all your future plans! Hans, sometimes I like to recall those days when we were in Theo's lab, looking for random seeds just outside Frank's window… You have so much talent; don't ever think of leaving the academia! It was lucky to have you around twice and I believe we're going to do some serious canoeing…maybe in search of new speciesJ? Francesco, thank you for being always so much fun! If we don't end up in the same lab, at least we'll meet at conferences where we can discuss the "subon-

eme" over and over again! Melis, thank you for all our wonderful conversations... and jumping through the waves (also literally!). Good luck with everything! Xin, thank you for taking care of me when I was still a lab baby and appreciating whatever came out of my oven! Tanja and Zohreh, thanks for sharing your experience with me and always having something wise to say. Frank, thank you for the very warm welcome and getting me started. Steffen and Tom, many thanks for the work on our cyclin story and being always open for discussion. Jop, you introduced me to the cell size world… Shall I thank you for this or hire a voodoo priest ;)? I'm glad we could write a paper together (at least one more to come!). Good luck with all your projects! Ramzi and Wilbert, thank you for all your work which (relatively fast) sprouted into a nice publication. Ramzi, I wish you all the best with your life overseas! Ankie, you're the lab angel! Your work is simply priceless; no one in the world is as accurate and devoted as you are. Rob, we've truly had a great time together. Thank you for explaining things in a way that tricked me to believe I understoodJ. We shared a very special experience – we're the only ones who have encountered the most peculiar animal of all … the wild rooster, naturally! Yvonne, you always keep things on a leash, thank you for organizing our crazy lab life! But also – thank you for your warmth; you understand my dilemmas without me having to explain! Judith, you're officially the best pest fighter I've ever known. Always alert and ready for a battle! Together with Yvonne, Ankie and Rob you've created a sense of home for me. I know you all kept your fingers crossed for me when I needed it. I'm very, very grateful! Hans (van Aken J), we shared our lab lives for a short while but I want to thank you especially for always having something interesting to discuss! Divya, girl, there's a tiger's spirit in that little body of yours. Enjoy the last lap of the "race" and keep laughing! Joke, you know very well how happy it made me to work with you. You're faster than a lightning. How do you achieve such speed carrying a huge heart at the same time? Thanks for everything! Frits and Ronald, I really appreciate all your help and kindness. None of my data would ever see the daylight without your assistance! Henri, thank you for your humorous stories and true passion for biology! Thijs, you should have your own radio programme for desperate PhDs "Lost a publication? Ask Doctor Thijs"- you'd become a superstar!

Paulien, thanks for bringing the freshness and an organizer's spirit to our group! Good luck with all you challenges and plans you've set for yourself! Katie, I'm so glad you joined our team, you're a beautiful combination of brains, warmth and uniqueness (will you marry me?J). Marleen, you're a twinkling star, thank you for always being helpful, positive and genuine. All the best with everything! Aniu, kochana, zycze Ci, zebys wszystko szlo po Twojej mysli – naukowo i "nienaukowo". Dziekuje losowi, ze moglysmy sie poznac! Jestem pewna, ze nie dasz sie zadnym przeciwnosciom, ze swoim super-slowianskim charakterem i poczuciem humoru zawojujesz caly swiat! Debatosh, lots of luck with your project and exploring healthy cuisineJ. I'll be waiting for your graduation impatiently. My students - Anita, Cheryl and Sven- thanks for all your hard work and contributing to the research! Good luck, Cheryl, with your PhD, I'm sure you'll learn A LOT. You're stubborn and persistent,

never give up!

My beloved sisters, Carmie, Min and Ania (Szypcia, rzecz jasnaJ). I want to thank you for being my family. We met right after I arrived and you have stayed with me for good and for worse. Even though it sounds cliché and corny, you guys have always been there for me without expecting anything in return. Carmie, the first time I saw you in the corridor of JBI, I knew we would become friends (in the European sense, hehe). Min, and there you were, right after Carmie and I started talking. I know I don't have to explain how much it means to me to have you here. You never gave up on me, also when I was too weak to have faith in myself. Aniusia, dzieki Tobie moge sobie choc po czesci wyobrazic, jak to jest miec siostre. Jestes mi blizsza niz czubek wlasnego nosa. Dziekuje Ci za million rzeczy, zwlaszcza za to, ze jestes naprawde wyjatkowa, a zarazem autentyczna. Mam nadzieje, ze choc troche razniej Ci zwalczac swoje koszmary, majac taki koszmarek jak ja u boku J! Musisz mi obiecac, ze bedziecie do nas przyjezdzac. Popularne powiedzenie mowi, ze przyjaciol poznajemy w dziecinstwie, a pozniej to juz lipa. Nie zgadzam sie! Ale moze ten aspekt przedyskutujemy innym razem (to znaczy, ja wyslucham Twoich przemyslen ☺hihihi).

Ana and Fra, thank you for our moments spent on Hoogravenseweg ;). I'm glad we shared a bit of happiness; I will never forget our parties and the blast we had together! Pity it didn't last forever but I always think warm about you hoping you're healthy and happy! Many thanks also to Javi, Hector, Arjen, Esteban and Dave for always being fun… Suma, thanks for sharing a piece of yourself with me and always being supportive. Good luck with everything! Nikianaki, I'm happy the Greek-Polish union started the way it did and took its today's course. Thank you for our special moments and for staying in touch despite the distance!

Przybis, jestem szczesciara, ze mam Ciebie w zanadrzu ;). Jedno z moich wielkich marzen jest takie, zebysmy zawsze mieszkaly blisko siebie (najlepiej w jednej wielkiej willi z basenem, przy slonecznej plazy, gdzie po drugiej stronie ogrodu gorskie stoki sa zawsze osniezone, gdzie w kuchni stoi niezastapiony termomix gotowy robic nam truskawkowe przysmakiJ, hahahah). Pamietaj, ze nasza historia dopiero sie rozkreca i wiele niesamowitych przygod przed nami! Powodzenia na ostatnim okrazeniu, niechaj towarzyszy Ci tekst roku 2008, czyli "Dobra jestes" J. Trzymam za Ciebie kciuki, pozostan zawsze moim usmiechnietym Przybisiem!

Sabine, I'm so grateful for you helping me to find my way back to a healthy life. Even though our sessions seem far in the past, I still remember what you have done to help me. Gabi, I like to think we both benefitted from our meetings. I think you have a great talent, warmth and natural radiance… My research and this book would never come to existence if I hadn't met you. DANK JE! Kim, thank you for all the beautiful yoga classes. Thanks to you I started digging deeper into my practice and developed passion for the Ashtanga series. All the best with your little angels and I truly hope we meet on the mat soon!

Guy, what can I say? I thank the Universe for making us meet. If I were to thank you for everything, it would take me too much time and you know how impatient I amJ. You're one of the few people that have a natural Buddhist wisdom with-

out years of studying it.

אנא, דע כי אני מעריצה ואוהבת אותך הכי בעולם.אני יודעת שאינך מאמין במסע,הרוחות

אך אל דאגה,פרק החיים הבא מיעד אותנו לחיות ביחד.

Gideon and Catherine, thank you for being full of support for both of us and always being so sweet to me! Toda raba!

Mamusiu i Tatusiu, ostatni paragraf, ale pierwsze miejsce w moim sercu. Dziękuję Wam za to, że jesteście najlepszymi Rodzicami na świecie i stworzyliscie mi dom cudowny, cieply i inspirujacy. Mami, jesteś moim ideałem kobiety, silnej i szalonej. Twoje cechy dodają mi nadziei, że może wkrótce genetyka zacznie działać . Twoj śmiech to najlepsze lekarstwo na wszelkie troski, a pasja do życia i zdolność dostrzegania piękna to coś, co tylko Ty posiadasz! Tatko, zaczęło sie od opowieści i podroży… i od książek o ptakach. Moja miłość do biologii jest Twoją zasługą, dziękuję, że pokazałeś mi jej uroki, kiedy byłam małym szkrabem, a dziś jesteś zawsze wsparciem i inspiracją. Moja praca nigdy nie dosięgnie pięt Twojemu prawdziwemu powołaniu, ale mam nadzieję, że jesteś troszke dumny. Dziękuję Wam, Kochani Rodzice, za to co jest motorem działania każdego biologa. Życie i fascynacja nim!

Curriculum vitae

Joanna Polko was born on the 22nd of February 1983 in Tychy, Poland. She did her bachelor studies at the University of Wroclaw. In 2006 she conducted a six month-research project in the laboratory of Plant Physiology, University of Groningen under the supervision of Prof. Theo Elzenga and Dr. Frank Lanfermeijer. In 2007 she obtained her master degree which she had conducted in the Laboratory of Pland Morphology and Development at the University of Wroclaw. Her master project, *"The involvement of polar auxin transport in the formation of vascular system in Arabidopsis thaliana on embryonic and postembryonic level"* was supervised by Prof. Beata Zagórska–Marek and Dr. Alicja Banasiak. In August 2007 she started her PhD work in the group of Plant Ecophysiology at the University of Utrecht. The major results of that project are presented in this is dissertation.

Publications

Polko JK, van Zanten M, van Rooij JA, Marée AFM, Voesenek LACJ, Peeters AJM, Pierik R. **2011.** Ethylene-induced differential petiole growth in *Arabidopsis thaliana* involves local microtubule reorientation and cell expansion. *New Phytologist*. **193**: 339-348.

Van Zanten M, Ritsema T, **Polko JK**, Leon-Reyes, Voesenek LACJ, Millenaar FF, Pieterse CMJ, Peeters AJM. **2011**. Modulation of ethylene and heat-controlled hyponastic leaf movement in Arabidopsis thaliana by the plant defense hormones jasmonate and salicylate. *Planta*. doi: 10.1007/s00425-011-1528-3.

Polko JK, Voesenek LACJ, Peeters AJM, Pierik R. **2011**. Petiole hyponasty: a response to the environment regulated by ethylene. *AoB Plants;* doi: 10.1093/aobpla/plr031.

Polko JK, Temanni MH, van Zanten M, van Workum W, Iburg S, Pierik R, Voesenek LACJ, Peeters AJM. **2012** Illumina sequencing technology as a method of identifying T-DNA insertion loci in activation-tagged *Arabidopsis thaliana* plants. *Molecular Plant*; in press.